STRATIGRAPHIC STUDIES IN THE SNOW AND FIRN OF THE GREENLAND ICE SHEET

Thesis by

Carl S. Benson

In Partial Fulfillment of the Requirements

For the Degree of

Doctor of Philosophy

California Institute of Technology

Pasadena, California

1960

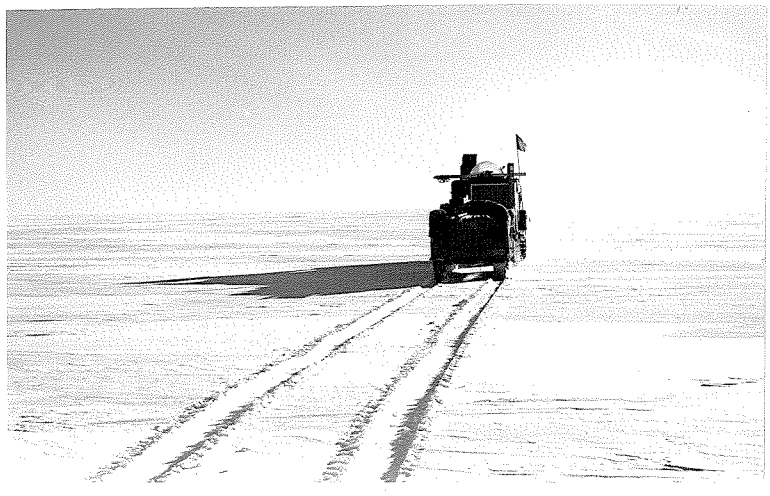

I

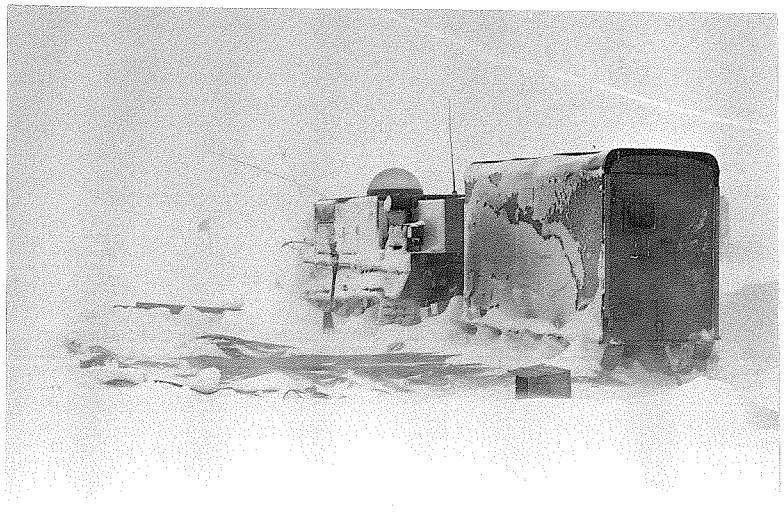

II

FRONTISPIECE

THE GREENLAND ICE SHEET

I. On the trail during a clear day with a smooth and firm snow surface.

II. Station 2-50, 4 August 1953, during a 3-day blizzard. The pit, lying to the left of the wannigan, is covered by a tarpaulin supported by a framework of timbers. Glaciological measurements were made in covered pits during storms with but minor interruption of schedule (Fig. 4g). The ability to navigate and work regardless of weather was essential, especially in planning and keeping up to the 1955 time table.

PREFACE

This thesis presents the results of 19 months of field work in Greenland during 1952, 1953, 1954, and 1955 while the writer was a staff member of the Snow Ice and Permafrost Research Establishment (SIPRE); it will be published by SIPRE as Research Paper 70.

A primary question about ice masses of the world today concerns their material balance, i.e., are they in balance with present-day climate or not? In order to answer this question it is necessary to know current rates of accumulation and ablation. A major part of this study is the determination of the amount and distribution of accumulation on the Greenland ice sheet. But the basic purpose has been to extend our knowledge of the overall physical environment of the ice sheet--the accumulation picture is only a part of this. Improvement in our knowledge of the Greenland ice sheet contributes to understanding the nature of ice sheets in general, including extinct ones of the Pleistocene.

During the course of 4 years field work in northwest and central Greenland I have become indebted to many individuals and several organizations. Without the aid of men of the North Atlantic Constructors (NAC) it would have been very difficult to outfit the expeditions. Especially in 1955, Mr. Wm. E. Perkins contributed generously of his time and opened NAC shops to us when "official channels" were jammed. The Transportation Arctic Group, Northeast Air Command and First Engineer Arctic Task Force provided the bulk of logistic support from Thule, Greenland. The 6614th Air Transport Group carried out 4 perfect air drops to the 1955 expedition. These were free-drops (i.e., without parachutes) with aircraft flying within 20 feet of the snow surface, during each free-drop pass, at altitudes on the ice sheet exceeding 10,000 ft above sea level. From the receiving end the drops were 100% successful and beautiful to watch. Grateful acknowledgment is extended to the men and officers of these organizations.

Special acknowledgment is due to Mr. J. Peter Johnson (now at St. Lawrence University, Canton, N. Y.), the writer's co-worker throughout the 140 day field season of 1953.

Invaluable assistance, under extreme environmental conditions, was rendered by Mr. George R. Toney (U. S. Weather Bureau) and Mr. Stephen W. Miller (Stanford Research Institute) in 1953, and by Mr. Dale Beranek (Trans Arctic Group) in 1954.

Mr. James A. Bender and Mr. Richard H. Ragle (both of SIPRE) were assistant party leaders during the first and second halves, respectively, of the 1954 field season. Without their aid the work would have been more difficult, less enjoyable, and far less productive. Mr. Ragle also provided valuable assistance in preparation of glaciological and altimetry data from the 1954 season and was assistant party leader in 1955. Ragle was an indispensable man in 1955; he designed and built the gyro-navigation system (based on a surplus aircraft, vacuum-type gyroscope),

and in Thule he played the major role in constructing our two wannigans, from runners up, largely from material drawn from the dunnage heaps. These details, so often overlooked in planning or in final acknowledgments, are the difference between results or excuses at the close of the operation.

Special thanks go to Mr. B. W. Gardner, Jr., Associate Chief, Animal Products Division of the Quartermaster Food and Container Institute, for providing the 1955 expedition with 1500 lbs of light-weight test-items of frozen and dehydrated foods. This contribution made it possible to operate at 4.7 lb food-cargo per man day as opposed to 10 lb per man day which is standard for Army sled trains; thus, it increased our range of travel and permitted greater independence from time consuming air drops.

Mr. A. N. Brunson of Brunson Instrument Company provided a newly designed Sun Compass for us to test and use in 1955. This sun compass constituted an essential part of our navigation system.

The personnel of the 1955 expedition contributed invaluably to the final success of the operation. Each man was extremely well qualified in his specialty and assisted in the routine work which is so abundant on a small mobile group. Grateful appreciation is extended to: Robert W. Christie, M. D. (expedition physician), James B. Holston, B. A. (expedition radioman), Richard H. Ragle, M. S. (glaciologist and assistant leader of the expedition), Alan C. Skinrood, M. S. (Mechanical Engineer--expedition mechanic), and George Wallerstein, Ph. D. (Astrophysicist--expedition navigator).

I take this opportunity to express my sincere gratitude to Dr. Henri Bader, Chief Scientist of SIPRE, for granting me complete freedom in planning and complete support in carrying out this study. The support has varied all the way from allowing modifications of vehicles for the specific purpose of a glaciological expedition to defraying expenses of drafting and photography in the thesis.

I gratefully acknowledge discussions with Mr. Don L. Anderson and Drs. W. Barclay Kamb and Robert P. Sharp of the California Institute of Technology. In particular, the discussions with Mr. Anderson on densification of snow were very helpful. Special thanks are due to Professor Sharp for his sustained interest and encouragement and for reading and criticizing the manuscript in its several stages.

Mr. and Mrs. John T. Crowell opened their home in Thule, Greenland to extend warm and friendly hospitality in 1952 and 1953 which I shall never forget.

Finally, the acknowledgments would be grossly incomplete without mention of my wife Ruth Gronlid Benson. I am everlastingly grateful for her patience, encouragement, and understanding during this nearly eight year affair with the Greenland ice sheet. In particular, her reams of letters during 24 long months of separation were indispensable.

ABSTRACT

The Greenland ice sheet is treated as a monomineralic rock formation, primarily metamorphic, but with a sedimentary veneer of snow and firn. This sedimentary member is perennial above the firn line, and the classical methods of stratigraphy and sedimentation can be profitably applied to it.

During a 4-year period 146 pit studies and 288 supplementary Rammsonde profiles were made along 1100 miles of over-snow traverse (Fig. 1). Temperature, density, ram hardness, and grain size were measured in the strata exposed in each pit.

Stratification of snow results from variations in the conditions of deposition and is emphasized by subsequent diagenesis. Summer layers are coarser-grained and have generally lower density and hardness values than winter layers; they may also show evidence of surface melt. The onset of fall is usually identified by an abrupt increase in density and hardness accompanied by a decrease in grain size. This stratigraphic discontinuity is used as the annual reference plane.

Strata in the upper 10 to 20 meters compose a succession of annual sequences which are preserved in recognizable form for at least several decades. Correlation of annual layers between pits, spaced 10 to 25 miles apart along the traverse of Figure 1, gives a picture of annual accumulation during the past 5 to 20 years for western Greenland between 69 and 77°N. The control established by these data, together with information from earlier expeditions (primarily those of Koch-Wegener and DeQuervain) and from permanent coastal meteorological stations, have been used to make a map showing the distribution of gross annual accumulation, essentially the equivalent of annual precipitation, for the entire ice sheet (Fig. 30). In general, the accumulation contours follow the north-south trend of the coast lines, with extremes of less than 10 cm H_2O in the northeast and more than 90 cm H_2O per year in the south; the average for the ice sheet is 34 cm H_2O per year. The zone of maximum precipitation lies close to the coast in two regions, one on the east coast between Angmagssalik and Scoresbysund, the other on the west coast between Upernavik and Thule.

In addition to the existence of a useful stratigraphic record four diagenetic facies are recognized on the ice sheet.

(1) The ablation facies extends from the outer edge, or terminus, of the glacier to the firn line. The firn line is the highest elevation to which the annual snow cover recedes during the melt season.

(2) The soaked facies becomes wet throughout during the melting season and extends from the firn line to the saturation line, i.e., the uppermost limit of complete wetting. The saturation line is the highest altitude at which the 0°C isothermal surface penetrates to the melt surface of the previous summer.

(3) The percolation facies is subjected to localized percolation of melt water from the surface without becoming wet throughout. Percolation can occur in snow and firn of sub-freezing temperatures with only the pipe-like percolation channels being at the melting point. A network of ice glands, lenses, and layers forms when refreezing occurs. This facies extends from the saturation line to the upper limit of surface melting, the dry-snow line. Negligible soaking and percolation occur above the dry-snow line.

(4) The dry-snow facies includes all of the glacier lying above the dry-snow line, and negligible melting occurs in it.

The saturation line can be identified by discontinuities in temperature, density, and ram hardness data, and it may also be located by examination of melt evidence in strata exposed on pit walls. It is as sharply defined as the firn line; but the dry-snow line, although determined by the same methods, is an ill-defined transition zone 10- to 20-miles wide.

The facies represent a response to climate, therefore changes in the location of facies boundaries may be used as indicators of secular climatic change. Since facies are not restricted to the Greenland ice sheet, they provide the basis for a general classification of glaciers. This "facies classification" is areal in nature and gives a greater resolution of characteristics than Ahlmann's "geophysical classification." In particular, the "facies classification" permits subdividion of large glaciers which span the entire range of environments from temperate to polar. Ahlmann's useful distinction between temperate and polar glaciers takes on new meaning in the light of glacier facies. Thus, a temperate glacier exhibits only the two facies below the saturation line whereas one or both of the facies above the saturation line are present on polar glaciers. An attempt has been made to map the distribution of facies on the Greenland ice sheet (Fig. 48).

The distribution of mean annual temperature on the ice sheet may be approximated by gradients with respect to altitude and latitude of $1^{\circ}C/100$ m and $1^{\circ}C$ per degree latitude respectively. The altitude gradient is controlled by strong outgoing radiation, producing deep inversions and katabatic winds. The katabatic winds are warmed adiabatically as they descend along the surface of the ice sheet, and this is the primary control determining the temperature gradient along the snow surface. The latitude gradient is based on temperature measurements made above 2000 m on the ice sheet, and on average values from meteorological stations spanning 20° of latitude on the west coast. A contour map of isotherms based on these gradients compares well with temperature values obtained from pits on the ice sheet (Fig. 40).

The densification of snow and firn is discussed for the case where melting is negligible. The assumption is that accumulation remains constant at a given location and, under this assumption, the depth-density curve is invariant with time as stated by Sorge's law. As a layer is

buried it moves through a pressure gradient under steady-state conditions, and it is assumed that the decrease in pore space with increasing load is simply proportional to the pore space, i.e.,

$$\frac{dv}{d\sigma} = -m(v - v_i) \tag{8}$$

where

$v = \frac{1}{\rho}$ = specific volume of firn (ρ = firn density),

v_i = specific volume of ice = 1.09 cm^3/g,

$\sigma = \int_0^z \rho \, dz$ = load at depth z below the snow surface

and

m = a constant which depends on the mechanism of densification.

The depth-density equation obtained from equation 8 is

$$z = \frac{1}{m\rho_i}[K - (\epsilon + \ln \epsilon)] \tag{14}$$

where

$K = \epsilon_o + \ln \epsilon_o$,

$\epsilon = \frac{\rho_i - \rho}{\rho}$ = void ratio for snow of density ρ, and

$\epsilon_o = \frac{\rho_i - \rho_o}{\rho_o}$ = void ratio for snow of density ρ_o,

ρ_o = density of snow when $\sigma = 0$.

The consequences of the assumption in equation 8 compare favorably with observation. A fundamental change in the mechanism of densification is recognized within 10 m of the snow surface. The concept of a "critical density" is introduced. Before the density of snow attains the critical value it is compacted primarily by packing of the grains. The critical density represents the maximum value obtainable by packing and further compaction must proceed by other mechanisms. The rate of change of volume with increasing load decreases by a factor of 4 when the critical density is exceeded. The same equations hold in the case where melt is not negligible but the rates of densification are higher.

Bauer's (1955) estimate for the balance of the ice sheet is revised. Two corrections are applied: (1) the average annual accumulation value of 31 cm H_2O originally estimated by Loewe (1936) is revised to 34 cm H_2O as a result of this study; (2) the relative areas of ablation and accumulation zones in Greenland north of 76°N are more accurately defined. The net result is a slightly positive balance which is interpreted to mean that the Greenland ice sheet is essentially in equilibrium with present day climate.

TABLE OF CONTENTS

PAGE

PAGE

APPENDICES

LIST OF TABLES

LIST OF FIGURES

CHAPTER I

INTRODUCTION

The primary objective of this study is to demonstrate that the methods of stratigraphy and sedimentation can be successfully applied to the study of snow and firn. Such stratigraphic investigations differ from those of other rock formations primarily in technique. The parameters used in interpretation consist of measured variations in density, hardness, grain size, and (when present) observations of melt and wind evidence. This approach has proved fruitful in determining the prevailing climatological conditions on the Greenland ice sheet.

The term "ice sheet" is defined in Ahlmann's (1948) classification of glaciers, which is summarized with special reference to the Greenland Ice Sheet in Appendix I. The emphasis on the stratigraphic nature of the ice sheet in this study has le͡d to a more quantitative classification of glaciers than has been possible before.

Determination of annual accumulation, one of the most important results obtained from snow stratigraphy on the ice sheet, depends on the ability to identify annual units in the strata. In Sorge's (1933, 1935) classical study he found that annual units could be identified at Eismitte (Fig. 1) by measuring firn density, winter layers were slightly denser than summer layers. Fortunately, Eismitte was located where annual units are thick (about 1 meter)

and where density differences between summer and winter strata are pronounced. Sorge's research program, done at a single station, did not include correlation of several year's strata on a regional scale.

Koch and Wegener (1930) correlated the "Jungschneedecke" across Greenland during the summer of 1913 (Fig. 1). Their "Jungschneedecke" consisted of a layer of fine grained snow and firn which was underlain by a coarse grained low-density layer. They assumed that the Jungschneedecke represented the accumulation since fall of 1912. Theirs is the best recorded example of stratigraphic correlation in snow of the Greenland ice sheet.

In the present study the Greenland ice sheet has been treated as a monomineralic rock formation,* primarily metamorphic, but with a sedimentary veneer. In terms of areal exposure, this is the most extensive formation in Greenland, covering 1,726,400 km^2 (675,000 mi^2) or about 80% of the total surface area (including islands). The metamorphic member consists of glacier ice which has been metamorphosed through flowage caused by unbalanced stresses. Herein, attention is confined to the sedimentary member which is perennial above the firn line, has a maximum thickness of

---

*The term "Greenland ice sheet" is a suitable formation name without addition of the "formation." This is convenient because it does not entail new terminology. The Greenland ice sheet is often referred to as the "Greenland ice cap" or "inland ice."

about 90 meters, and consists of snow and firn.

The sedimentary member of the Greenland ice sheet is especially important because of its intimate relationship with climate. The annual climatic cycle produces recognizable annual sequences of strata, and the interpretation and correlation of these units forms an important part of this study. It is important to note that measurement of water equivalent of annual layers on the ice sheet is the only satisfactory method of determining the amount of precipitation in Greenland. Precipitation gages at meteorological stations along the coast are strongly influenced by local conditions of exposure, and give readings which are invariably too low and only for a single point location. In contrast to this situation the ice sheet is an infinite set of automatically recording precipitation gages. It is only necessary for one to learn how to read the records.

Correlation of annual stratigraphic units from the edge of the ice sheet to the high-altitude, interior regions led to the development of the concept of diagenetic facies on glaciers. In 1952, regional differences were recognized in physical properties of the upper snow layers which were clearly related to the decrease in temperature with altitude. However, the 1952 data were not sufficient to permit recognition of the facies (nor, for that matter could detailed correlation be done between all of the 7 pits which were spaced about 50 miles apart). Subsequent field

work has clarified the picture and the combined results from 1952, 1953, and 1954 (Benson, 1959) permitted interpretation and correlation of 17 years of snow and firn strata and established the concept of diagenetic facies on the ice sheet.

Essentially the research has taken on two main aspects: first, the recognition of annual stratigraphic units, involving detailed analysis at each station; and second, the comparison of gross variations in properties between facies. Both aspects of the study combine in defining a quantitative classification of glaciers based on the existence of facies on the ice sheet.

Sedimentation on the ice sheet may be compared with underwater transportation and deposition in a basin. On the ice sheet there is a "dome or highland of deposition" rather than a basin. Masses of air transport a load of water vapor which condenses, crystallizes, and is precipitated as the air cools on ascending the slope of the ice sheet. After, or during, a snowfall, winds transport snow grains by saltation and in suspension along the surface. To some extent this smooths local irregularities in the original distribution of the snow. At this point, the blowing and drifting snow is an aeolian sediment and surface features of wind erosion and deposition, such as sastrugi, barchans, and ripple marks are observed (Fig. 7).

Post-depositional, i.e., diagenetic, changes transform the snow into firn. The diagenetic environment extends downward for an unspecified depth, but includes most of the sedimentary member. The firn layers record specific meteorological conditions or events, such as warm spells which produce various degrees of melting, and windstorms or blizzards which produce hard wind slabs. In general, meteorology, sedimentation, and diagenesis are so closely inter-related on the ice sheet, that the stratigraphy provides a climatic record.

Presentation of the data, gathered over a four-year period, from 434 test sites, along 1100 miles of traverse, posed a problem which has been partially solved by assembling the data from 79 representative pit stations on 10 data sheets (in a pocket at the end of this thesis). The data sheets comprise the "spinal column" of this work; however, to avoid constant reference to them, special points have been abstracted into figures throughout the text. This approach has necessitated some redrafting but the writer hopes it has made the results of this study more accessible to the reader.

---

*The term "metamorphism" was used by Bader et al. (1939) to describe the phenomena called "diagenesis" in the present paper. According to accepted usage, it is preferable to refer to post-depositional changes in sedimentary layers as "diagenetic changes." Metamorphic processes occur in glacier ice of the metamorphic member of the Greenland ice sheet and will not be considered in this paper.

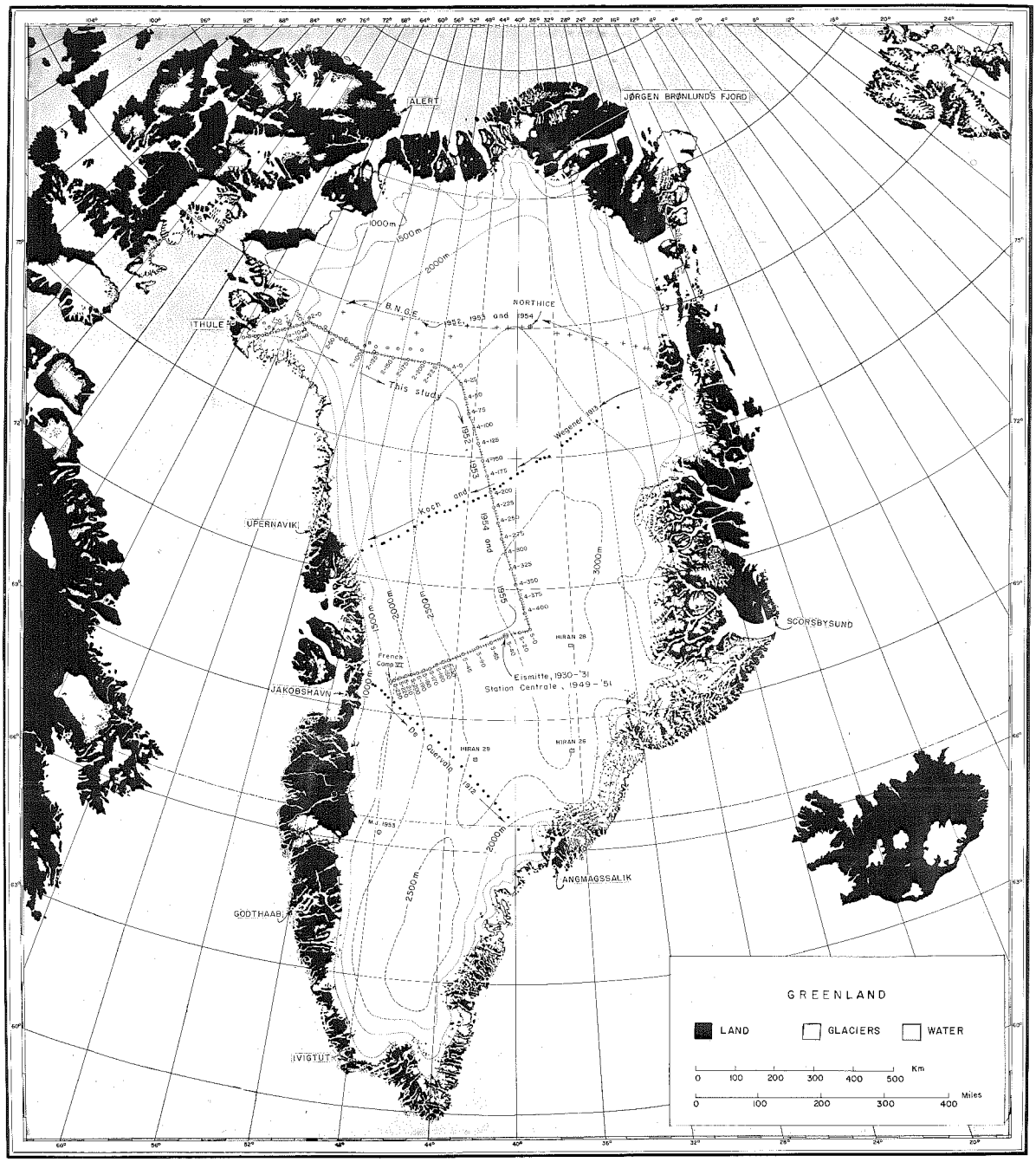

Figure 1.--Location of traverses. Circled points along the traverse of this study represent pit stations, the tick marks represent Rammsonde stations. See Figure 2 (in pocket) for a detailed map of the stations in northwest Greenland. The other traverses shown are referred to in the bibliography as: De Quervain and Mercanton (1925), Koch and Wegener (1930), and Bull (1958; British North Greenland Expedition, B.N.G.E.). the HIRAN Stations were part of a U. S. Air Force project in 1956. The location of Project Mint Julep (Schuster, 1954) is indicated by the point labeled M. J. 1953.

CHAPTER II

METHODS OF INVESTIGATION

Region of Investigation

The overall region of investigation is shown in Figure 1. Pit stations are indicated by circled points, and the tick-marks indicate ram hardness tests. During 1952, 1953, and 1954 the work was confined to northwestern Greenland between Thule and Station 4-0 (Fig. 2). The density of stations is greatest in this area and one or more pit studies were made during each year of the project at many of the stations. The major objective during the first three years was a detailed study of the strata deposited between 1937 and 1954 (Benson, 1959). During 1955, stratigraphic control was extended, along the traverse shown in Figure 1, and the combined results of the four field seasons are presented herein.

The peninsular region on the west coast of Greenland between 76 and 79°N enters the discussion several times and it is convenient to introduce the following terminology:

(a) Thule Peninsula lies between Melville and Ingelfield Bays, and produces a ridge on the ice sheet which is well defined for over 150 miles.

(b) Ingelfield Peninsula lies between Ingelfield Bay and the Kane Basin, it also produces a well defined ridge on the ice sheet.

The ridge crests of Thule and Ingelfield peninsulas meet at about 52°W (Figs. 1 and 2).

The entire traverse, shown in Figures 1 and 2, is subdivided into seven trail segments. These are labeled with numbers as follows: 00, 0, 1, 1a, 2, 4, and 5. Any point on the traverse may be located by two numbers: the first refers to one of the trail-segments, the second to the number of miles along the trail-segment from its origin. A total of 434 test sites were occupied (146 pit studies, and 288 Rammsonde profiles measured at points between pit stations), each test site is located by two numbers as described above.

Two points of access to the ice sheet were used. One was camp "NUTO" on Nuntarssuaq, the other was camp "TUTO" located 12 miles from Thule Air Base. The trails from these origin points converge at Station 1-0. Station 1-0 is known as "Station Morris" and was called "point Alpha" prior to May 1955. Stations along the trail from TUTO to Morris are numbered "0-n," where n has any value from 0 to 60. Stations between NUTO and Morris are numbered "00-n," where n has any value between 0 and 30.

The trail between 1-0 and 2-0 is 60 miles long and has remained constant during the four years considered here. It is labeled "segment 1." The 20 mile trail labeled "1a" originating at Station 1-50 was covered in 1955 only.

The trail between 2-0 and 4-0 (segment "2") is 250 miles long and has varied slightly in detail as shown in

Figure 2. Work extended to 2-125 in 1952, to 2-200 in 1953, to 2-100 in 1954 and to 2-250 (i.e., 4-0) in 1955.

The north-south segment is labeled 4 and the southern east-west segment is number 5. There is no trail segment number 3.

Operations and Logistics

Operational and logistical problems have been both cumbersome and complex. It is beyond the scope of this thesis to discuss the details. A full treatment of this part of the program is in preparation and some aspects of it have been described (Benson 1955b, 1955c; Benson and Ragle, 1956). Only the order of magnitude and general nature of the problem will be stated here.

The total one-way length of traverse was 1,100 miles (Fig. 1), but the total vehicle mileage recorded, during the four field seasons, was 12,860. Weasels (M29c Cargo Carriers), modified for arctic use, together with cargo sleds and wannigans (built by the members of the expeditions), provided transportation and living quarters (see Frontispiece). Resupply in the field was provided by aircraft based at Thule and Sondrestromfjord Air Bases. The major logistic burdens of fuel, food, trail markers, and technical equipment, exceeded 100,000 lbs of cargo. Most of this was free-dropped (i.e., without parachutes) from low-flying aircraft (about 20 feet above the snow surface).

Pit Studies

Pits 3-6 m deep were dug in areas undisturbed by foot or vehicle traffic (Fig. 3). Extreme care was taken to avoid disturbance of the section exposed on the test wall (Fig. 4). Pits were always covered at night and during stormy or windy days (Fig. 4d and Frontispiece II). Without cover, 4-m pits have been completely filled with drift snow in less than 10 hours. Work can proceed satisfactorily in a covered pit during storms.

Stratigraphic control was extended below the pit floors by core drilling at most stations (Fig. 4f). The 3-in diameter hand auger, developed by the Arctic Construction Laboratory and modified by SIPRE, was used. The maximum length of core obtained, 11 meters, was at Station 2-0 (1954) giving a total depth penetration of 17 m (56 ft) at that station. The depth of core drilling was determined solely by the amount of time available to obtain, describe, cut, measure, and weigh the core samples. A reasonable estimate is 1 hour for each meter of core. The following measurements were made at test stations.

Temperature

A temperature profile was measured at 10-cm intervals on the pit wall with Weston bimetallic thermometers. This was done concurrently with the excavation to avoid significant disturbance of natural thermal conditions. Additional

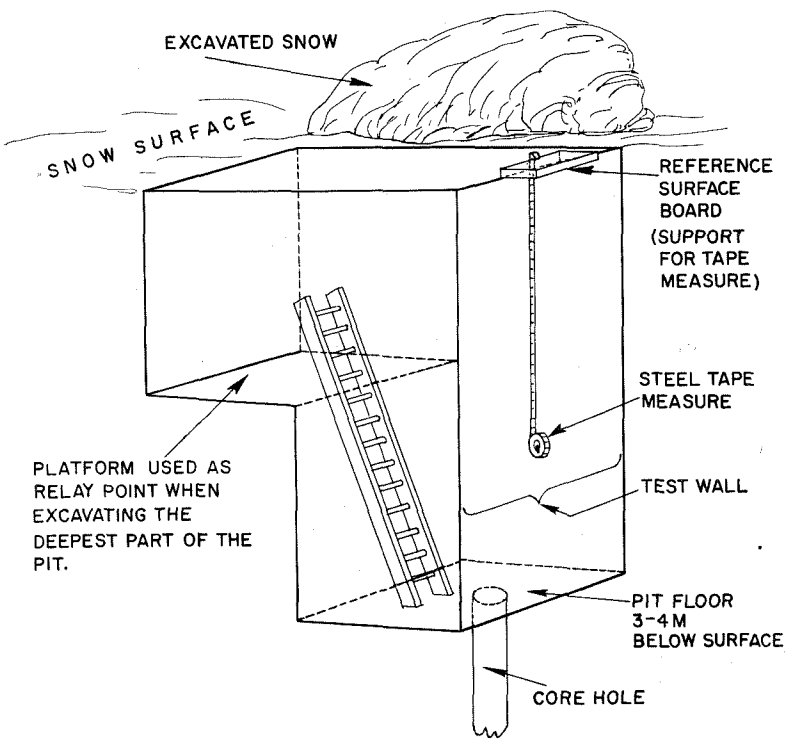

Figure 3.--Sketch of a typical test pit. Pits were dug in places undisturbed by foot or vehicle traffic. Waste snow was not thrown over the test wall and no one walked within several feet of its edge. Test walls, located on the south side to avoid direct sunshine, were made clean and vertical. A board on the snow surface served as a mount for the steel tape measure and also as a radiation shield for thermometers in the snow (see also Figs. 4a and h).

Figure 4a.--Test wall of a pit being brushed to make strata stand out clearly in the upper 6 m where resistance to this "erosion" varies markedly. Note the undisturbed surface at edge of the test wall.

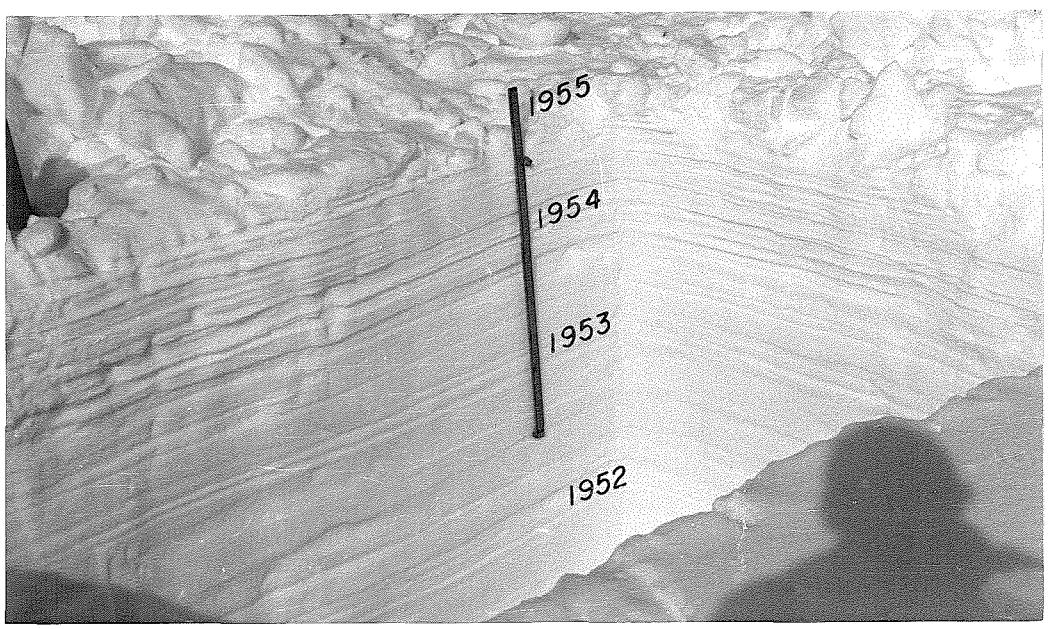

Figure 4b.--Rear walls of a test pit showing individual strata which can be traced around the four walls of the pit. The summer layers of 1952, 1953, 1954 and 1955 are labeled, they are slightly softer than the winter layers.

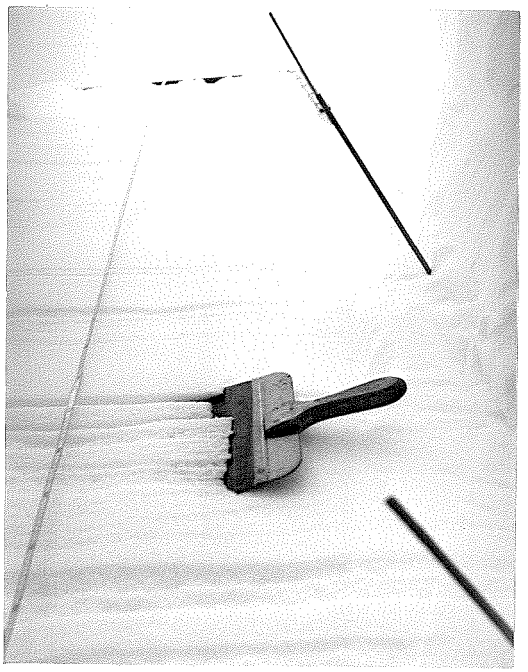

Figure 4c.--Test wall of the pit at Station 2-60 (1954) prepared for sampling.

Figure 4d.--Inserting density sample tubes. A thin metal plate was used to push sample tubes beyond the face of the test wall. This makes the lines seen cutting across the circles on the test wall. Samples were placed in an attempt to get representative measurements for individual layers, but sometimes it is impossible to avoid sampling across layer boundaries. The placement of tubes with respect to a hard layer is shown.

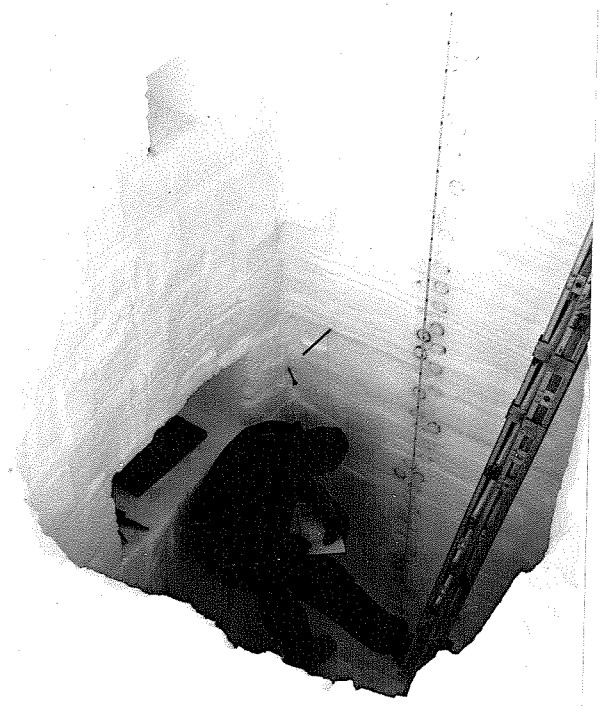

Figure 4e.--When all tubes were placed (70-80) and their locations recorded, a detailed stratigraphic description was made with special attention paid to evidence of melt and wind action. Noteworthy relations between tubes and layer boundaries, especially when boundaries were cut by tubes, were shown by brief sketches.

Figure 4f.--Stratigraphic control was extended below the pit floors by core drilling (see p. 10).

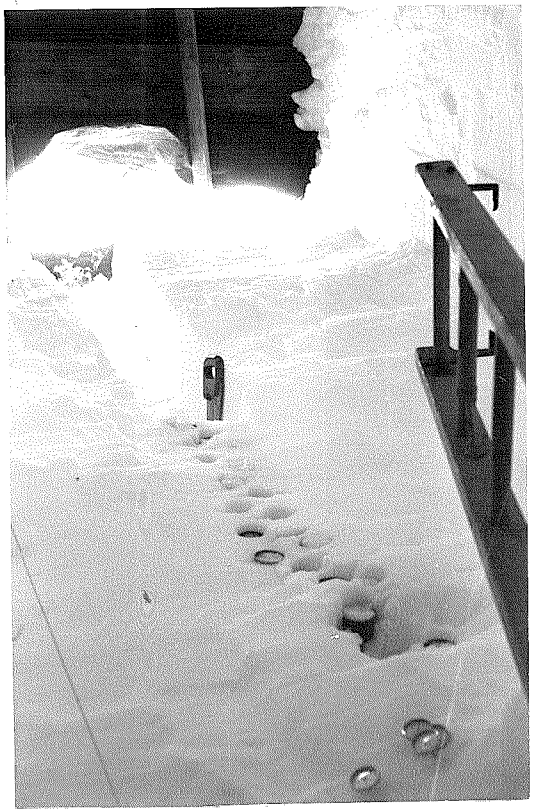

4g

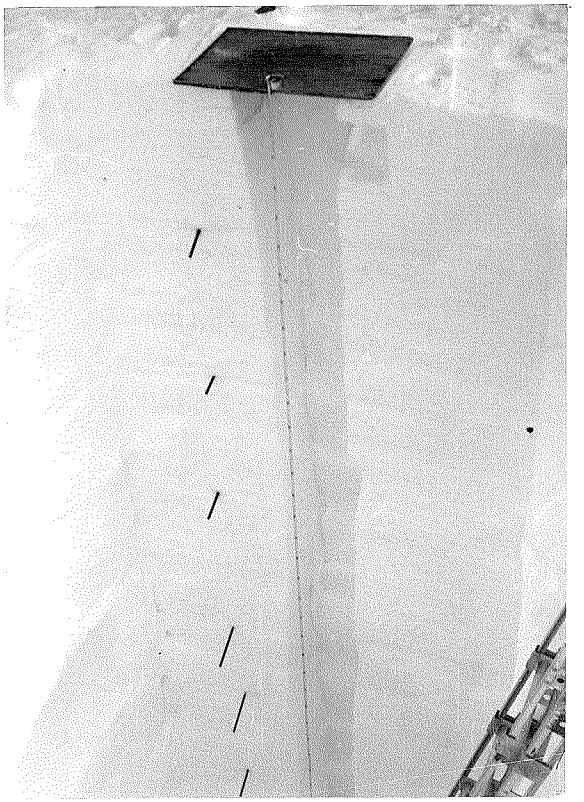

4 h

Figure 4g.--Pit at Station 2-30 (1954), covered because of wind. The right edge of the "slot," left when density tubes are sawed out, is nearly vertical so that a thin slice can be cut from it to prepare photo sections as shown in Figs. 5 and 8.

Figure 4h.--Test wall at Station 4-0 (1955), a thin section has been cut from the left edge of the slot. Dowels are placed in prominent low-density summer layers. The 1951 summer is not marked; it was abnormally cool and produced a minimum discontinuity between summer and winter layers (See data sheets, Fig. 31, and p. 90).

temperature measurements were obtained from the bottom of the core holes. The thermal effect of an open pit on the surrounding snow is indicated in Figure 33 by curves 3 and 3a from Station 2-50. The test pit of 4 August was left open and revisited 17 days later (21 August); it had been completely filled by drifting snow. The snow that filled the pit was at the temperature of the snow surface, and since August is one of the warmer months, heat was added to the surrounding firn.

Hardness

The Rammsonde penetrometer measures the resistance of snow to the penetration of a cone. It was developed by Haefeli (Bader et al., 1939, p. 128-132) and was slightly modified at SIPRE following the 1952 field season. It is used as the standard for hardness measurement in this work. The Rammsonde has a distinct advantage over other hardness-measuring instruments because reliable profiles can be obtained from the surface to a depth of 4 m without digging a pit. Such profiles, obtained at points between pit stations, have proved useful in making stratigraphic correlations from pit to pit.

The Canadian hardness gage was also used in 1952. It did not add to the general stratigraphic picture in proportion to the time required for its proper use, as five measurements for each layer were required to obtain an average value. It is also more subject to operator variance

than the Rammsonde. Comparison of several hardness measuring instruments in south Greenland (Schuster, 1954) supports this conclusion.

Density, stratigraphy, and grain size

The standard SIPRE 500 cm^3 snow-sampling tubes were used for density measurements.

Stratifications in firn, as in other sediments, reflects differences in the environment of deposition and diagenesis. Snow is unlike other sediments in that it does not record variations in the source of supply. Discontinuities between firn layers are often abrupt and stand out clearly when the test-wall is brushed (Fig. 4b). Brushing was done before the tubes were placed, so that sampling across layer boundaries could be avoided as much as possible (Fig. 4a,d). The brushing technique is not useful below 6 m because of increased hardness. The procedure is illustrated in Figures 4a through h.

Characteristics of individual snow and firn layers vary in a manner that affects the accuracy attainable in density measurements. The reproducible accuracy in homogeneous ice-free firn layers varied from $\pm$ 0.003 to $\pm$ 0.005 g/cm^3. Layers affected by melt are more difficult to sample, iced firn being the worst. Accuracy is possibly $\pm$ 0.01 g/cm^3 in such material. Throughout this work the overall accuracy was of the order of $\pm$ 0.005 g/cm^3.

Significant variations in density between firn layers are greater. Changes of 0.02 to 0.03 g/cm^3 are common and abrupt changes of 0.10 g/cm^3 are not rare.

Grain size differences were determined by sieve analyses made on selected layers (Figs. 17, 18). The sieving was done in the pit bottoms where air temperature was below -15°C. Photomicrographs of grains (magnifications of 9, 18 and 27 diameters) were taken as a record (Fig. 19).

Photography

Common practice in geologic field work is to take rock samples to the office or laboratory for subsequent study. The handling of firn in a similar manner is prohibitively expensive and inconvenient. Since photographs of properly brushed pit walls do not always reveal sufficient detail, as is apparent in Figures 4a through h, two techniques were developed to obtain photographic records of stratigraphic features to supplement field notes.

Stratigraphic photo sections ("thin sections"). When the density tubes have been completely removed from the test wall, a slot remains (Figs. 4g and 4h). The walls of this slot were made as smooth and vertical as possible; horizontal cuts through them were avoided. A thin slice 8 to 10-cm thick was sawed from one side of the slot from snow surface to base of the test wall. Such sections have

considerable strength and were carried out of the pits and assembled in proper order on the snow surface even though some layers were loosely bonded. They were trimmed with a saw to a thickness of 1 to 2 cm (Fig. 5a,b) assembled with top at left (observer facing sun), and finally cleaned with a trowel and whiskbroom until nearly uniform in thickness. Dowels were set at 1-m intervals along the final assembly. An overall photograph was made of each "stratigraphic section" (Fig. 5a) followed by a close-up photo of each meter (Fig. 5d).

Strata of high and low density correlate well with dark and light layers respectively on the photos (Fig. 8). However, slight differences in the transmission of light through firn layers cannot be correlated directly with density because factors such as icing, grain size variations, and thickness of the section are also involved. Nevertheless these photos provide a permanent record with a wealth of detail.

Pit wall photography. The above technique is effective on clear days when direct sunlight is available, but it does not work on cloudy days or during "whiteouts." If photo records of stratigraphic features were desired on such days, the technique shown in Figure 6a was used. When bright sunlight is available, the upper meter of the test wall may be photographed after brushing, taking full advantage of shadows (Fig. 6b). Details of deformed

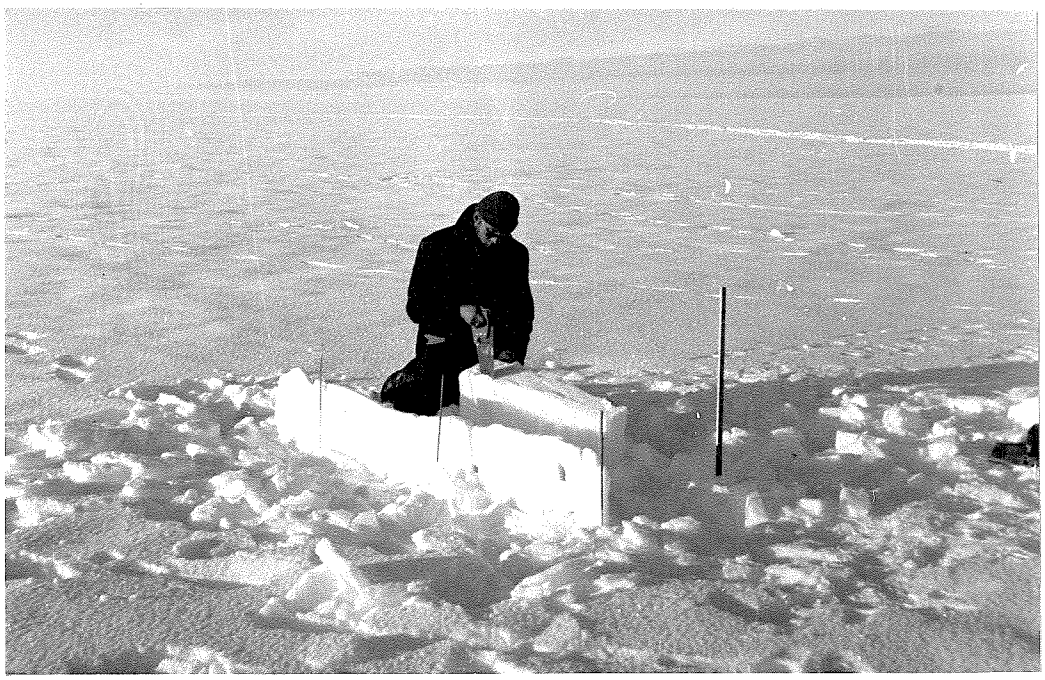

Figure 5a.--Slices, about 10 cm wide, sawed from slots in the test walls (Figs. 4g and h) were carried to the snow surface where thin sections were sawed from them.

Figure 5b.--Thin sections, trimmed with trowel and broom to a final thickness of 1 to 2 cm, are assembled with top at left and ready to be photographed.

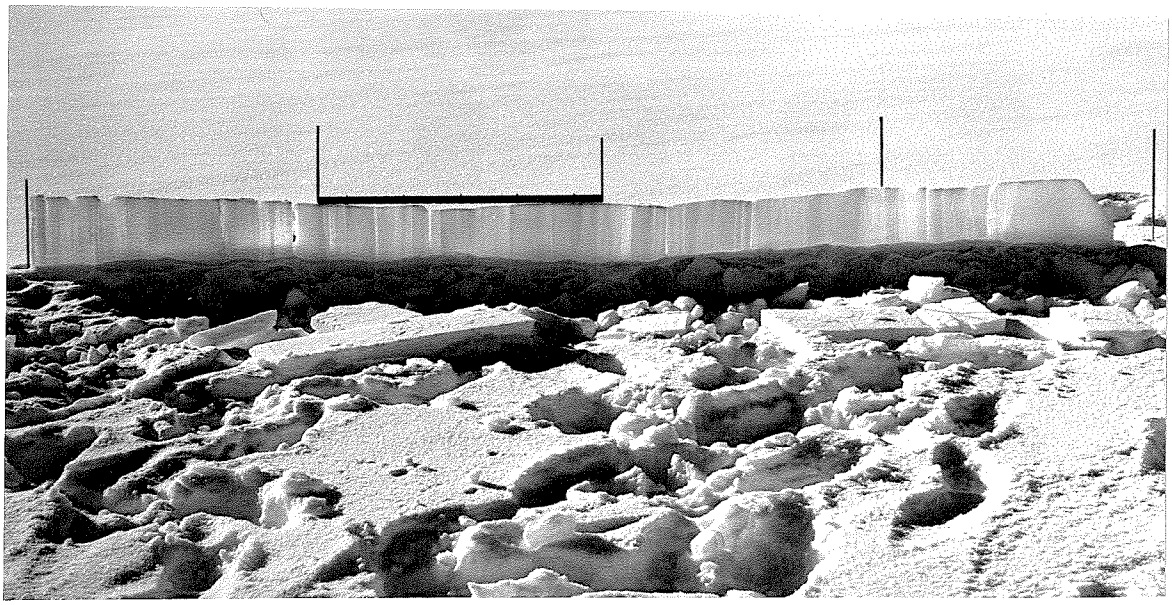

Figure 5c.--Stratigraphic section from top 4 m at Station 2-90 (1954). Dowels indicate 1 meter intervals, top of section is at the left.

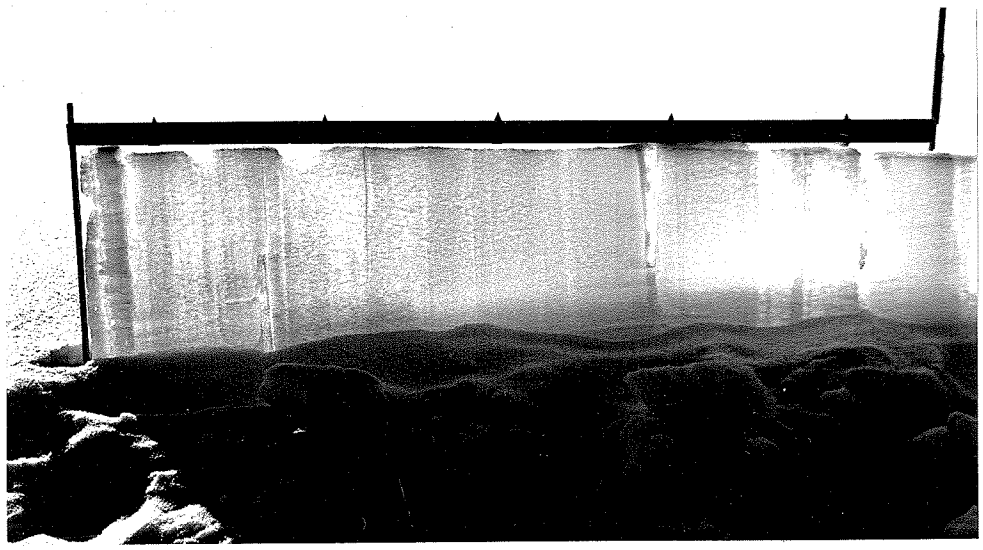

Figure 5d.--Top meter of the section shown in Fig. 5c. Close up photos, such as this, taken of each meter at most stations in 1954 and 1955 serve as detailed supplements to the stratigraphic field notes. Brass clips fastened to the meter stick facilitate measurements on the photos. In these photos the clips are at 10, 30, 50, 70, and 90 cm.

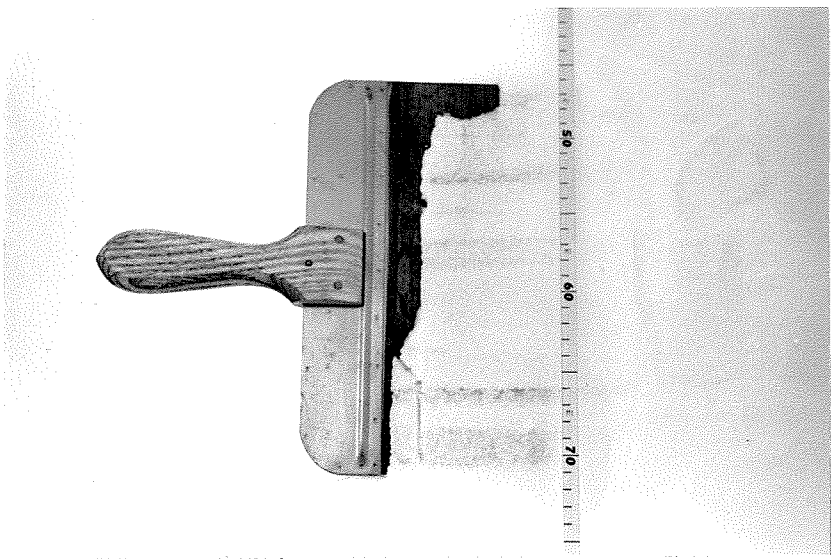

Figure 6a.--Station 2-100 (1953) depth range 140 to 177 cm. Stratigraphic detail photographed by inserting a dark colored trowel behind the pit wall. The trowel, seen through the snow, must be inserted very carefully to avoid breaking the brittle snow.

Figure 6b.--The top 90 cm at Station 1-50 (1954). Photographed by making use of shadows. The 5 cm soft layer overlain by three closely spaced wind crusts at 45 cm was identified at Stations 1-50, 2-0, 2-10, and 2-20, i.e., for 30 miles (see 1954 data sheets).

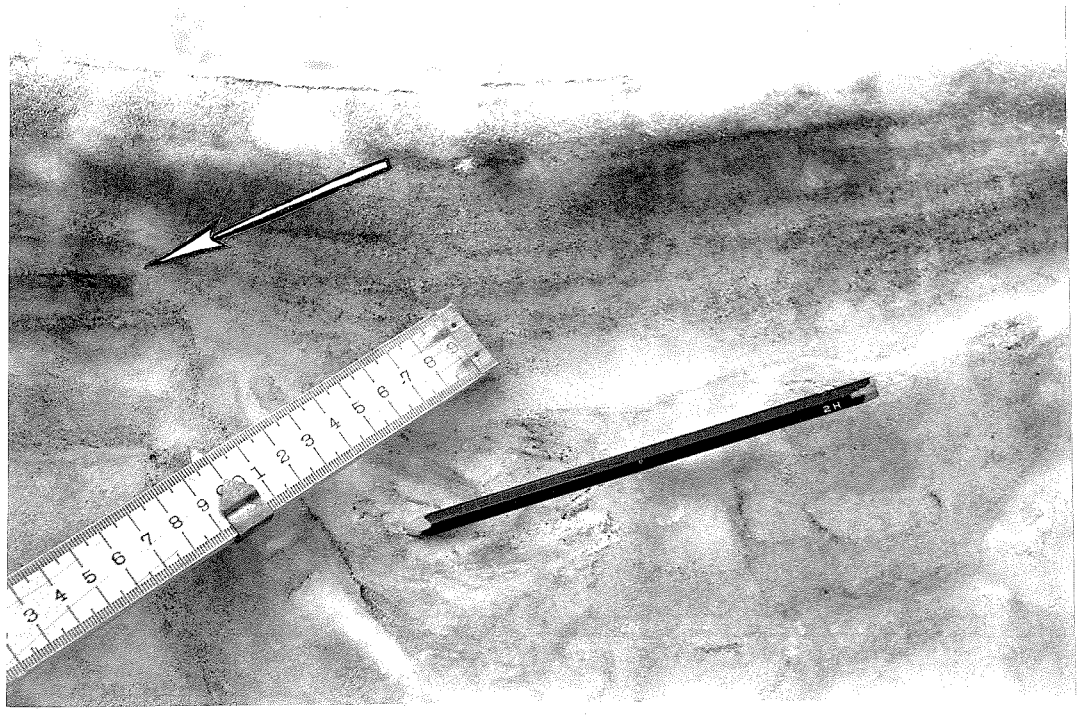

Figure 6c.--Close up of strata exposed at Station 2-30 (1954). The pit wall was exposed to the flame and smoke of a blow torch to make details more photogenic. The buried surface of 2 August 1953 has been broken by a footprint at the point marked by the arrow, unbroken layers have drifted into the footprint.

strata (p. 27) can be made more photogenic by exposing a cleanly-brushed section to the flame and smoke of a blow-torch, because capillary absorption of the moisture so produced differs within the strata (Fig. 6c).

Elevation Measurements

In 1953 two separate records of elevation measurements were kept: one by George Toney of the U. S. Weather Bureau, and one by Robert Zavadil in connection with his gravity studies. Corrections for atmospheric pressure changes were applied from records at Thule and at several stations maintained on the ice sheet during the field season.

In 1954 elevation differences between stations were recorded by a Paulin-system surveying altimeter with readings made at 1-mile intervals. The time scheduled was 1 mile in 10 minutes, thus, the 10-mile moves between stations were completed in 1 hr and 40 min and the number of barometric changes important to the elevation program were reduced. Portions of the trail in 1954 were covered four times and the entire trail was covered twice. The records from 1953 and 1954 agree well with each other (Benson, 1959).

In 1955 the altimetry program was carried on by reading elevation differences between stations as in 1954 with the added improvement of using two altimeters. The

expedition vehicles were split into two groups of two weasels each. One group recorded barometric variations at a pit station while the other group made altimeter readings every mile enroute to the next station. The time schedule required motion of both groups for about 2 of the 5 hours required for the 25-mile move between stations.

CHAPTER III

STRATIGRAPHY AND ACCUMULATION

Introduction

Stratigraphic work in firn consists of identifying variations in a layered sequence, and extending recognizable features laterally by correlation with other measured sections. The objectives are similar to those of stratigraphic studies of other rock formations, but there are obvious differences in technique. Although differences between firn layers are often easy to see or feel, it is necessary to make measurements of density, hardness and grain size in order to express them quantitatively. The walls of hand-excavated pits constitute the "exposed sections." The primary objective is to determine the prevailing environmental conditions on the ice sheet, and the identification of annual units of accumulation is one of the more significant results obtained.

Stratigraphic relations were initially studied by excavating pits each year at selected sites. It was found that individual firn layers maintain their identity as they are buried under the snowfall of succeeding years. Also, it was ascertained that strata could be correlated between adjacent pits across traverses several hundred miles long. Knowledge gained from such studies made it possible to identify annual firn layers in pits dug in

regions not previously visited.

Stratigraphic interpretations were checked by using certain artificially established surfaces. The simplest is the location of buried surfaces disturbed by foot and vehicle traffic (Fig. 6c). Such surfaces are observed by digging special pits at places known to have been previously disturbed by traffic. The 1953 summer surface was marked by spreading soot at certain locations. This works well where melting is slight. Also, dated aluminum tags were fastened 2 m above the snow surface on bamboo poles. In 1954 plywood boards about 30 cm (1 ft) square were placed on the snow surface, located between two poles near each pit station. These boards identify precisely dated snow surfaces.

Markers placed on a pole do not, in themselves, provide valid measurements of accumulation because of snow settling around the pole. Pole-marker measurements have been used only as a supplement in this work, and accumulation measurements are not based on them alone.

Since planes between strata exposed in pit walls represent buried snow surfaces, examination of the snow surface and the processes which operate on it is useful. The area under consideration is primarily a wind blown desert of dry-snow throughout the year. Typical snow surfaces are illustrated in Figures 7a-k.

Data from all stations are assembled on data

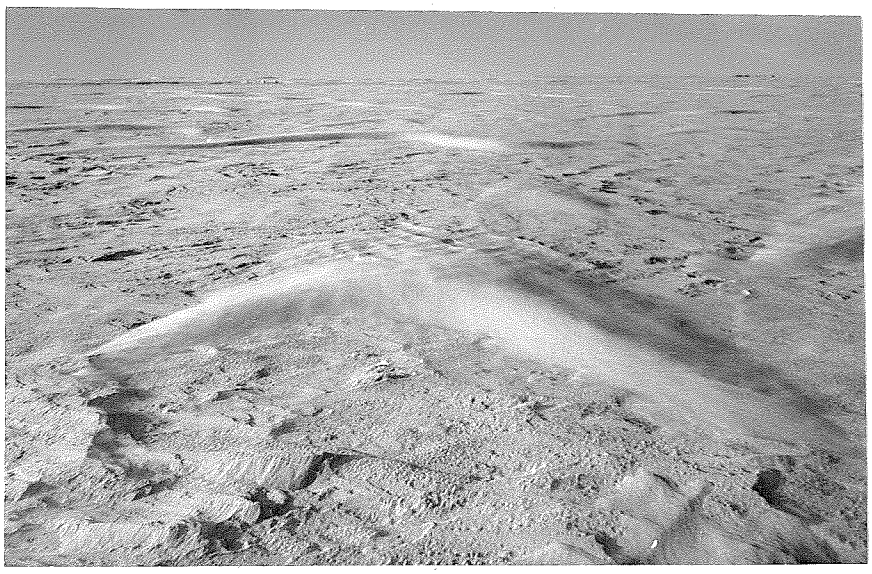

7a

7b

Figures 7a,b.--Snow barchans near Station 2-90, July 1954. In these photos the snow surface is being subjected to wind erosion and deposition. Material picked up from the surface is deposited on the crescent shaped dunes, "barchans." These snow barchans migrate at a rate of about one meter per hour; they are moving toward the camera in Fig. 7a and away from it in Fig. 7b. The foreground of each photo is a typical eroded snow surface.

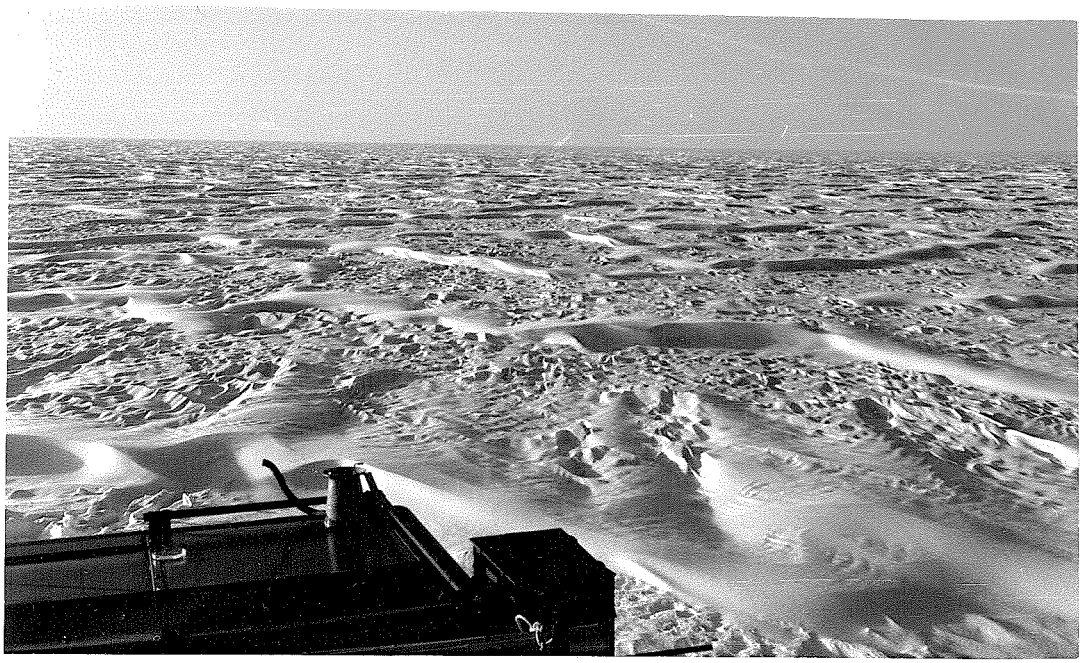

7c

7d

Figures 7c,d.--Snow barchans near Station 1a-20, May 1955. In Fig. 7c the barchans are moving toward the observer, in Fig. 7d they are moving from right to left. Note erosion features in center of 7d.

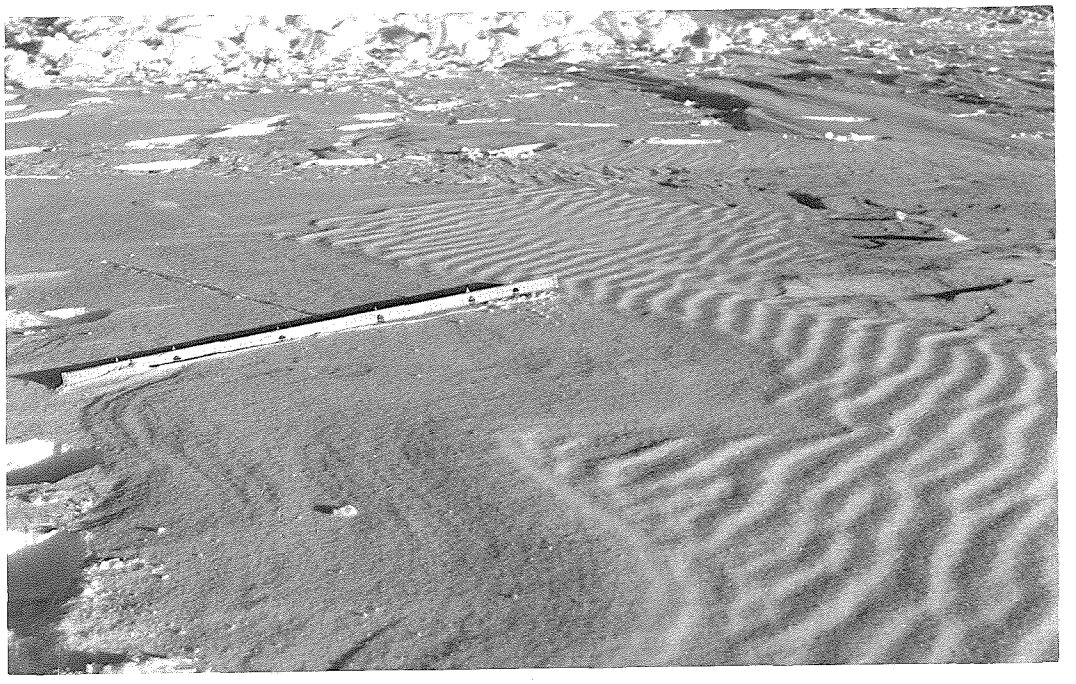

7 e

7 f

Figures 7e,f.--Ripple marks on lee side of smooth areas. Wind movement from left to right in Fig. 7e and from right to left in Fig. 7f. Note erosional features in center of Fig. 7f. Snow surface was so hard in 7f that it was not broken by men on foot (note absence of footprints to and from shovel).

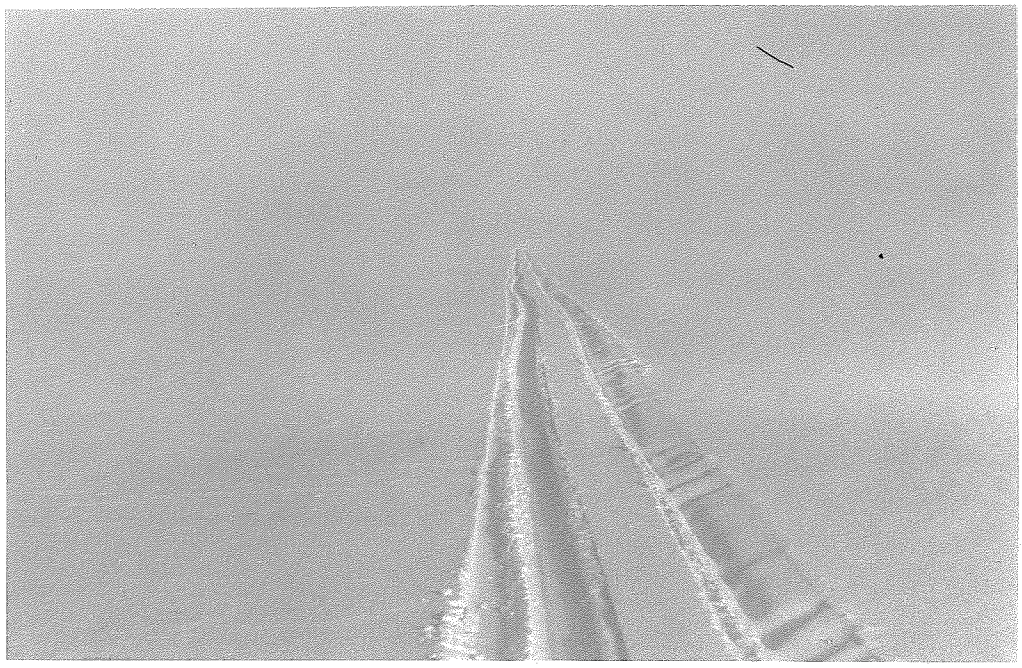

Figure 7g.--Drifting snow moving from right to left across a smooth surface covered by 3 cm of new snow. The drifting is so slight that the right-hand track is nearly filled with snow after 3 hours while the left track is clean.

Figure 7h.--Drifting snow moving from right to left at a more rapid rate than in Fig. 7g. Surface erosion is taking place and barchans are beginning to form.

Figure 7i.--Blowing snow at the tail end of a severe blizzard (gusts over 70 mph). The camp of four weasels is shown after 12 hours at Station 00-20, 12 June 1954.

Figure 7j.--Snow drift formed between 02:00 and 14:00 at Station 00-20 on 12 June 1954. The tracks which go under the drift were made 12 hours before this photo was taken.

Figure 7k.--Sastrugi at Station 2-0, 4 September 1952. Sastrugi are erosion-deposition features formed by wind. They are often very hard (Fig. 20) and have caused serious damage to vehicles and sleds. The surface shown here is typical of that present between Stations 1-30 and 2-30 following the blizzard of 2 September 1952 (see pages 64 and 65 and Fig. 20).

sheets* and included in a pocket at the end of this thesis. The location of each data sheet is indicated in Figure 55. In the text the data sheets will be referred to by the numbers assigned in Figure 55.

An example of the correlation between pit data and the mosaic of thin-section photos is illustrated in Figure 8. The reason for drawing sharp boundaries between firn layers in the stratigraphic column and in the density profile is clear from the photo mosaic in this figure.

Diagenesis without Melt

Diagenetic changes in snow and firn are accelerated at higher temperatures. This behavior is related to poorly known details of atomic structure in the surface layers of ice and how this structure is influenced by temperature. Two related phenomena easily observed within 15 degrees of the melting point are; (1) an increase in vapor pressure with temperature, especially above -10°C,** and (2) the

---

*The format of the data sheets is explained in Appendix III.

**See Bader, et al. (1939), p. 9, for a useful P-T diagram of the ice-water-vapor system. The following values are listed for convenient reference:

Temperature (°C)	Vapor pressure of ice (mm Hg)
0	4.58
-5	3.30
-10	1.97
-15	1.26
-20	0.79
-25	0.48

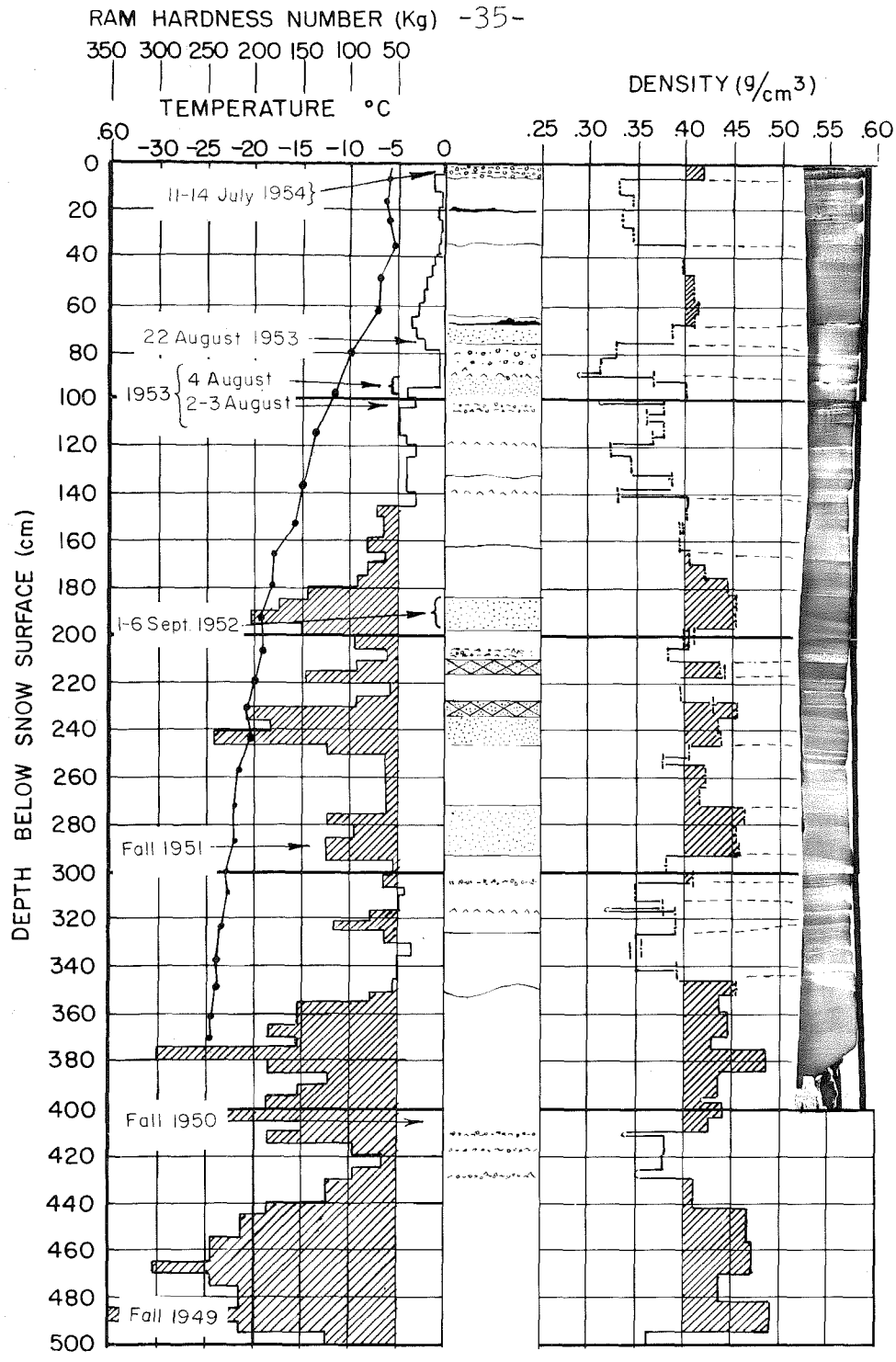

Figure 8.--Stratigraphic data and photo section for Station 2-90, 20 July 1954. The usefulness of stratigraphic photo sections as a supplement to descriptive notes is clear in this figure. Strata of high and low density generally correlate with dark and light strata respectively on the photos (See pages 19 and 34). Layer boundaries are usually well defined although not always horizontal. The wavy layers near 350 cm depth probably represent a buried snow surface similar to the ones shown in Figures 7a, b, c, d, and k.

presence of a liquid-like film on ice surfaces, evidence of which is greatest within five degrees of the melting point and nearly absent below -15°C (Weyl, 1951; Nakaya and Matsumoto, 1953).

In firn strata these phenomena give rise to vapor transfer and sublimation, together with migration of near surface molecules; the net results are changes in grain size and shape, and in the bonds between grains. Such changes are most pronounced in newly-fallen snow and in layers of very fine-grained firn, because they have maximum surface area per unit mass (Bader, et al., 1939; deQuervain, 1945).

Diagenesis with Melt

The extent of summer melting varies greatly over the traverse, and the following concepts are useful:

Soaking

When a given mass of snow is at 0°C and wet throughout, it is said to be "water-saturated" or "soaked." When soaked firn refreezes it becomes "iced firn." Iced firn layers in the stratigraphic section indicate melt which occurred on the snow surface (Fig. 9).

The following definition is useful: If the snow at a particular location becomes soaked down to the level which had been soaked during the previous summer, then that location is subject to complete soaking.

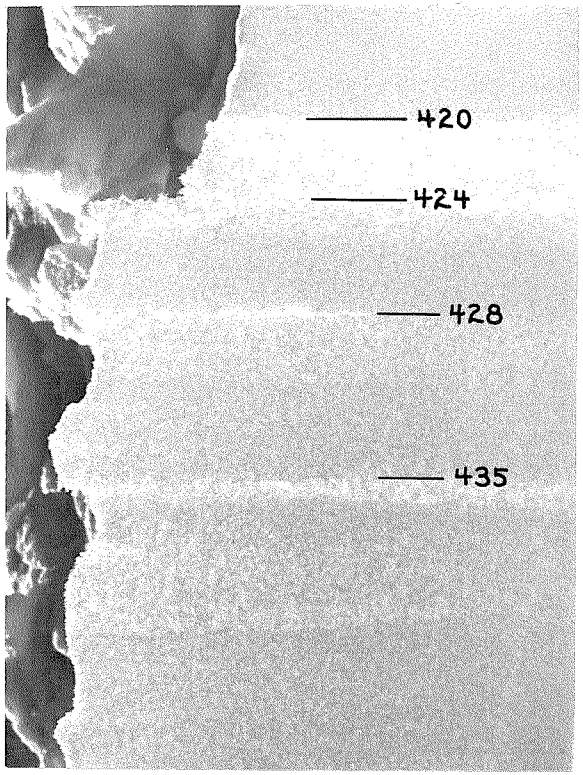

9 a

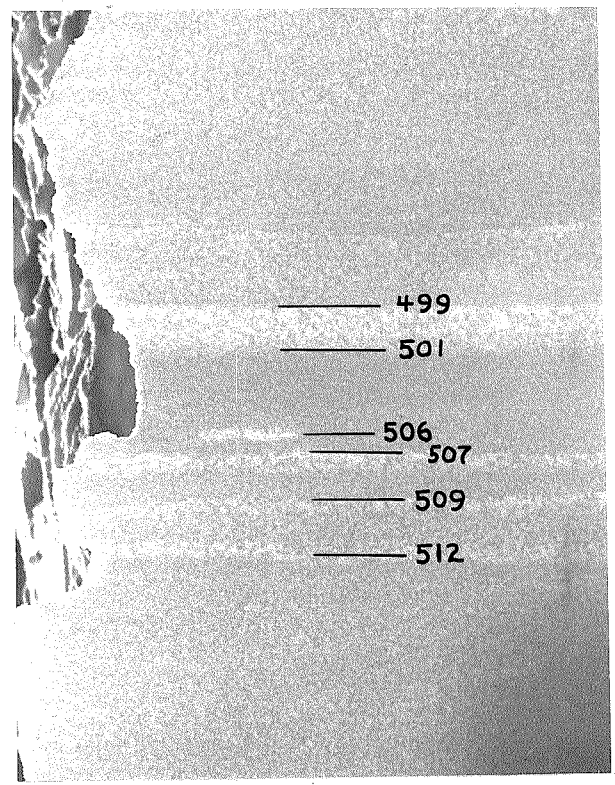

9 b

Figure 9. Layers of Iced Firn at Station 2-100, 1953

Figure 9a.--Detail of the iced-firn layer of 1949 at 420 to 424 cm. The small ice lens at 428 cm was formed by percolation (Fig. 10). The thin layer of coarse bonded grains at 435 cm resulted from an earlier period of surface soaking during the same year.

Figure 9b.--Detail of the 1948 summer melt layers. The iced firn between 499 and 501 cm resulted from the warmest period of the 1948 summer. The small ice lens at 506 cm resulted from percolation. Other melt crusts are shown at depths 507, 509, and 512 cm. All depths measured from the snow surface of August 1953.

Localized percolation

Melt water can percolate downward along restricted "channels," and move laterally along favorable layers. This can occur in snow with negative temperatures, only the percolation channels being at the melting point. While active, the percolation channels appear slightly slushy (Fig. 13), they refreeze to form ice glands, lenses, and layers (Fig. 10a,b).

Ice layers, lenses, and glands are described as follows:

(a) Ice layers extend over large areas parallel to the strata with only minor interruptions.

(b) Ice lenses are lens-shaped layers which pinch out laterally. They are parallel to the firn strata.

(c) Ice glands are pipe-like vertically extending masses which occasionally spread laterally to form lenses and layers. They are the frozen percolation channels which feed lenses and layers.

Lenses and layers are "concordant structures" whereas glands are "discordant."

Percolation of moisture through snow and firn is primarily a wetting process, and subsurface melting is not an essential part of the mechanism. The fact that melting is not required was demonstrated by pouring gasoline on the surface of snow well below the freezing temperature and after two minutes a vertical cut was made

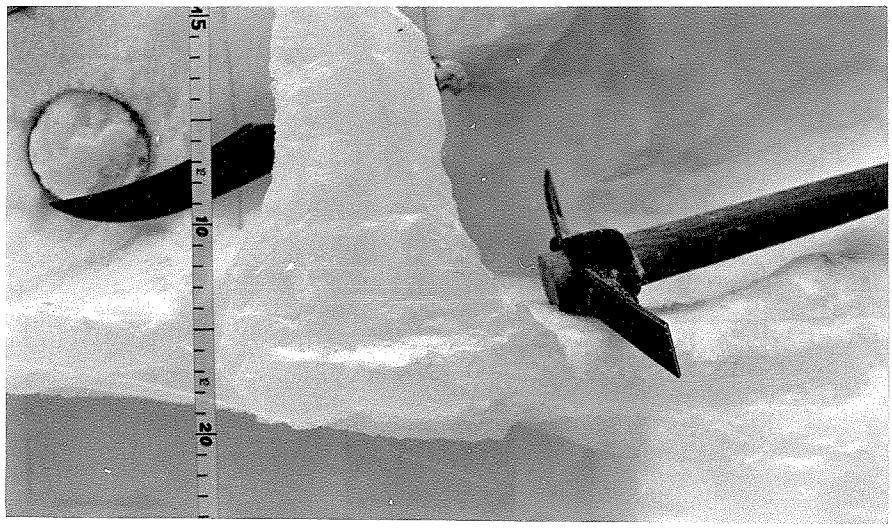

10 a

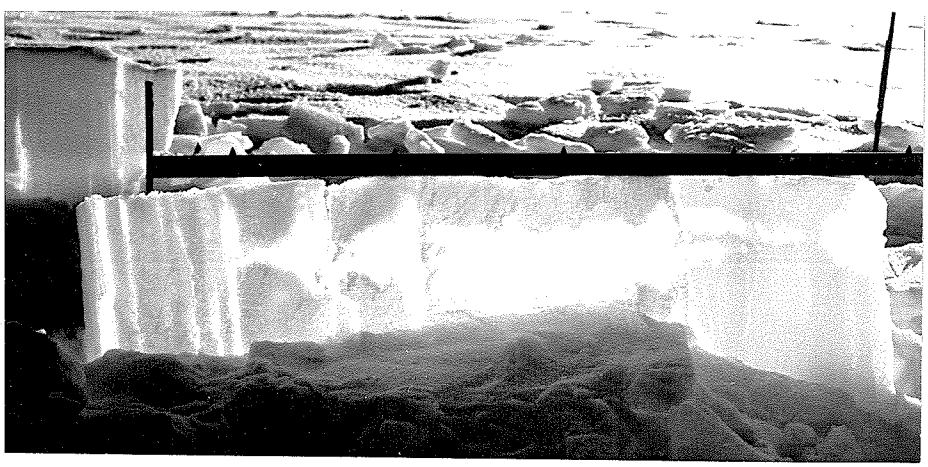

10 b

Figure 10. Ice Masses in Snow Strata

Figure 10a.--Ice gland formed during the summer of 1950 at Station 1-0 and observed 5 m below the snow surface of July 1953 (see data sheet 3).

Figure 10b.--This ice gland, with layers and lenses formed at Station 2-70 during the heat wave of 11 to 14 July 1954 (Fig. 12). The zero point on the meter stick is at the left and marks the 1 m depth in the pit. The ice layer at 110 cm, and the lens at 130 cm formed on depth hoar layers (see Station 2-70, data sheet 5). Percolating meltwater, originating at the snow surface during four warm days, penetrated nearly two meters below the snow surface which at this station includes two years accumulation. The ordinary effect of a summer here is to produce only a crust of iced firn like those shown in Figure 9.

exposing a network of glands and lenses identical to those formed by percolating melt water (Fig. 11).

When the percolating liquid is water, the temperature of the percolation "channels" is raised to the melting point. However, temperatures several degrees below the melting point have been measured between channels within the percolation network.

Melt phenomena observed at Station 2-70, 12-15 July 1954

The entire process of surface melt, percolation, and refreezing to form iced firn on the surface, and ice glands, lenses, and layers at depth, was observed at Station 2-70 during the exceptional "heat-wave" of 12-15 July, 1954. The heat-wave was accompanied by a slight drizzle (apparently produced by the occlusion of a front over the area centered at 2-0) up to altitudes of about 7000 ft. Summer rains are common at sea level in polar regions but very rare at altitudes above 6000 ft at 77°N latitude. Air temperature records during this heat wave and the one of 10-15 August 1954 are summarized in Figure 12. Negligible melt occurred above 7500 ft, but the effects of the heat wave, and its precipitation, were recorded by the formation of a wind slab (see p. 67 and Fig. 32c). The melt process observed at 2-70 during the 12-15 July "heat wave" will be described in some detail because it illustrates the general mechanism.

Figure 11.--Percolation of gasoline in snow at -30°C at Station O-5, 27 March 1953. Percolation proceeds by a wetting action and melting is not required. This was shown by pouring gasoline on the snow surface and after two minutes a vertical cut exposed the network of glands and lenses shown here. The temperature profile measured in the snow during this test is listed below:

	Depth (cm)	Temperature (°C) (to the nearest half degree)
(snow surface)	0	-30.0
	8	-29.5
	19	-29.0
	25	-28.0
	32	-26.5
	40	-25.0
	47	-25.0
	52	-23.5
	61	-23.0
	68	-23.0

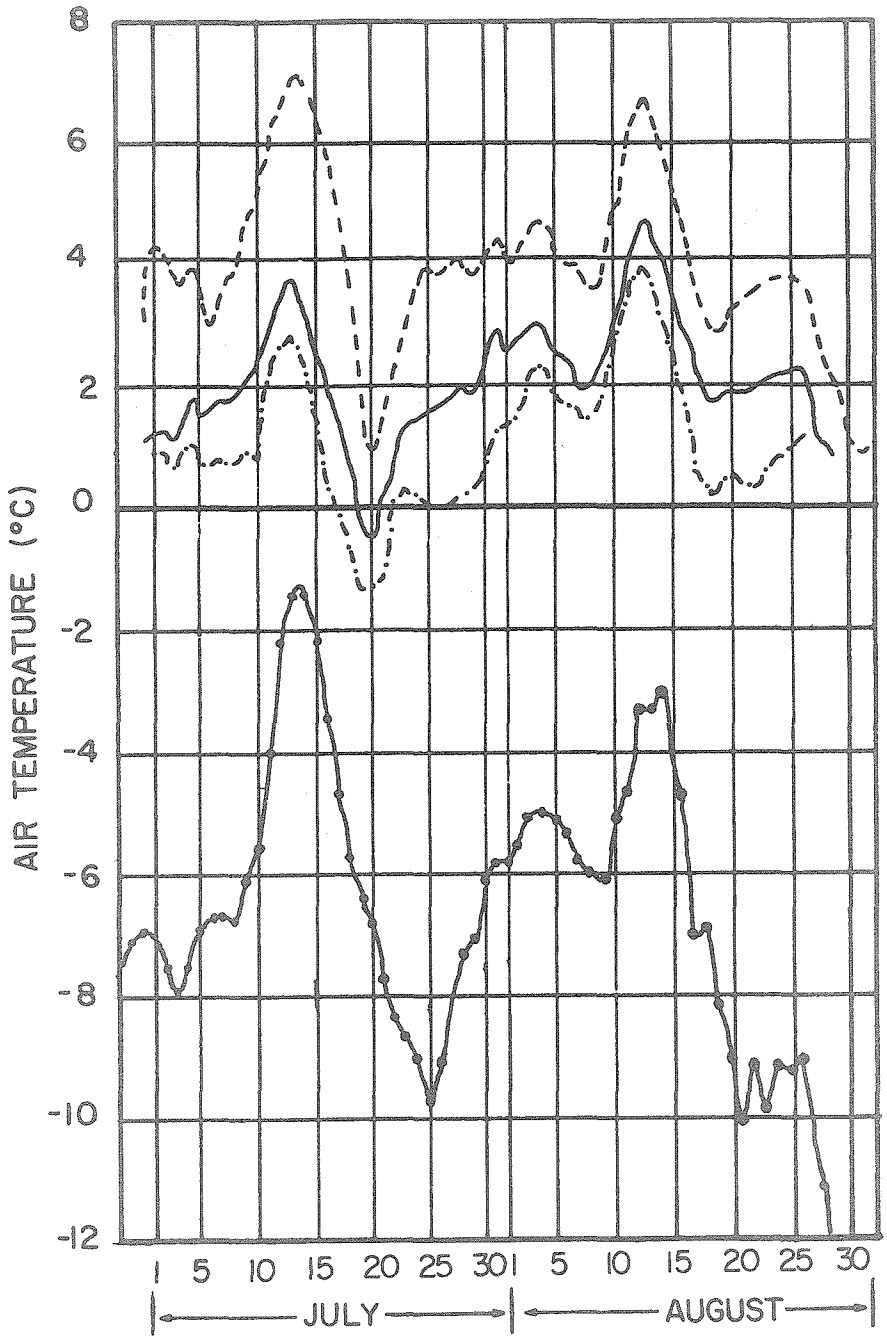

Figure 12.--Daily mean air temperature (5-day running means) at:

Station		Elevation (m)		
0-0	(Camp TUTO)	480	— — — — —	Schytt (1955, p.5)
0-1	(Thule Ramp)	569	———	" "
0-6	(Hardtop)	736	—·—·—·—	" "
2-100	(Site II)	1990	—●—●—●—	Site II Meteorological Data (USAF Air Weather Service)

A pit was dug on 13 July solely for the purpose of observing melt action in the firn. The snow surface was at 0°C, and damp. Slightly damp slushy lenses, layers and glands were observed on the pit walls (Fig. 13). They were best developed at one corner of the pit near a large ice gland. The snow and firn near the active percolation channels remained at subfreezing temperature.

On 15 July the percolation network had refrozen and ice masses were exposed on the walls of the pit dug on 15 July for stratigraphic studies. The main ice lenses and layers spread out from the large ice gland shown in Figure 10b. Three temperature profiles measured in the top 2 m of the 15 July pit are shown on data sheet 5, and in Figure 25. Profile No. 1, from the test wall, was not near a major ice gland and shows the normal mid-July decrease in temperature with depth. Profiles No. 2 and 3 show the warming effect of the percolation network surrounding the ice gland of Figure 10b.

The snow surface showed two interesting features after the heat wave:

(1) The top 3 to 5 cm consisted of a crust of iced firn with a pock-marked surface (Fig. 14).

(2) Slight depressions, spaced several meters apart, were everywhere (Fig. 14). Such surface depressions are probably located directly over major ice glands as hypothesized by Sharp (1951). Ice glands represent ex-

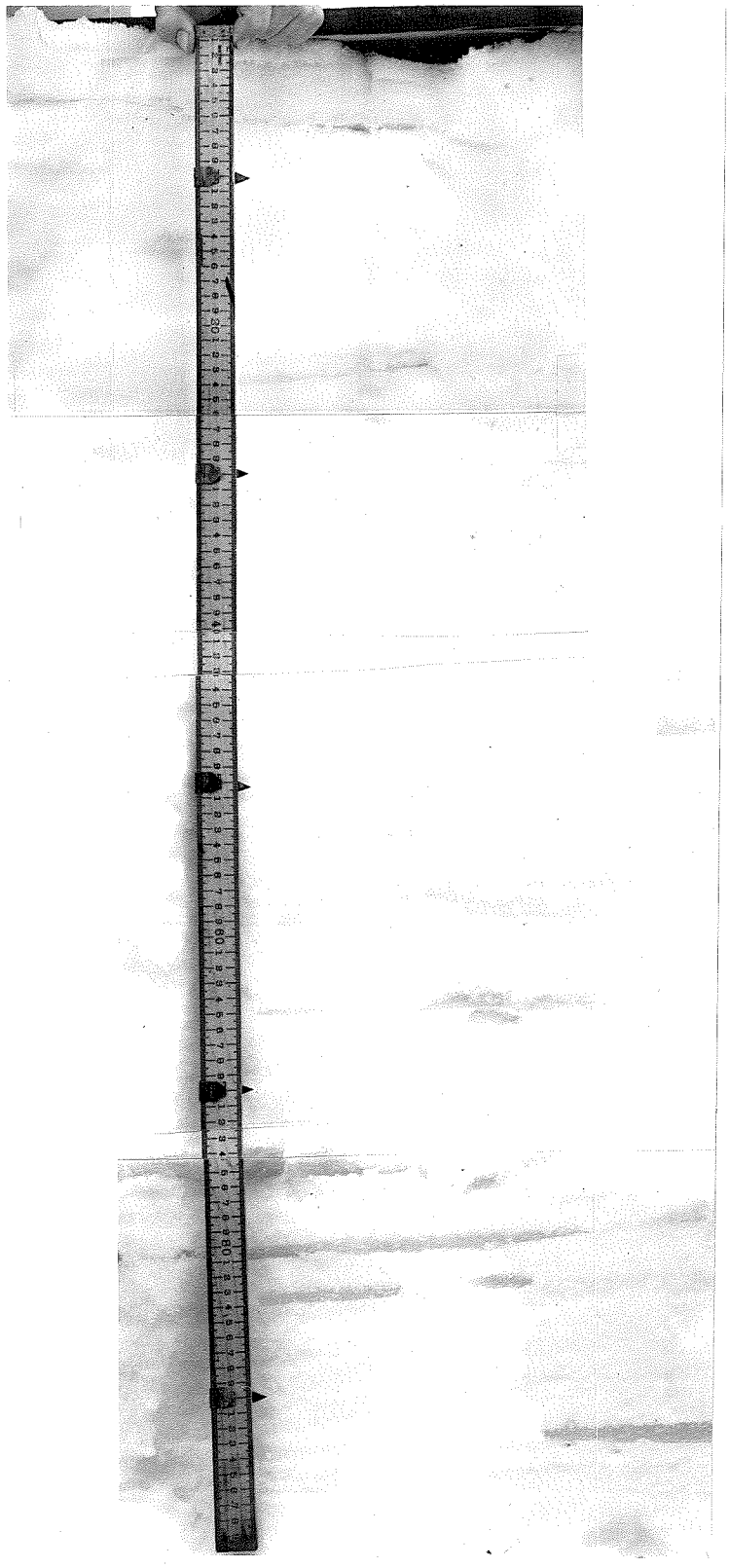

Figure 13.--Active percolation channels. The pit wall shown was exposed on 13 July 1954 at Station 2-70. The ambient snow temperature was -6 to -10°C (see data sheet 5 and Fig. 25), yet percolation channels caused the slushy lenses shown here. Temperatures as low as -6°C were recorded between the wet slush-lenses at 70 and 91 cm.

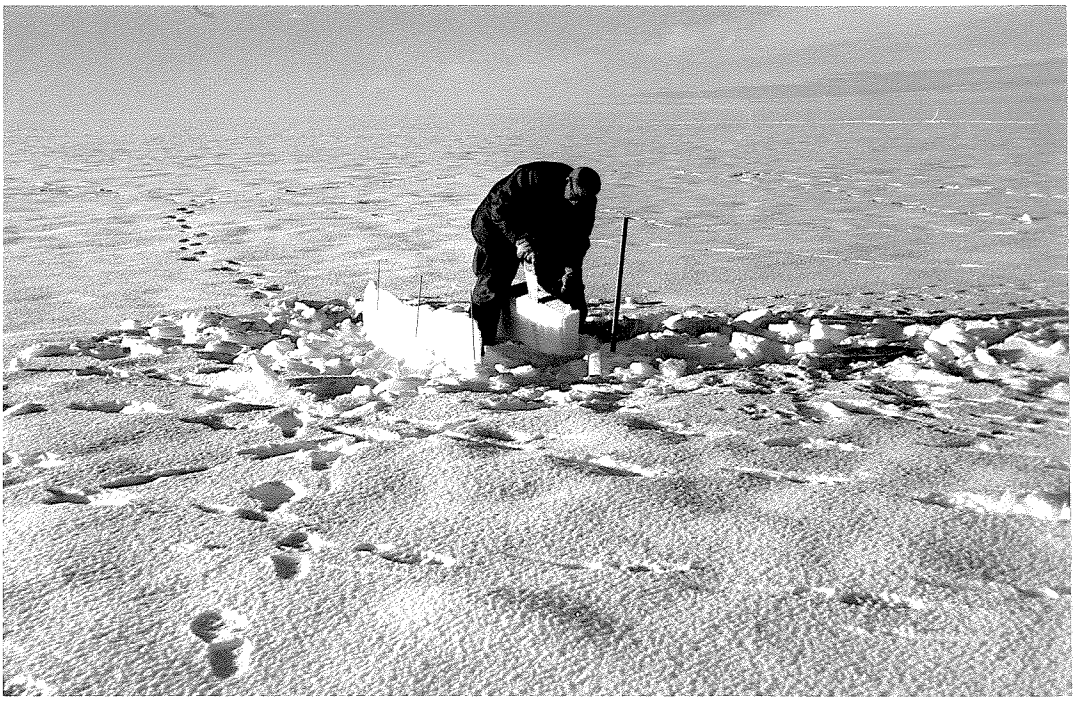

Figure 14.--Frozen melt crust at Station 2-70, 15 July 1954. The melt crust was 3 to 4 cm thick and resulted from the mid-July heat wave (Fig. 12). The depressions spaced about 1 to 2 m apart probably form over large ice glands such as illustrated in Fig. 10b. The spacing of the large ice glands is about the same as the spacing between depressions. The glands and depressions both formed during 11-14 July 1954 (see p. 43).

treme local densification and the snow surface is the most likely place to expect an expression of this reduction in volume. This hypothesis was not checked by digging beneath the depressions in search of ice glands, but the spacing and arrangement of major glands is similar to that of major surface depressions. Also, depressions and glands formed simultaneously, at Station 2-70, during the only time that the formation of either was actually observed. Furthermore, surface depressions, like those of Figure 14, were seen only on this occasion in the percolation facies and were never seen in the dry-snow facies.

Summary

It is important to distinguish between the two basic types of melt which may be generally classed as "surface" and "subsurface."

Surface melt features. Surface melt usually results in layers of iced firn which consist of clusters of grains bonded together by frozen melt water. They form continuous, concordant strata which may be traced around the four walls of a test pit and are excellent stratigraphic horizons. Small ice glands and lenses are often found directly beneath layers of iced firn (Fig. 9).

Subsurface melt features. Subsurface melt features are produced by surface melting, percolation, and subsequent refreezing of the melt water. They are relatively clear ice masses with variable dimensions and during an

exceptionally warm period, may penetrate the firn of several previous years (Fig. 10b). The ice masses are usually so irregular that they cannot be traced around the four walls of a test pit. Individual ice lenses or layers are not good stratigraphic marker beds; however, a zone of abundant icing beneath a crust of iced firn constitutes a good stratigraphic unit. In lenses of variable thickness, the lower contacts are more nearly parallel to the strata. The latter observation has also been made in Spitsbergen (Ahlmann, 1948, p. 17).

Diagenetic Facies Defined on Glaciers

Even a cursory glance at the data sheets reveals regional differences in the physical properties of the upper firn layers (compare data sheets 1, 6, 7, and 10). The differences are caused primarily by variations in the effect of summer melt. A spectrum of melt action exists on the ice sheet. It varies from the extreme of melting the entire annual accumulation at some locations, to the complete absence of melt at others. This spectrum may be subdivided into four distinctive regions. Stratigraphically, these regions are facies. The ice sheet is thin in relation to its areal extent, and the facies actually represent lateral variations in the properties of a single stratigraphic unit, even though altitude, rather than distance, is used as a parameter in defining them.

Regional differences apparent on the data sheets are partly time-dependent as the observations span nearly 7 of the 12 months in a year. The concept of facies includes the element of time because the boundaries are established with respect to that time when maximum melt conditions prevail. During winter at 77°N the environment of deposition and diagenesis varies little from the edge of the ice sheet to the center. During summer, this region shows wide variation in its diagenetic environment, and these variations produce the facies.

Consider the diagenetic environment of a single annual layer of snow accumulation, spanning a range of elevations from sea level to the crest of the ice sheet, during the peak of the melt season. Below the firn line, the snow cover is stripped away revealing bare glacier ice (the metamorphic member). Complete soaking (see p. 36) occurs between the firn line and the upper limit of complete soaking, the saturation line. Localized melt-water percolation (see p. 38) occurs between the saturation line and the upper limit of surface melting, the dry-snow line. The firn line, saturation line, and dry-snow line are facies boundaries separating the ablation, soaked, percolation, and dry-snow facies. Figure 15 is a diagramatic sketch of these relations.

A quantitative classification of glaciers can be established on the basis of diagenetic facies. This will

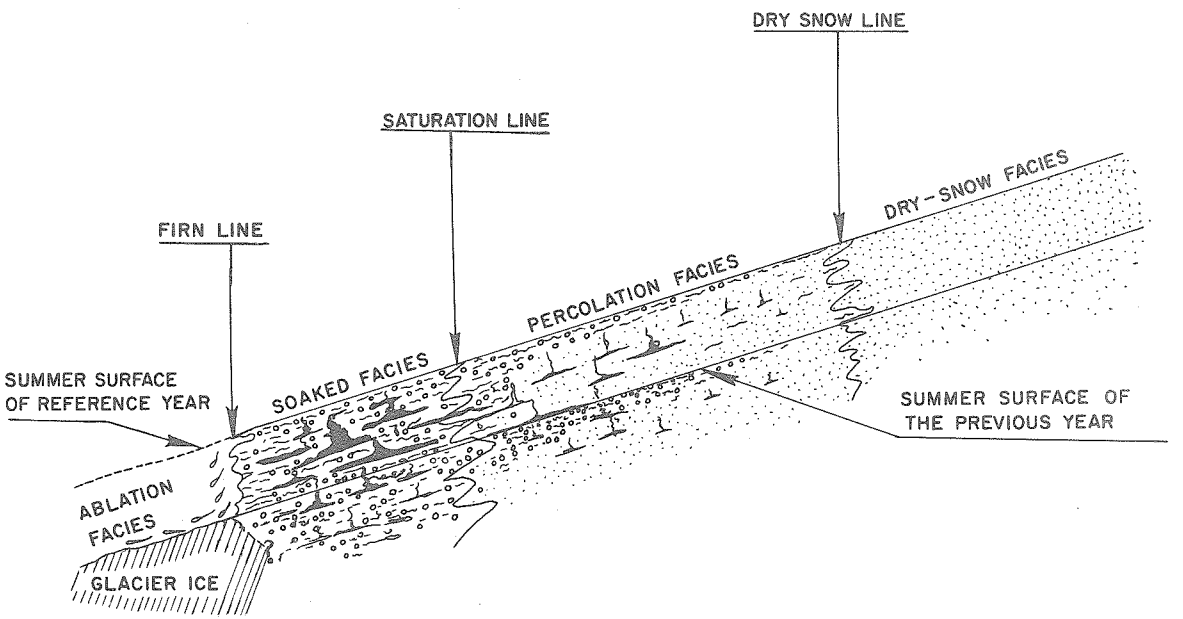

Figure 15.--Generalized cross-section of glacier facies. The snow cover is completely stripped away in the ablation facies. The entire year's accumulation is raised to the melting point and wetted in the soaked facies. In the percolation facies the annual increment of new snow is not completely wetted nor raised to the melting point, and the amount of percolation decreases with altitude becoming negligible at the dry-snow line. Negligible melt occurs in the dry-snow facies.

be presented at the end of Chapter IV after demonstrating how facies boundaries are defined by measurements of firn temperature, ram hardness, and firn density.

Grain Size

The international classification of snow grain size proposed by Schaefer, Klein, and deQuervain (1951) was used in this study with a subdivision of the medium-grain range (Fig. 16). Fine dust-like snow which drifts along the surface (Fig. 7h,i) has grains less than 0.1 mm in diameter, while grains in soaked layers often exceed 4 mm. By far the majority of measured grains in non-soaked strata lie within the two Wentworth grades bounded by 1/2 and 2 mm, or between +1 and -1 on the phi-scale of Krumbein (1934); the median diameter is between 0.5 and 1.0 mm. Grain size distribution histograms using the subdivisions of Figure 16 are shown in Figure 17.

Most samples are well sorted, although not to the extreme found in some beach deposits. They are comparable to the St. Peter sandstone. Cumulative curves from several sediments are compared in Figure 18. Detailed analyses as shown in Figures 17 and 18 are not necessary for routine stratigraphic observations.

Grains in firn strata which have not been exposed to melt action are often slightly angular and predominantly less than 1 mm (Fig. 19a). When surface melt and

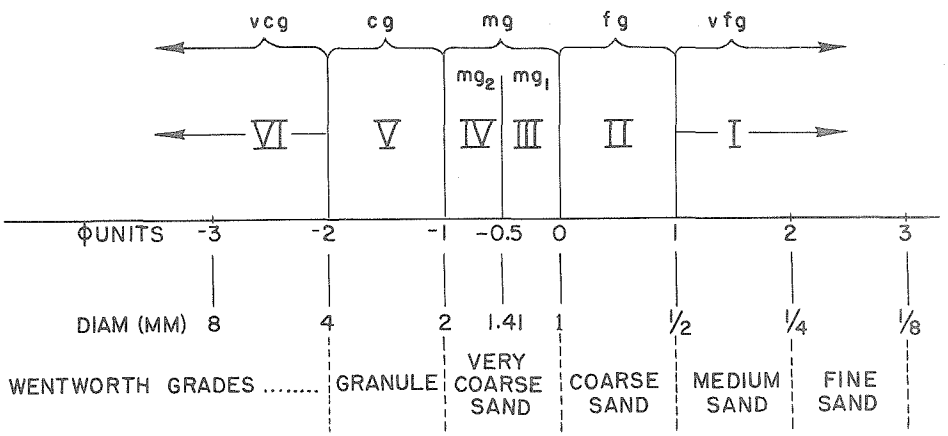

Figure 16

Grain Size Classification

Classification of Schaefer, Klein, and de Quervain (1951)

vfg	very fine	< 0.5 (mm)	a
fg	fine	0.5-1.0	b
mg	medium	1.0-2.0	c
cg	coarse	2.0-4.0	d
vcg	very coarse	> 4.0	e

The numbers I through VI were used in this work with the medium grain range subdivided as shown.

The φ scale is defined as follows:

$$\varphi = -\log_2 \xi \quad , \text{ or } \quad \xi = 2^{-\varphi}$$

where ξ = diameter in mm (Krumbein, 1934).

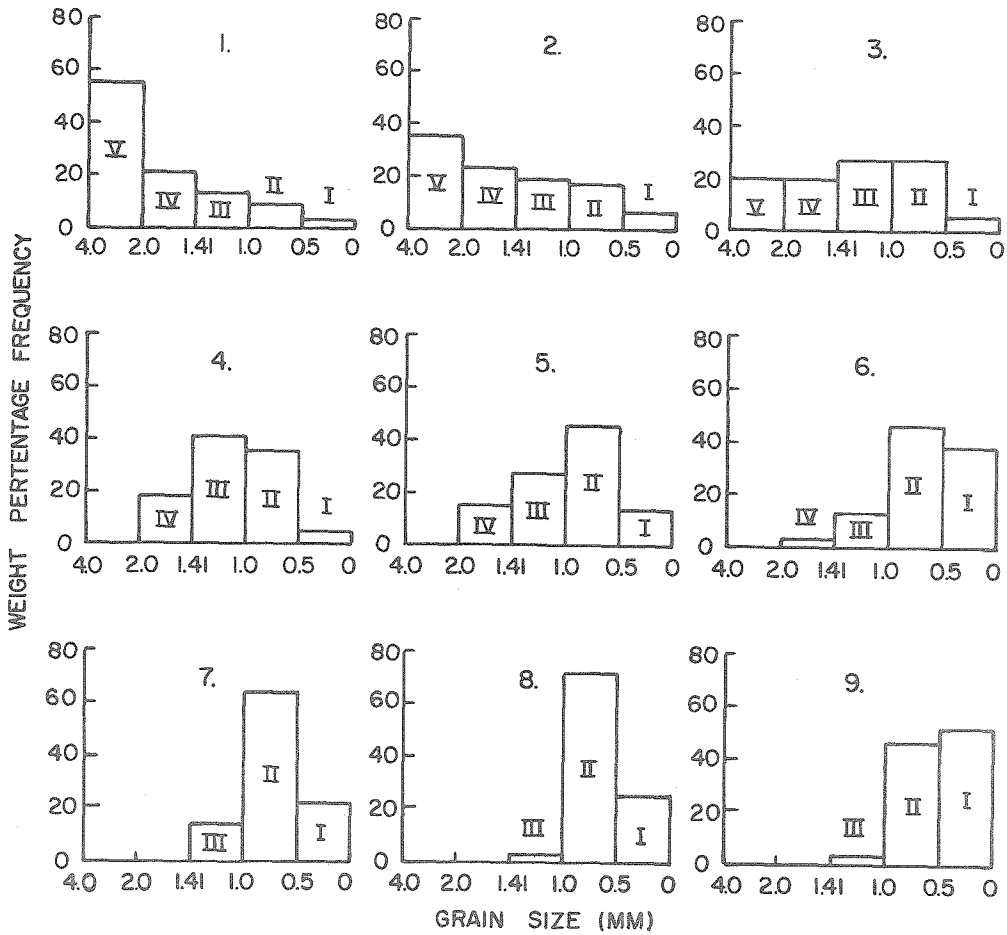

Figure 17.--Histograms of snow grain size arranged in order of decreasing grain size from the coarest to finest observed in non-soaked facies.

Sample	Station	Depth (cm)
1	4-0	275-276
2	2-0	378
3	2-0	162
4	2-225	78-83
5	1-0	110
6	1-0	240
7	2-30	60
8	2-30	160
9	1-0	30

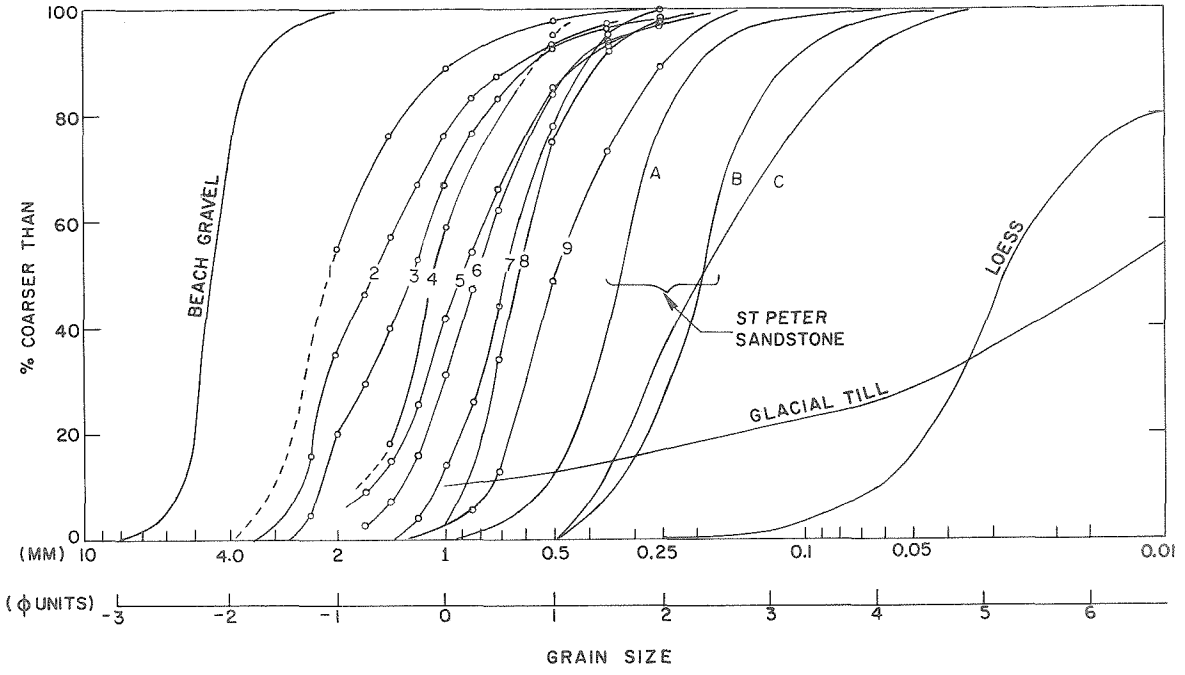

Figure 18.--Cumulative curves. Curves 1 through 9 from the Greenland ice sheet were plotted from the data of Fig. 17. Curves from the St. Peter Sandstone were obtained by Thiel (1935) in the upper Mississippi Valley as follows:

Curve	Identification
A	0-10 ft. from top
B	30-40 ft. from top
C	average of 72 samples

The other cruves were obtained from the following sources:

Beach gravel curve, Krumbein (1936)
Glacial till curve, Krumbein (1933)
Loess curve, Krumbein and Sloss (1951)

Facing p. 54

Figure 19

Photomicrographs of Firn Grains

The samples were scraped from the pit wall at Station 1-0, 1953 at the following depths: "a" from 120 cm (typical of the material from 57 to 126 cm); "b" and "c" from depth hoarlayer at 185 cm; "d" and "e" from 203 cm (see Fig. 22 and data sheet 3).

Figure 19a.--These grains were taken from strata deposited during the 1952-53 winter and unaffected by the 1953 summer; they are predominantly less than 1 mm and slightly angular.

Figure 19b,c.--The layers between 157 and 190 cm were subjected to surface melt and some soaking in 1952, as a result the grains became large, well rounded, and bonded into clusters. The grains shown are from a 1 cm layer of very loosely bonded grains with depth hoar crystals. They indicate melt-water soaking, refreezing,and subsequent sublimation. Sharp irregular growth of depth hoar are apparent on the rounded grains and several hexagonal cup-shaped hoar crystals may be seen in c.

Figure 19d,e.--From 196 to 240 cm percolation took place in 1952 and the upper layers were close to 0°C without being soaked. The grains are rounded and bonded into clusters, but their surfaces are smooth and this is interpreted to mean that sublimation was not as important here as in the grains shown in b and c. Note that the scale in e is twice that of the other photos, 18 diameters as opposed to 9.

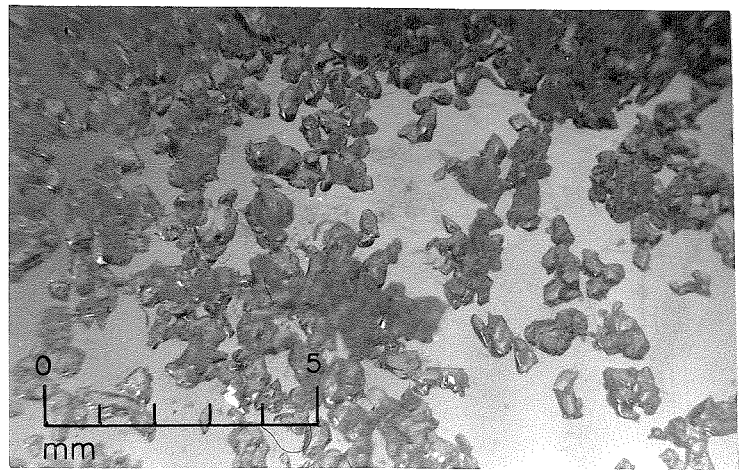

Figure 19a

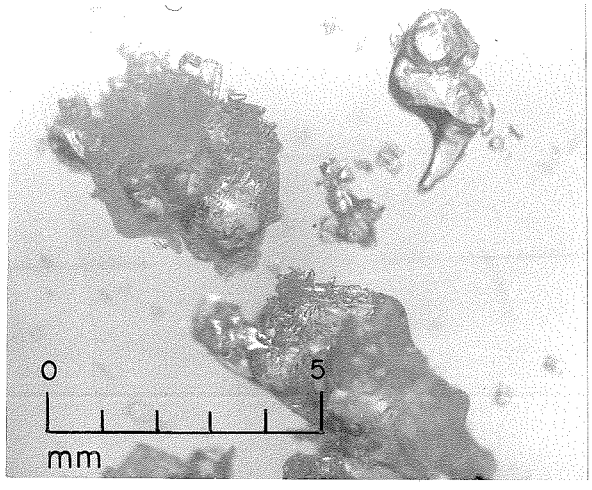

Figure 19b

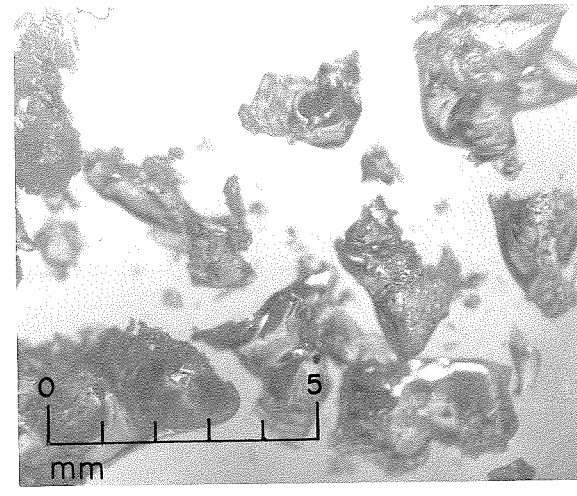

Figure 19c

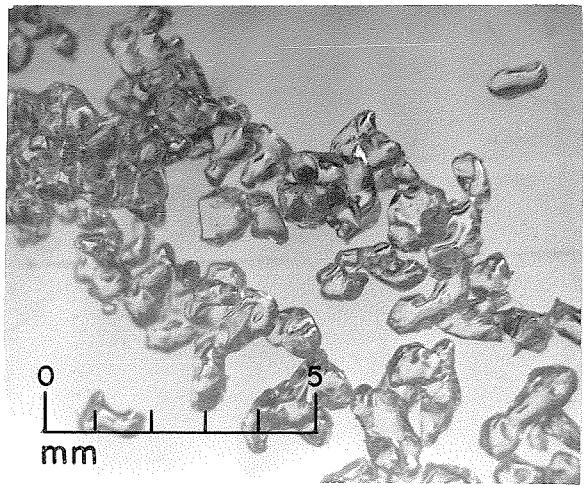

Figure 19d

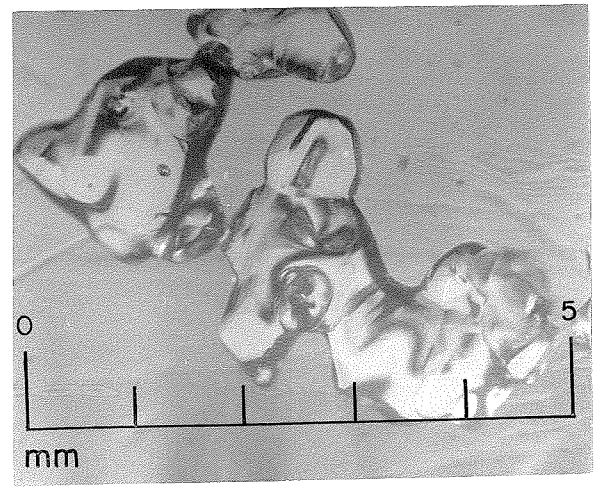

Figure 19e

soaking occur, grains become larger, more rounded, and are often bonded into clusters. The dimensions of clusters may exceed 5 mm and individual grains are mostly larger than 2 mm with only about 10% less than 1 mm (Fig. 19b,c). Grains exposed to temperatures within about five degrees of melting, but not soaked, fall in the medium-size range, between 1 and 2 mm. Their appearance differs from that of soaked grains only in degree; they are rounded and sometimes bonded together but both the individual grains and the clusters are smaller than those of soaked layers (Fig. 19d,e).

Crystal growth by sublimation produces hexagonal cup-shaped crystals (Fig. 19c) and irregular growth of depth hoar on individual grains or grain clusters (Fig. 19b,c). Grains rounded by melt and refrozen, but not subjected to significant crystal growth by sublimation, retain smooth surfaces (Fig. 19d,e).

Description of Three Stratigraphic Features

In addition to the melt products described above, other stratigraphic features, useful in correlation, are: depth-hoar layers, wind slabs, and wind crusts.

Depth-hoar layers

> "Depth hoar . . . is the most coarse-grained type of snow that can form without the presence of the liquid phase. It has a porosity of 67 to 78 percent and consists mostly of well-developed,

> clearly hemimorphic crystals with a base, a prism, and pyramids. . . . Complete cup formations are often in evidence" (Bader et al., 1939, p. 16).

Some depth-hoar layers have vugs with dimensions of several cm.

In addition to layers clearly recognized as depth hoar other soft loosely-bonded layers consisting mostly of rounded grains exist. These are classified as depth-hoar layers in description of the stratigraphic section, or simply as coarse loosely-bonded layers. They most likely represent depth-hoar layers in which the grains have become rounded by sublimation over a period of several years.

There is very little bonding between grains in a depth-hoar layer. It consists of a loose skeleton structure of ice crystals which will often collapse if disturbed giving rise to the phenomenon called "Firnstoss" (see pp. 159 and 160). Depth-hoar layers, especially thick ones, are excellent stratigraphic horizons which can be correlated for hundreds of miles.

Wind slabs

Wind slabs consist of rounded, firmly-bonded, fine or very-fine grains. Viewed from a little distance they appear dull, lusterless, and chalky. Maximum values on the hardness profiles are associated with wind slabs and layers of ice or iced firn. The density of wind slabs (even very hard ones) is not exceptionally high. As an example, the ram

profile exceeding 300 kg in Figure 20 was made through a wind slab of density 0.37 g/cm^3.

As stratigraphic units, wind slabs are usually variable in thickness and may lens out within the walls of a test pit (Fig. 21). However, the lenticularity may, in itself, provide a basis for correlation if a zone of wind slabs can be recognized in the stratigraphic sequence over a traverse. Lenticular wind slabs observed in pit walls result from burial of surfaces of erosion such as shown in Figure 7a,b, c,d,h, and k. Stratigraphically these buried erosion surfaces are unconformities; and they are good stratigraphic horizons, because conditions leading to erosion, with sastrugi and dune formation on the snow surface, with

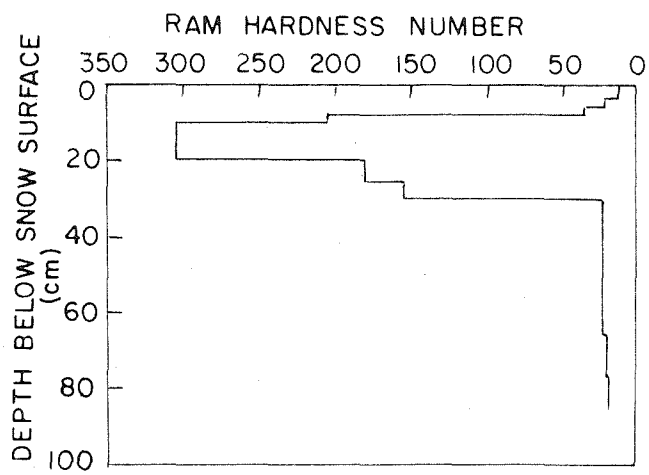

Figure 20.--Rammsonde profile through wind slab at Station 1-23, 4 September, 1952.

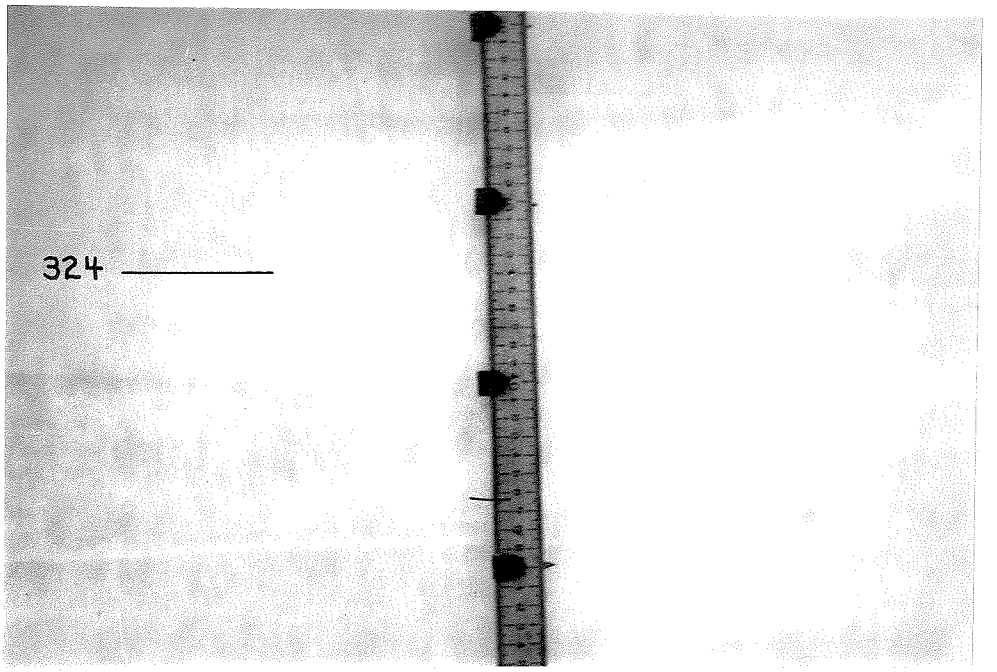

Figure 21a.--Wind slab lensing out in pit wall at Station 4-250, 1955.

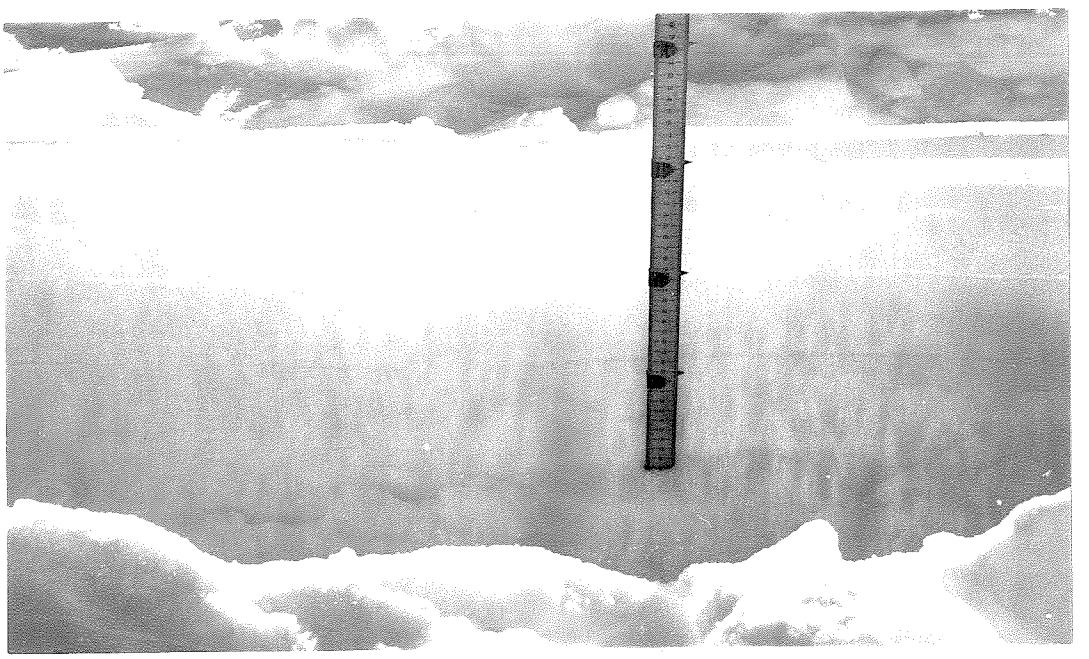

Figure 21b.--Wind slab formed on snow surface at Station 4-250, 2 July 1955. Several loose, low-density layers alternate with finer grained harder layers. This is typical of summer strata. The wind slab on the surface varies from 2 cm at the right to a thin wind crust at the left, and it was more than 5 cm thick to the right of this photo.

or without new deposition, are widespread. Sometimes the degree of induration of a hard layer, which can be correlated for 100 miles or more, varies laterally with bona fide wind slabs representing local extremes. Individual wind slabs at a given location are preserved for several years (see data sheet 4).

The nature of depth-hoar layers and wind slabs will be discussed further in connection with the reference datum within the annual sequence.

Wind crusts

Wind crusts are thin (1 or 2 mm) layers of firmly-bonded, rounded, fine or very-fine grains. When the pit wall is brushed with a whisk broom they stand out like layers of stiff paper (Figs. 4b and 6b). They are abundant, and to some extent this reduces their usefulness as units for stratigraphic correlation. However, certain prominent individual, or characteristic groups of wind crusts have been useful in correlation. The three wind crusts shown in Figure 6b, with the loosely bonded layer immediately below, were traced for 40 miles in 1954 (see Stations 1-50, 2-0, 2-10, 2-20, and 2-30 on data sheets 3 and 5).

Principles of Stratigraphic Interpretation

Interpretation of firn strata is based more on recognition of similar layered sequences rather than on the positive identification of a specific layer, such as a particular wind crust or ice stratum. The stratigraphic sequence represents a response to change in environment and, since these changes occur over an annual cycle, similar sequences are produced each year. Summer strata are generally coarser-grained and have lower density and hardness values than winter layers; they may also show evidence of surface melt. Also, there is usually more variability in summer layers, with coarse-grained, loose layers alternating with finer-grained, higher density layers or even wind slabs of variable thickness. Winter layers are generally more homogeneous, with higher density and finer grain size than summer layers. Typical summer layers are seen in Figure 21b, and the differences between summer and winter strata are most clearly seen in Figure 8. To measure annual accumulation by integrating depth-density profiles, a specific reference datum in this annual sequence is needed. It should form within a short time interval and must be recognizable in all facies. A part of the annual sequence fulfills this purpose.

Selection of a reference datum in the annual stratigraphic sequence

The short "fall season" produces a unique record in the firn. It is represented by a stratigraphic discontinuity in the form of a coarse-grained, low-density layer--often containing depth-hoar crystals--overlain by a finer-grained, harder layer of higher density. In regions where surface melt occurs, the discontinuity lies slightly above the topmost evidence of surface melt. The discontinuity at the base of the first year's snow is apparently the base of the "Jungschneedecke" of Koch and Wegener (1930 pp. 371-372).

Time of formation and stratigraphic nature of the discontinuity. The time of formation of the sequence containing the discontinuity was determined by the exact dating of specific layers, such as the one shown in Figure 6c. In 1953 the low density layer formed during middle and late August; and the discontinuity between it and the overlying higher density layer was fully developed by early September. Specifically, at 77°N latitude the discontinuity forms between 20 August and 10 September.

The discontinuity is easily recognized and may be traced continuously over long traverses. In 1953, 1954, and 1955, it was recorded at each of the 36, 68, and 27 stations, respectively, between 0-0 (TUTO) and 2-100. Sometimes the upper layer is a wind slab (see Fig. 20,

and Stations 1-50, 2-0, -30, -40, -50, -60, -70, -80, -90, and 2-100 on data sheets 3 and 5); sometimes it contains a series of thin, closely-spaced wind crusts (Fig. 6b; and data sheets 3 and 5 for Stations 1-50, 2-0, -10, and 2-20); but always it is harder and of higher density than the layer below.

At some stations ice masses in the firn make it difficult to obtain accurate firn density measurements (Stations 1-0 and 1-20 for the years 1948 to 1950 on data sheet 3). In these cases the ram hardness profiles are helpful in locating the discontinuity. Below the saturation line the discontinuity may be largely obscured by melt water soaking and percolation by early July.

Mechanism of formation of the discontinuity. At the end of August and during early September the temperature gradient in the upper firn layers is steep, i.e., 0.3°C/cm or more (Fig. 33; Station 1-0, curves 6,7, and 9; Station 2-0, curves 4 and 5; Station 2-50, curves 4 and 5; Station 2-120, curve C). These temperature gradients produce vapor pressure gradients which cause upward diffusion of water vapor and the possible loss of mass to the atmosphere.

By assuming an idealized situation with no movement of air through the firn, Bader (1939) computed the amount of moisture transferred by diffusion alone. His result was of the order of milligrams per cm^2 per day for the temperature

range 0 to -10°C. Because this is so small, he concluded that movement of air through the snow is essential to significant transport of moisture within or between layers.

Winds, especially very gusty ones, produce rapid fluctuations of air pressure within the upper snow layers, and increase the rate of vapor transfer. As a result, material is redistributed within the upper layers, and some material is removed. Actual removal of some water vapor from the snow by wind was observed by Seligman (1936, p. 107). It is also apparent from the low density of depth hoar layers in pits (between 0.20 and 0.30 g/cm^3) that moisture was extracted during their formation.

A combination of strong wind and steep temperature gradient in the fall would account for the formation of the low density layer. It would also account for the observation that this layer is thickest in the ablation, soaked, and lower part of the percolation facies. (See data sheets, especially Numbers 1 through 6.). Temperatures in the near-surface layers are highest in these facies. This results in maximum losses of mass by sublimation and evaporation, because the difference in vapor pressure between two firn levels depends on the range of temperature involved as well as on the temperature gradient. As an example, the temperature range 0 to -10°C produces more than twice the difference in vapor pressure produced by the range -10 to -20°C (2.61 as compared with 1.18 mm Hg).

Part of the upward migrating water vapor escapes to the atmosphere, but the remainder is redeposited within the upper layers. According to Bader's computation for the case with no wind, these amounts are nearly equivalent. If new or drift snow is being deposited on the surface, this material will be indurated by the vapor deposited in it. The condensing (by sublimation) vapor will first fill in the cracks between grains, because vapor pressure is lowest there. This strengthens grain bonds and in the extreme case forms a wind slab. This process was described as wind packing by Seligman who concluded:

> ". . . that wind-packing consists of the compacting of snow grains by the condensation of water vapour among them when subjected to the action of a moisture bearing wind. It is practically certain that at any rate some of this moisture is derived from the grains themselves. We can therefore define wind-packing as a special form of firnification accelerated by a wet wind. The mechanism of the processes is probably one of wind-accelerated diffusion which may or may not be influenced by the pulsations or pressure variations of the wind" (Seligman, 1936, p. 200).

It is suggested here that much of the moisture referred to as coming "from the grains themselves," is indeed from the low density layer below the wind slab.

The best example of wind-slab formation observed during the course of this work occurred on the first and second of September, 1952. On 3 September this wind slab covered the region 1-0 to 2-100, being most pronounced between 1-20

and 2-20 (Fig. 20)*; at 1-50 its formation involved the alteration of much of the 1952 layer (this is the only example of what one might call "wind erosion" of a significant portion of the annual accumulation, see data sheet 4). The prevailing meteorological conditions satisfied Seligman's requirements as seen in the following summary:

(1) Observations in the vicinity of 2-120:--
Low clouds and light snowfall on 1 September turned into a blizzard during the night which lasted throughout the day of 2 September. Winds exceeded 40 mph, new snow was combined with blowing and drifting snow and the air temperature remained near or above -5°C during the storm. On the morning of 3 September the sky was clear and the air temperature was below -25°C (see Fig. 33, Station 2-120, curve C).

(2) Observations on the trail between 2-100 and 1-0:--
The weather remained cool and clear until 5 September.

(3) Observations between 1-0 and 0-35:--
Wet snow fell during the night of 5 September followed by warm weather (near 0°C) and rainfall on 6 September occurred up to elevations of 4000 feet.

Evidence of surface melt from 5-6 September exists above the wind slab of 1-2 September in the 1952 strata at some stations. Wind slabs formed during summer are especially prominent because they are overlain and underlain by coarser-grained, lower density snow (Figs. 22 and 32c).

Another example of wind-slab formation is associated with the 15 July 1954 heat wave. The cooling period which

---

*The observed maximum wind effects in the vicinity of 2-0 are attributed to the location of this region near the crest of the ridge forming Thule peninsula. In May 1955 the wind-blown surface between 1-30 and 2-10 (Figs. 7c, d, k) caused broken runners on sleds.

followed the heat wave (Fig. 12) produced a strong temperature gradient in the freshly deposited snow. The thermal conditions were similar to those which contribute to the fall discontinuity. At Station 4-75, the heat wave resulted in a wind slab (Fig. 32c and data sheet 7). The O^{18}/O^{16} data support the inference that snow comprising this wind slab actually was deposited during the heat wave, because it has the highest δ value in the 1954 summer layer (Fig. 32c).

Examples of stratigraphic interpretation

Application of the above principles is illustrated in the following examples:

Four years data at Station 1-0. The four pits, presented in Figure 22, were made within 100 m of each other. In 1954 two pit studies were made, one before and one after the melt season. The 19 August, 1954 profile extended only to 160 cm, at which time the density and hardness profiles exceed those of 3 June as indicated by the stippled areas.

The sequence of strata recorded in the 1952 pit is preserved and easily identified in the pits of 1953 and 1954. The 1951 summer sequence, together with the nearly homogeneous interval down to the 1950 summer surface, was recognized with especial ease in each of three years of observation. The 1954 profile shows more evidence of percolation from the 1953 summer than does the 1953 profile; although this could be partly due to local variations in percolation, it is primarily

because warm weather continued for several weeks at 1-0 after the 1953 pit was completed.

Three years data at Station 0-35. The pit studies of 1953, 1954, and 1955 at 0-35 are assembled in Figure 23. The amount of melting at this station differs significantly from that at 1-0. Station 0-35 is below the saturation line, thus its entire annual accumulation increment is completely soaked each year. Stratigraphic correlation is difficult on the soaked facies because soaking of the firn produces rapid diagenetic changes. Features are not preserved for several years as shown in Figure 22.

Three years data at Station 1-50. The pit studies made in 1953, 1954, and 1955 at 1-50 are shown on data sheet 4 together with the two 1955 pit studies from the trail segment 1a (1a-10 and 1a-20). The latter trail segment made an angle of 90° with the segment 1-0 to 2-0. Pits 1a-10 and 1a-20 were made in an attempt to check the hypothesis (pp.77-79) that low accumulation on the lee-side of the ridge is caused by a precipitation shadow produced by the ridge.

Four years data at Stations 2-30 and 2-70. Pit studies made in 1952, 1953, 1954, and 1955 at Stations 2-30 and 2-70 are assembled in Figures 24 and 25 respectively. Except for the 1952 pits, (see Fig. 2) the pit studies at each station were made within 50 m of each other. Individual strata are correlated and the fall-datum of each year is indicated.

Figure 22.--Four years data at Station 1-O. The four pits were made within 100 m of each other on successive years; each in an area undisturbed by the previous years study. In 1954 two studies were made, one before and one after the melt season. The density and hardness values of the 19 August, 1954 pit exceed those of 3 June as indicated by the stippled areas. Note that the strata between fall 1951 and summer 1950 are well preserved and easily identified in the first 3 pit studies.

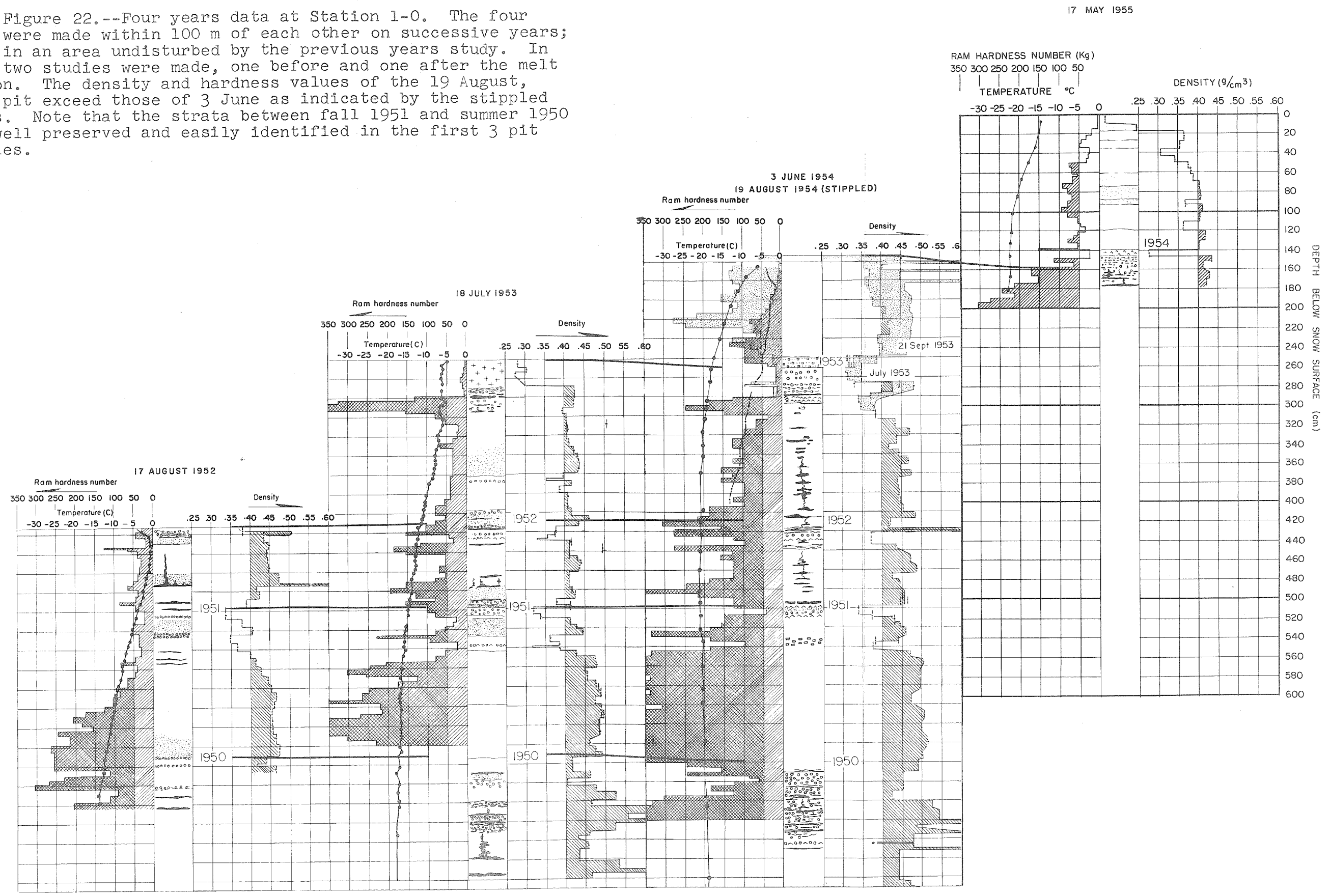

Figure 23.--Three years data at Station 0-35. This station lies in the soaked facies and stratigraphic details are not well preserved because of the amount of melt. However, the base of the first years accumulation is easily identified (especially before the melt season begins) by the contact between the low density depth hoar layer and the overlying fine grained snow (see p. 61).

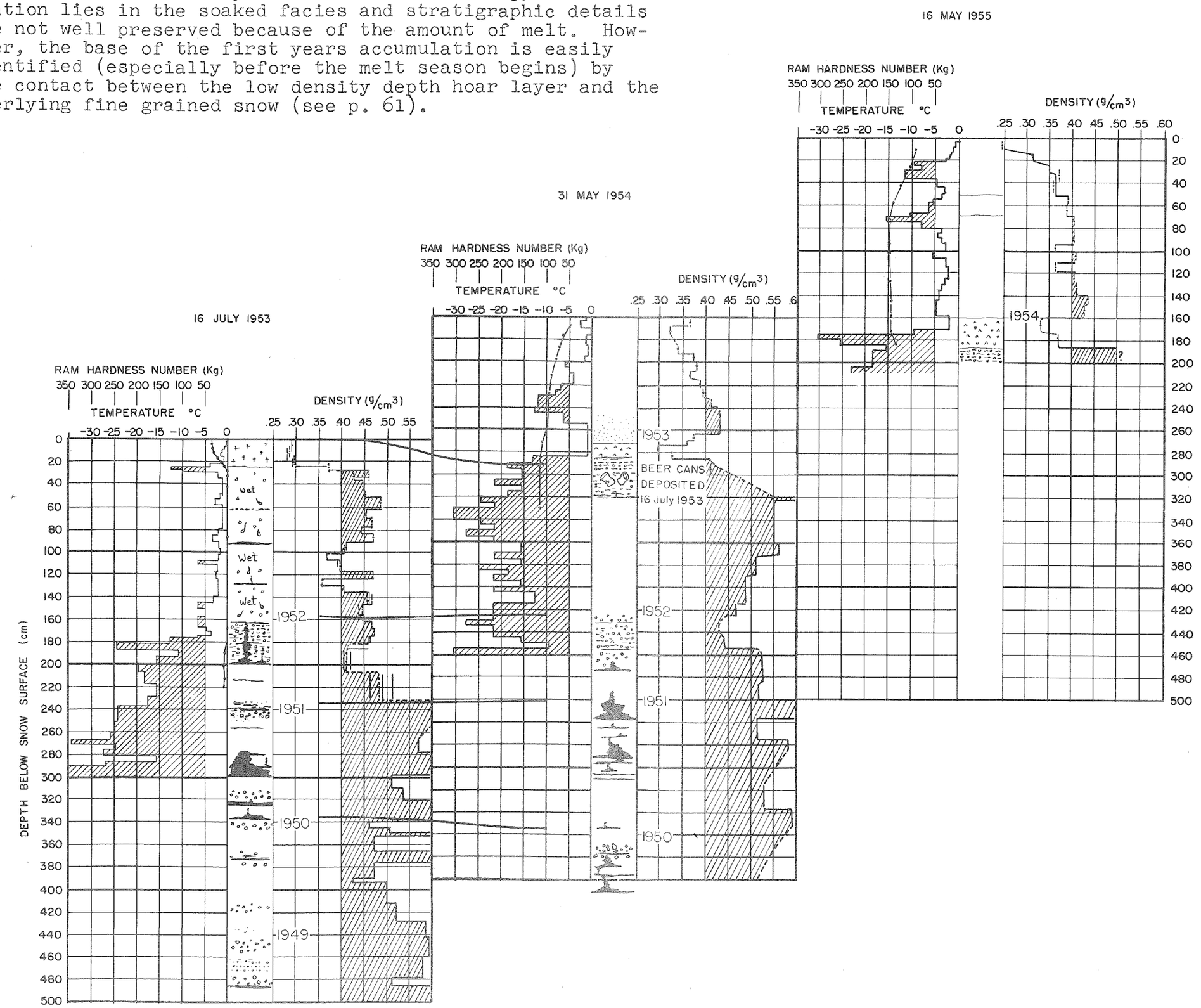

Figure 24.--Four years data at Station 2-30. The four pits were made within 100 m of each other on successive years except for the 1952 study which was about 3 miles northwest of the others (see Fig. 2).

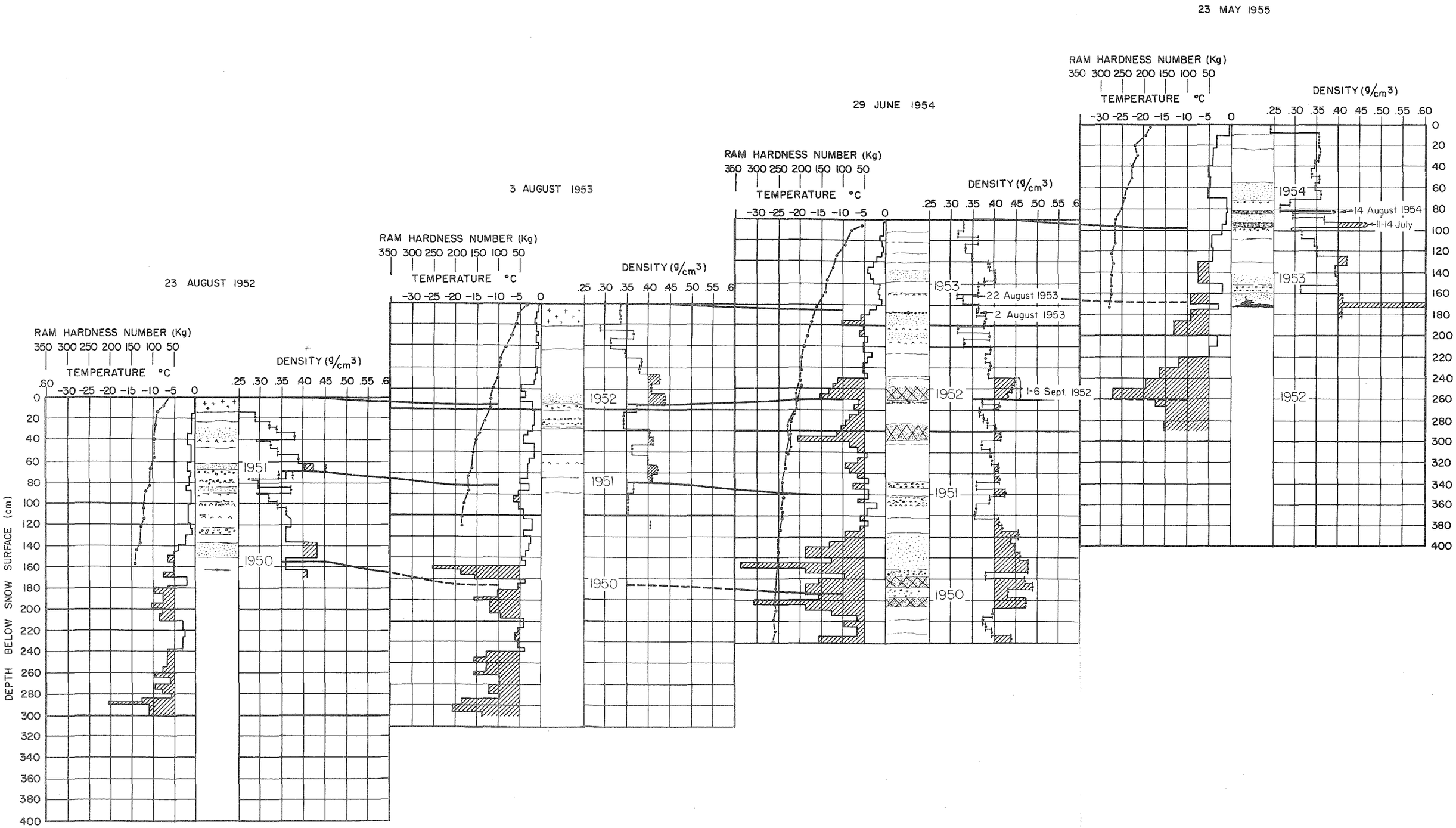

Figure 25.--Four years data at Station 2-70. The four pits were made within 100 m of each other on successive years except for the 1952 pit which was about 3 miles northwest of the others (see Fig. 2).

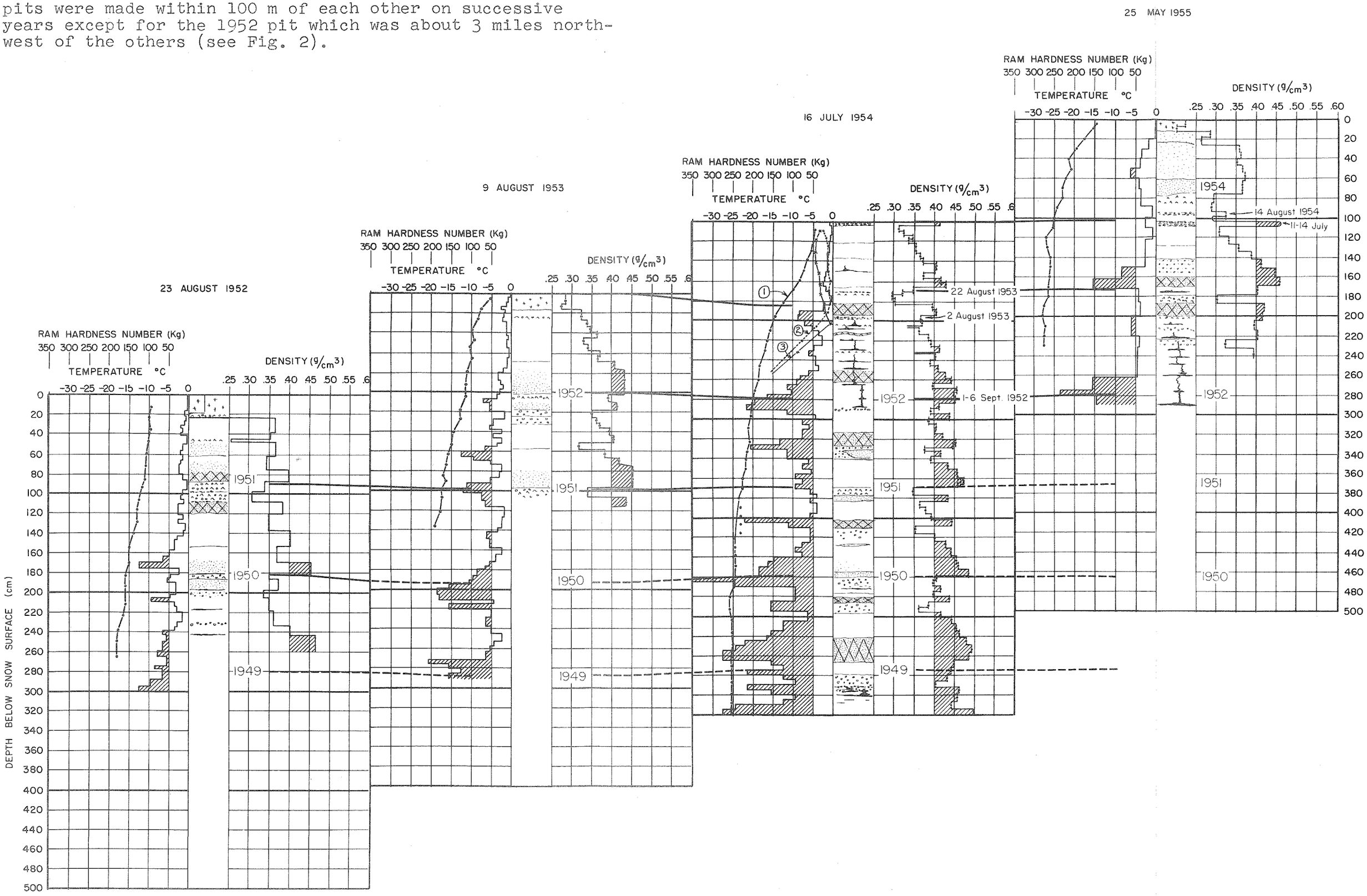

Stratigraphic Correlation

Data sheets

Stratigraphic interpretations made independently at each of the 79 stations shown on the 10 data sheets have been correlated with each other. The correlation lines are intended to pass through the fall layers of each year. Locations of specifically dated strata are indicated where known. The data sheets are discussed in Appendix III.

Measurement of accumulation

The only reliable method of measuring snow accumulation, in terms of an equivalent amount of water, is to integrate the depth-density profile between dated depth intervals. For example, the two pit studies at Station 1-0 in 1954 were stratigraphically correlated by matching identifiable layers at depths below 100 cm (Fig. 22). Integration of the depth-density profiles indicates a minimum increase of 10 cm H_2O in the upper 160 cm between 2 June and 19 August. This agrees well with the minimum of 12 cm H_2O obtained by direct measurement of snow added on surface marker boards at 1-0 during the same period of time. These are minimum values because the snow overlying the board on 19 August had been soaked and, as seen in Figure 22, some melt-water percolated downward; therefore, a larger accumulation between June and August might have been observed if the August pit had been deeper. It must also be pointed out that several large ice

masses were omitted from the integration of the August density profile. It is difficult to estimate the water equivalent of such masses because of their irregular shape and distribution, but in this case their contribution is about 3 to 5 cm H_2O.

The above results differ from those obtained by measuring the displacement of the snow surface relative to markers on poles. Such measurements are subject to error because the poles are set in firn which is undergoing compaction (Hubley, 1954) as illustrated in the following summary:

Height of marker above snow surface (cm) at Station 1-0	Date
200.0	21 September, 1953
121.5	2 June, 1954
98.5	14 June, 1954
112.0	19 August, 1954

Relative to the pole markers it is clear that: (1) The 9.5 cm rise of the snow surface, amounting to 4.3 cm H_2O, between 2 June and 19 August does not measure accumulation accurately because, as indicated above, an accumulation of at least 10 cm H_2O occurred during this time. (2) The 13.5 cm descent of the snow surface, between 14 June and 19 August, does not represent ablation because net accumulation of at least 5 cm H_2O is indicated by the surface marker board during this period. Densification apparently was sufficient to cause the snow surface to move downward, relative to the pole, in spite of net accumulation.

Pole-marker measurements also give inconsistent results at other stations as indicated in Figure 26. Net accumulation was measured on surface marker boards over the entire traverse during the period between the two series of measurements. Pole measurements indicate this above 1800 m (6000 ft); but, below this altitude melt action produced enough densification and settling to nullify or exceed the relative rise of the surface caused by accumulation.

Examples of water-content analyses

The depth-density profile from each station has been integrated to obtain a depth-load curve.* At a given station the load, in cm of water equivalent, at any depth may be read directly from the depth-load curve of that station. This makes it possible to determine the water equivalent of each identified annual layer, together with the average annual accumulation, at any station where the stratigraphy can be interpreted. By assuming constant annual accumulation at a given station one may use the observed depth-load curve to construct an idealized depth-time curve. The idealized depth-time curves for Stations 2-150, 2-225, 5-40, 5-90, and 5-180 all of 1955, are compared with data points in Figure 27.

---

*Typical depth-load curves are shown in Figure 45.

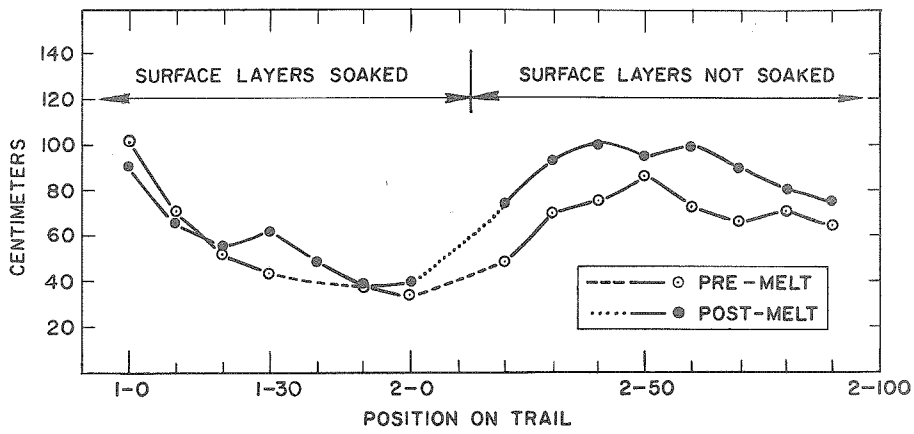

Figure 26.--Displacement of the 1954 summer snow-surface relative to markers placed on poles in 1953. The "pre-melt" series of measurements was made between 14 June and 5 July, and the "post-melt" series between 15 and 18 August. Net accumulation occurred over the entire traverse between measurements, but below 1830 m (6000 ft) summer melt produced sufficient densification and settling to nullify or exceed this upward displacement (relative to poles in the snow) of the surface.

Two qualifying statements are in order: 1) No marker was placed at 2-10 in 1953. 2) Errors were possibly introduced at 2-50 and 1-30 by the formation of large snow drifts around parked vehicles. The drifts probably influenced the accumulation registered on the poles even though the poles were not actually in the drifts. These errors were not compensated in preparing this figure.

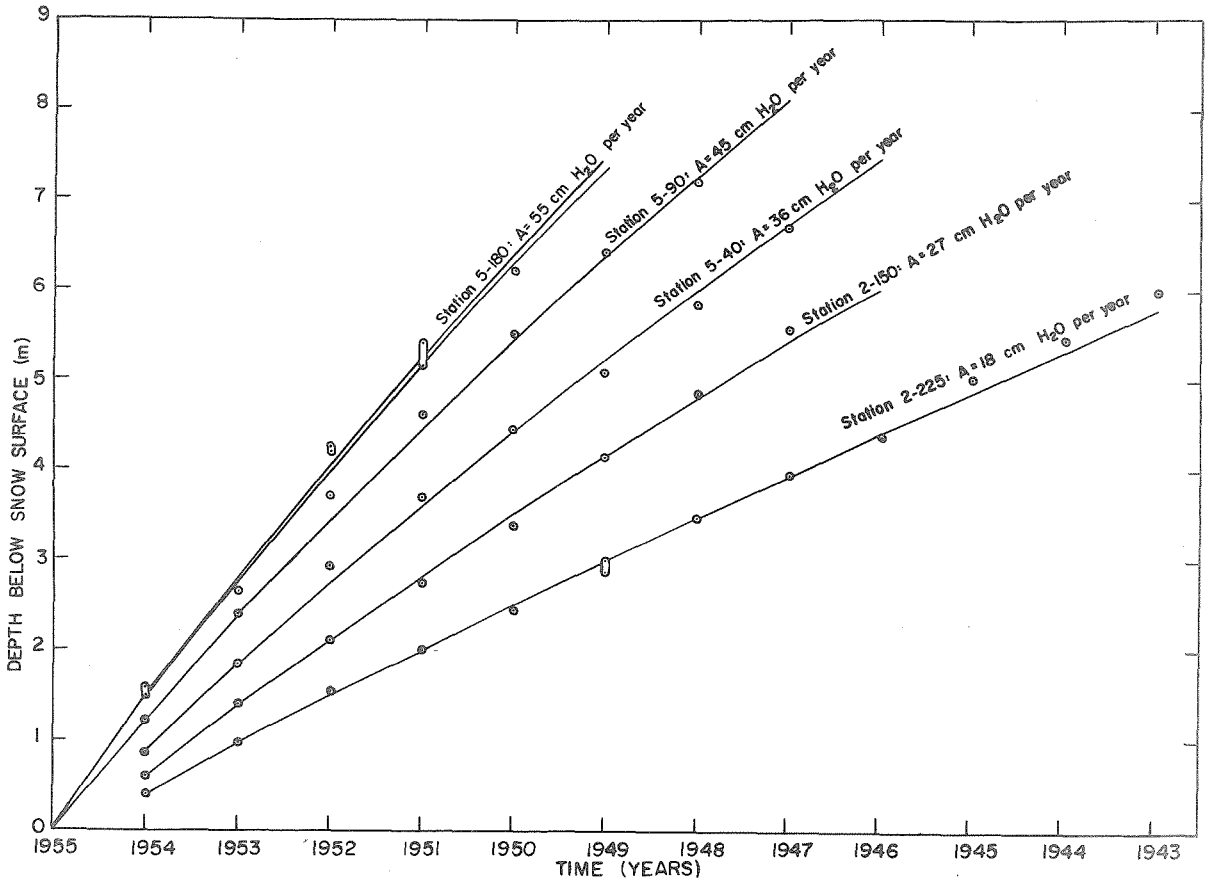

Figure 27.--Computed depth-time curves with data points for several 1955 stations. The curves were computed by assuming a constant rate of accumulation "A" cm H_2O per year.

Two curves are shown for Station 5-180; the upper one was computed by neglecting ice masses, the lower one includes estimates for the contribution of ice. The difference between depth-load curves with and without estimates for ice is less than 1% at the other stations shown (see p. 142).

At Stations 2-225 and 5-180 the depth to some yearly layers was not unequivocal and possible ranges are indicated. At Stations 2-150, 2-225 and 5-40 it was necessary to subtract 8, 5, and 6 cm H_2O respectively from the computed load values to adjust for the incomplete first year; the annual reference datum is the beginning of fall and these stations were made on 31 May, 7 June, and 23 July respectively.

Distribution of Annual Accumulation

Annual accumulation on the ice sheet provides a reasonable measurement of total snowfall; in fact, the results presented below, aside from uncorrected evaporative losses,* are essentially precipitation measurements.

Combined data from the four-years of observation reduced to water equivalent are shown in Figure 28. The snow surface of Fall 1955 is the reference datum. Data between 0-0 (TUTO) and 1-0 are from pits which penetrate a maximum of 2 to 4 years of firn; the variation in accumulation is greatest over this part of the trail because of irregular topography. Positions 0-27 and 0-31 lie near the lee side of large nunataks. All values between 0-0 and 1-0 lie within the range of 50 to 70 cm H_2O per year.

The minimum accumulation between 1-30 and 2-20 is attributed to topography. The trail between about 1-25 and 2-25 lies on the lee side of the Thule peninsula (Fig. 2).

---

*Because of low temperatures, evaporation is slight except in marginal parts of the ice sheet where temperatures above 0°C are encountered. However, stratigraphic measurements of accumulation, even though reduced by evaporation, exceed the precipitation measurements made at nearby meteorological stations with standard rain gages (see pp. 83 and 84).

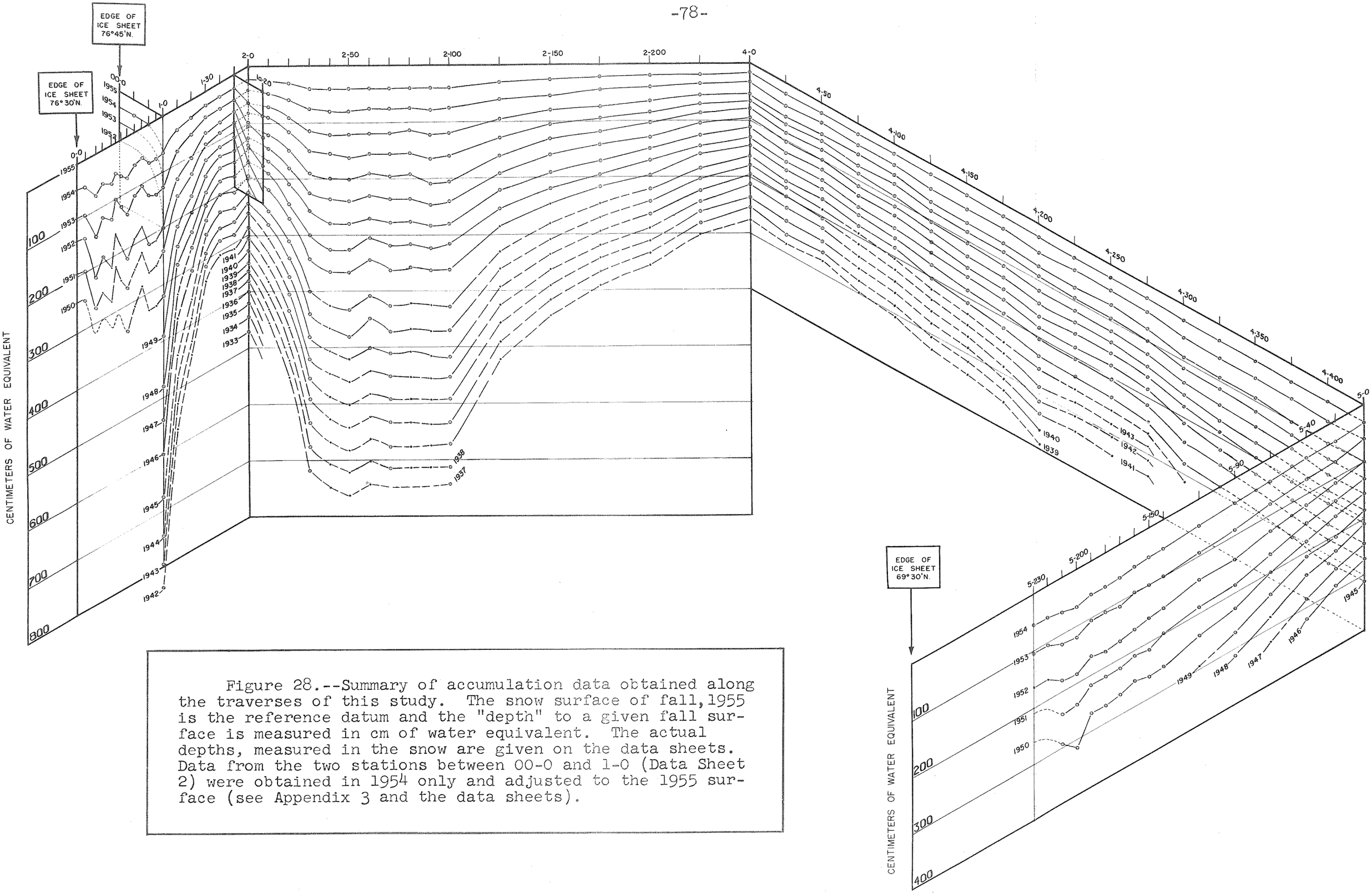

Figure 28.--Summary of accumulation data obtained along the traverses of this study. The snow surface of fall, 1955 is the reference datum and the "depth" to a given fall surface is measured in cm of water equivalent. The actual depths, measured in the snow are given on the data sheets. Data from the two stations between 00-0 and 1-0 (Data Sheet 2) were obtained in 1954 only and adjusted to the 1955 surface (see Appendix 3 and the data sheets).

The ridge is a topographic barrier to cyclonic storms which move onto the ice sheet from Melville Bay and points south. The area south and east of the crest serves as a catchment basin, while that to the northwest (the lee slope) lies in a precipitation shadow. Saturated air masses are cooled as they ascend the windward side of the ridge, producing precipitation. As they pass over the gentle crest of the ridge and begin to descend they are no longer being cooled, hence precipitation decreases. Further release of large amounts of precipitation does not take place until the air mass moves upward again on the north side of Inglefield Bay. As a consequence of this, the coast of Melville Bay is characterized by glaciers which flow into the sea, while the north side of Thule peninsula is comparatively free of glaciers. The Inglefield Land peninsula also has glaciers on its south side but not on its north coast.

In 1955 the above interpretation of a precipitation shadow caused by the ridge between 1-0 and 2-0 was checked in the field. The check consisted of running the traverse labeled "1a" to the windward from 1-50. The values of accumulation at 1a-10 and 1a-20 are 36% and 49% higher than that recorded at 1-50 on the lee side of the ridge. Station 1a-10 is near the ridge crest while 1a-20 is definitely on the windward side (see data sheet 4 and Figs. 2 and 28). A similar accumulation decrease occurs on the lee side of the ridge between 00-0 and 1-0 (see data sheet 2 and Fig. 28).

Accumulation-altitude relationship

The variation in precipitation with altitude, as a moisture bearing air mass ascends a slope, cannot be reduced to a fixed level as can be done with air temperature and pressure. Therefore, the usual precipitation map is the representation of actual isohyets (Conrad, 1944, pp. 182-183). In general,* it appears that precipitation increases with altitude on the windward slope, up to a certain level, above which it decreases as the air mass loses its water content. Precipitation continues to decrease up to the crest of the slope and on the lee side it decreases even more rapidly downhill into a precipitation shadow. Many factors influence the precipitation-altitude relation such as the temperature and humidity of the air as it begins its ascent, the duration and intensity of the storm, and the inclination of the slope. The latter factor is especially important because steeper slopes increase the amount of precipitation in addition to providing steeper precipitation gradients. The altitude of the zone of maximum precipitation varies seasonally, being highest in summer and lowest in winter. According to Henry (1919) it also varies slightly with latitude being less than 1000 m in the tropics and about 1500 m in temperate latitudes.

---

*Based on records from: California coastal mountains (Hamlin, 1904); India, Java, Hawaii, and mainland U.S.A. (Henry, 1919); and Sierra-Nevada and southern California mountains (Varney, 1925; Lee, 1941).

Average annual accumulation values for stations on south or west facing slopes,* which are windward slopes to the storm winds, are plotted against altitude in Figure 29. There is far less scatter among the points in this Figure than in precipitation-altitude diagrams for mountainous areas (see Lee, 1941, p. 58). This is because of the uniformity of exposure on the smooth, gently sloping surface of the ice sheet. Most meteorological stations in mountain regions are located at population centers, and their exposure to the moisture-bearing winds varies from station to station. This variability in exposure produces such irregularities in the data that Meyer (1941) doubted that an accurate precipitation-altitude relation could be obtained from them. On the ice sheet, in addition to uniform conditions of exposure, some uniformity also results from winds moving new snow along the surface, which tends to smoothen local irregularities in deposition from a single storm.

Figure 29 indicates maximum zones of accumulation at 2000 m at 70°N, and slightly above 1000 m at 77°N. Accumulation decreases with altitude above these altitudes at the rate of 3 cm H_2O per 100 m at 77°N and slightly less than this (about 2.7 cm H_2O per 100 m) at 70°N. It is interesting to note that this is close to the value (1.7 to

---

*Stations omitted are 0-27 and 0-31 because they lie on the lee side of large nunataks and Stations 1a-10 and 1-10 through 2-20 inclusive, because of their location on the crest or lee side of the Thule peninsula ridge.

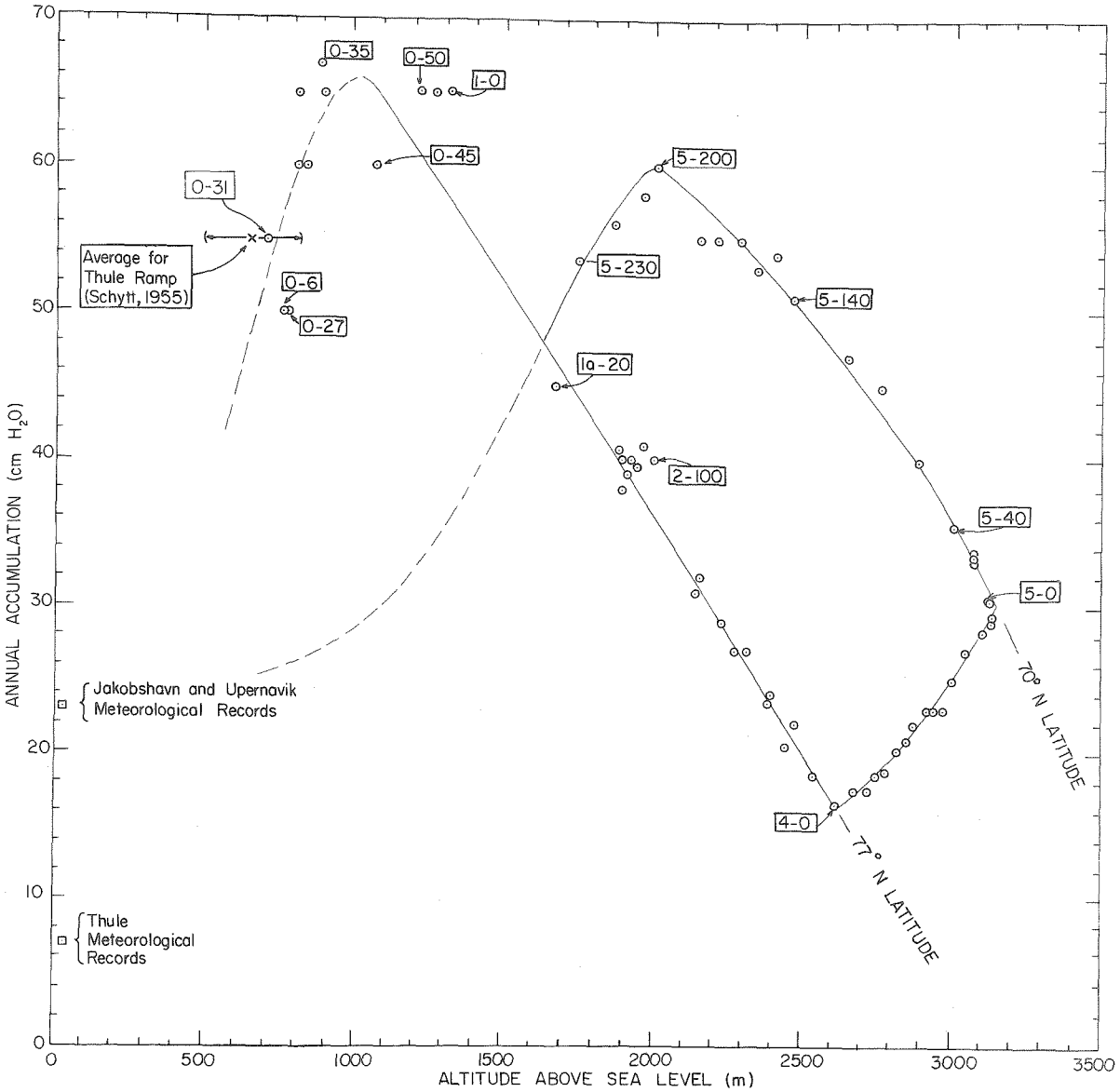

Figure 29.--Accumulation-altitude relationship on the west slope of the Greenland ice sheet. Points are from south- or west-facing slopes, i.e., windward slopes to storm winds (see p. 81). Each point represents an average of several years accumulation (see Fig. 28). Data from meteorological records are anomalously low because of incomplete gage-catch (p. 83). The Thule data are not representative for the coast of Melville Bay at 76°N because Thule lies in a precipitation shadow. The sea level accumulation value for south-facing slopes at 76-77°N is estimated to be at least 30 cm H_2O per year.

3.3 cm H_2O per 100 m) reported by Lee (1941) above the zone of maximum precipitation in the Sierra-Nevada Mountains.

Fewer data are available from windward slopes below the zones of maximum accumulation in Greenland than from above. Schytt's (1955) measurements of the 1953-1954 accumulation between 0-0 and 0-20 are compatible with the results of this study and his average of 55 cm H_2O is indicated in Figure 29. His minimum accumulation of 28 cm H_2O was definitely influenced by local topography on Thule Ramp (Schytt, 1955, p. 18). An estimate for the minimum annual accumulation in the TUTO area based on data sheet 1 and Schytt's work, is 45 ± 5 cm H_2O per year.

Average annual precipitation values from meteorological stations at Thule and Jakobshavn, located near sea level at the north and south extremes of the traverse, respectively, and Upernavik, midway between the extremes, are also indicated in Figure 29. However, it is necessary to qualify the use of these data on two points: (1) Measurements made at a meteorological station relate to a single point and the exact location and exposure of the precipitation gage is very important. For example, the Thule station is definitely in the precipitation shadow of Thule peninsula. Measurement of the water equivalent of yearly snow deposition over extended traverses, or snow-survey courses (Church, 1933, 1942), enables one to recognize such local irregularities. (2) The

percent of precipitation caught by standard, unshielded* precipitation gages decreases with increased wind speed (Brooks, 1938; Wilson, 1954). This is true regardless of whether the precipitation is in the form of rain or snow, but the lowest catch percentages, about 25%, occur in the case of snow storms. Black (1954) found that precipitation values recorded by the standard eight-inch precipitation gage at Barrow, Alaska were 2 to 4 times lower than those obtained by measuring the water equivalent of snow on the tundra. In general, precipitation in at least some, and perhaps many, arctic regions is greater than recorded values indicate. In Greenland, the two shortcomings of standard precipitation gages (location at a single point, and incomplete catch) can be eliminated by using the ice sheet as an infinite set of automatically recording precipitation gages.

Accumulation contour map

A contour map** of gross annual accumulation based on

---

*See Warnick (1953) for a discussion of recent experimental work aimed at improving the efficiency of precipitation gages by various types of shielding

**An accumulation contour map published by Diamond (1958) is erroneous because the published value (Benson, 1955a) of 60 cm H_2O per year at 1-0 was quoted as 20. Also the values quoted for the 1955 "JELLO" traverse were preliminary estimates prepared for internal use at SIPRE and not intended for publication. Since it was not known that these estimates were to be published the necessary corrections were not applied to them.

all available data,* is shown in Figure 30. In general, the accumulation contours follow the north-south trend of the coast lines. The zone of maximum precipitation lies close to the coast in two locations, one on the east coast between Angmagssalik and Scoresbysund, the other on the west coast between Upernavik and Thule.

The west coast swings from north-south to east-west to form the north shore of Melville Bay at 76°N. Cyclonic storms moving northward along the coast either ascend Thule peninsula here, or are deflected westward to Devon and Ellesmere Islands. Accordingly the ice sheet near the coast between 74°30' and 76°30'N, and the east facing shores of the Canadian Islands between 75 and 81°N receive relatively heavy precipitation.

Storms from the Icelandic low pressure region meet

---

*Mr. James A. Bender of SIPRE, using the methods described herein, measured the accumulation at each of the three HIRAN stations. Data from the British North Greenland Expedition are based on 5 pits and 30 Rammsonde profiles (Bull, 1958). The data of Koch-Wegener were obtained by using the same stratigraphic unit employed in this work, i.e. the discontinuity between the high density snow and the underlying softer snow. They also adjusted their data so that a full year's accumulation, from one fall level to the next was measured. This was necessary because they were in the area during June and July and therefore did not directly observe a full year's accumulation. The correction was of the same sort made in this work (see Fig. 26). DeQuervain's data were not adjusted and as annual values are at least 5 cm too low, therefore, 5 cm H_2O were added to his values before entering them in Figure 30. Recorded precipitation from coastal stations are listed; more than 50 years of record were averaged at all stations except Thule, Alert, and Brønlund Fjord which cover 8, 3, and 2 years respectively.

Figure 30.--Contours of gross annual accumulation. See Figure 1 for identity of data points. Data from this study are based on averages of several years accumulation (see Fig. 28). Data from Koch and Wegener (1930) were based on the same stratigraphic unit used in this study. Data from De Quervain and Mercanton (1925) have been adjusted by adding 5 cm H_2O to each value before entering it on the map. Data from the British North Greenland Expedition Bull (1958) are primarily based on Rammsonde profiles (see p. 85). Average precipitation values at coastal stations are indicated (see p. 85).

Greenland's highest mountain barrier, over 3000 m altitude, on the east coast between Angmagssalik and Scoresbysund. This results in heavy precipitation on the windward, i.e., south and east-facing, slopes here and a precipitation shadow to the north. Few data are available for this region and the contours are based on: (1) The 90 cm H_2O per year precipitation recorded at Angmagssalik compared with 23 cm measured 300 km north of Angmagssalik at 3000 m altitude on the ice sheet, (2) numerous glaciers flowing into the sea south of Scoresbysund compared to the dry, unglaciated regions to the north, (3) the assumption that the zone of maximum precipitation lies below 2000 m here as it does on the west side of the ice sheet (Fig. 29), and (4) the analogous effect on precipitation exerted by Thule peninsula in northwest Greenland.

Few data points are available on the ice sheet south of 66°N. Accumulation contours are extrapolated through this region, based on precipitation records at Godthaab, Ivigtut, and Angmagssalik and on the accumulation-altitude relations observed (Fig. 29) farther north.

Independent Checks on the Stratigraphic Interpretations

Stratigraphic correlation in northwest Greenland was well established by 1954 (see Figs. 22 to 25 and Benson [1959]). However, the work only included 100 miles of traverse in the

dry-snow facies. Stratigraphy in the dry-snow facies must be interpreted in the absence of melt evidence, whereas in the percolation facies, traces of melt evidence are useful in correlation. During the 1955 expedition, strata were successfully correlated from the percolation facies at 77°N through about 500 miles of the dry-snow facies and back into the percolation facies at 71°N (see data sheets). This, in itself, is considered a test of the method, but two independent checks exist and are described below.

Correlation between stratigraphic and meteorological records

Data at 1-0 extended 14.4 m below the snow surface in 1954. This represents a period of 11 years (1943 to 1954). The stratigraphic record shows that the degree of melt action varied considerably from year to year during this period. If the amount of summer melt can be related to summer warmth, then meteorological records from coastal stations may provide a useful check on stratigraphic interpretations, at stations near enough to be subject to the same general weather pattern. Thule is 70 miles from 1-0 and its meteorological records are continuous from 1947 to date. A single parameter, indicative of relative summer warmth may be obtained by summing degree days above freezing for each year. The calculations are based on average daily temperatures, i.e., if the average temperature on a particular day is 8°C, it is counted as 8 degree days above freezing. The results are plotted in Figure 31.

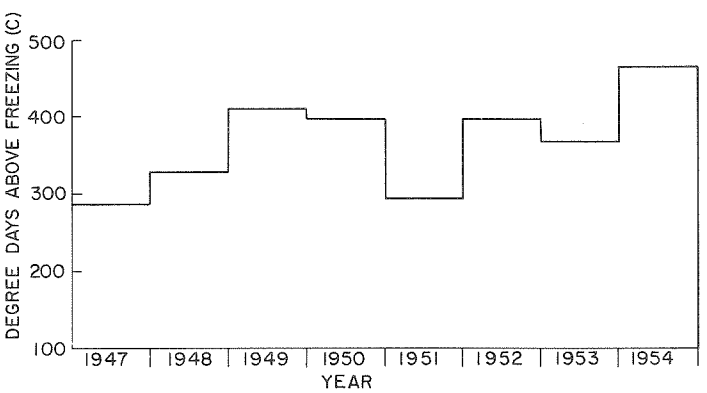

Figure 31.--Degree days above freezing at Thule, Greenland 1947-1954. Data from U.S. Weather Bureau and USAF Air Weather Service.

The years 1947 and 1951, which produced the least melt at 1-0, are the coldest recorded at Thule. The heaviest melt recorded between Thule and 2-150 occurred in July 1954, and this is the warmest year on the Thule record. The moderately heavy melt during 1949, 1950, 1952, and 1953 correspond to years which are colder than 1954 but warmer than 1947 or 1951.

A word of caution may be appropriate regarding the correlation of warm years with abundance of melt evidence. A few very warm days may produce heavy melt action in firn, and such a brief "heat wave" may occur during an otherwise cool summer. However, the general agreement between Figure 31 and the record at 1-0 on data sheet 3 is satisfying; it agrees with the interpretations shown in Figures 22 to 25 and provides an independent check on the stratigraphic methods.

O^{18}/O^{16} Ratios in snow and firn layers

Variations in the O^{18} content of waters from natural sources are discussed by Epstein and Mayeda (1953). The variation is temperature-dependent and it was expected that differences between summer and winter precipitation on the ice sheet would be recorded in the O^{18}/O^{16} ratios of firn strata. During 1954 and 1955 a total of 300 samples were taken for study of the general relationship between O^{18}/O^{16} ratios and firn stratigraphy on the Greenland ice sheet (Epstein and Benson [1959]). For the present it is sufficient

to state two major results:

(1) The altitudinal effect: Snow deposited from a single storm shows lower O^{18}/O^{16} ratios at higher altitudes.

> "In terms of per mil variation per 1,000 ft of altitude, it is approximately 1.8 in northern Greenland, 1.7 on the west slope of the Sierra Nevada in California, 1.6 in the Pasadena area, California, and 0.6 on the Saskatchewan Glacier. The last value may not be reliable because of incomplate sampling" (Epstein and Sharp, 1959, p. 91).

(2) The seasonal effect: Snow deposited in winter has less O^{18} than that deposited in summer. This produces an annual variation in O^{18}/O^{16} ratios which was observed by sampling every stratigraphic unit in the upper 4 meters at Stations 2-225 (total of 47 samples) and 4-200 (total of 59 samples). Samples through at least two yearly cycles were taken at Stations: 1-0 (1954), 2-70 (1954), 2-100 (1954), 1a-20 (1955), 2-150 (1955), 4-75 (1955), and 5-40 (1955); and samples across the fall discontinuity were taken at 12 of the stations between 4-275 and 5-230.

Comparison between O^{18}/O^{16} ratios and standard stratigraphic measurements are shown in Figure 32 and at Station 1a-20 on data sheet 4. Confidence in the interpretation of firn stratigraphy is gained by the agreement between the three independent methods of approaching the problem presented above.

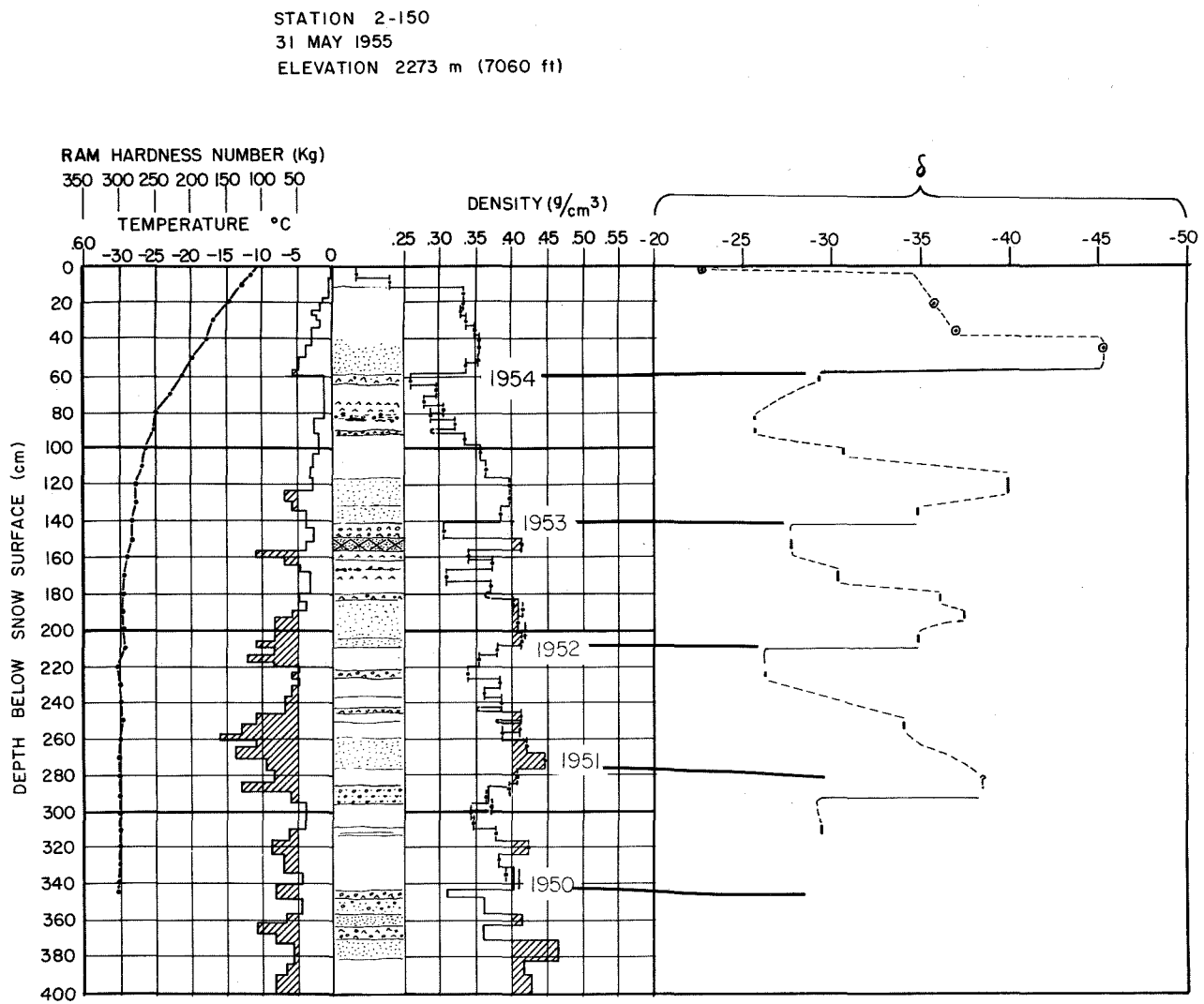

Figure 32a.--Standard stratigraphic data at Station 2-150 compared with O^{18}/O^{16} ratios; δ is the O^{18}/O^{16} ratio relative to mean ocean water, it is defined on page 94.

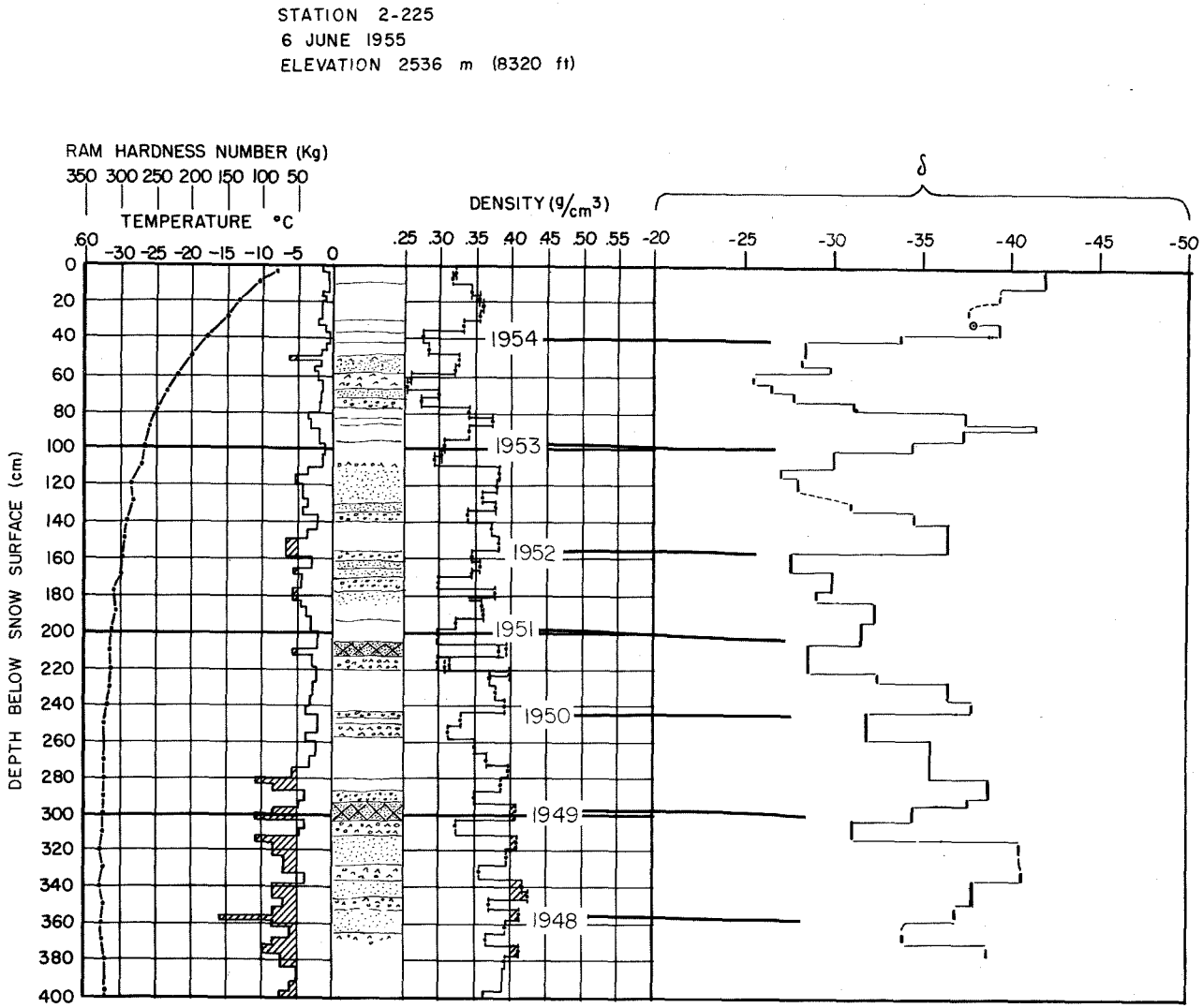

Figure 32b.--Standard stratigraphic data at Station 2-225 compared with O^{18}/O^{16} ratios; δ is the O^{18}/O^{16} ratio relative to mean ocean water, it is defined on page 94.

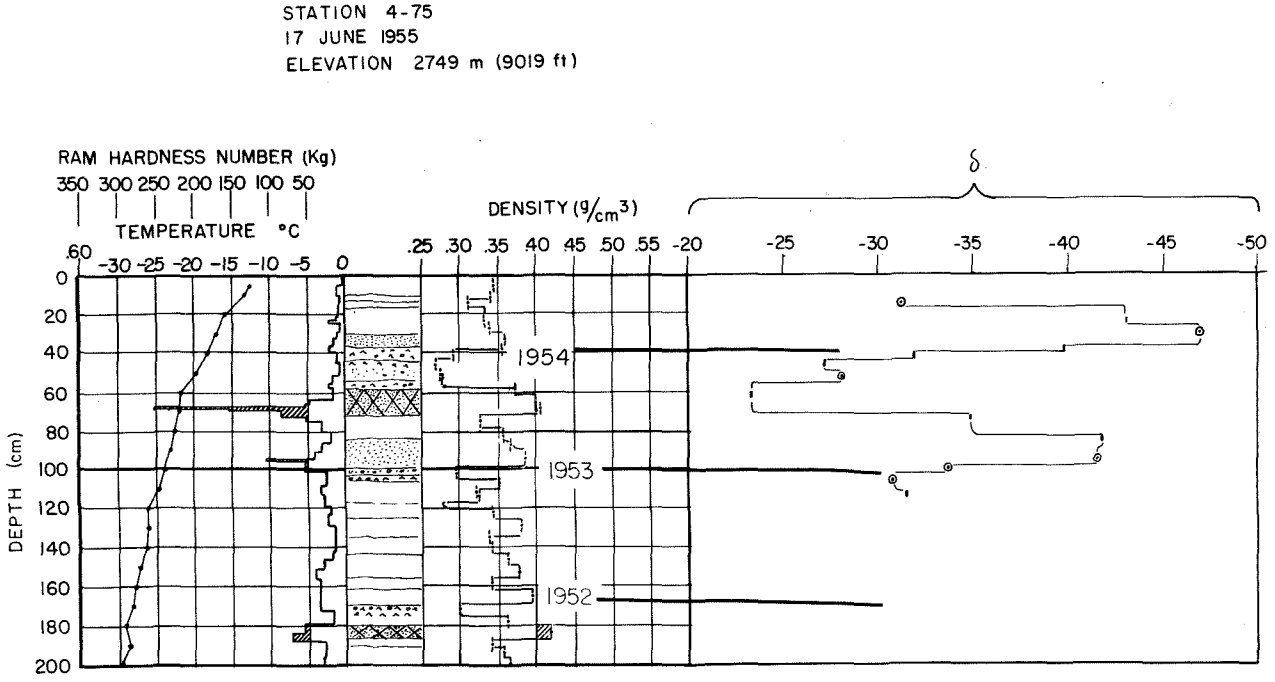

Figure 32c.--Standard stratigraphic data at Station 4-75 compared with O^{18}/O^{16} ratios. The data are expressed in terms of deviations from mean ocean water by the relation

$$\delta = \left[\frac{R_{(sample)} - R_{(standard)}}{R_{(standard)}}\right] \times 1000 = 1000 \left[\frac{R_{sample}}{R_{standard}} - 1\right] ,$$

where R is the ratio H_2O^{18}/H_2O^{16}.

δ = 0.00 for mean ocean water by definition (Epstein and Mayeda, 1953). Thus δ = -10 means that O^{18}/O^{16} ratio of the sample is 1% or 10‰ lower than that of mean ocean water. The fall discontinuity as seen in the stratigraphic record correlates well with an abrupt change in the O^{18}/O^{16} ratios. In Figure 32c the wind slab formed during the 1954 summer has the highest O^{18}/O^{16} ratio. This suggests that it was formed during the 11-14 July 1954 heat wave which left melt evidence at altitudes below 7000 ft at this latitude.

CHAPTER IV

DIAGENETIC FACIES--A CLASSIFICATION OF GLACIERS

Diagenetic facies on glaciers are defined on page 47. The purpose of this chapter is to demonstrate the differences between these facies and to show that their boundaries can be located by physical measurements.

Temperature

Seasonal temperature variation on the snow surface

Data. Air temperature measurements, made in a standard meteorological instrument shelter for periods of at least one year, are available from two locations on the ice sheet (2-100 and 5-40) as follows:

Station	Time interval	Observer
2-100 (site II)	7 July 1953 - 31 May 1956	U.S.A.F. Air Weather Service
*5-40 (French Central Station)	5 Sept 1949 - 15 Aug 1951	Expedition Polaires Francaise
5-40 (Eismitte)	1 Aug 1930 - 6 Aug 1931	Johannes Georgi

*(Not completely published as of June 1959).

Air temperatures measured in weather shelters are not obtained at constant height above the snow surface because

of accumulation of new snow and snow drifting. For example, Georgi's thermometer varied in height from 1.20 to 2.21 m above the snow surface. To obtain uniformity, Georgi devised and built an instrument to measure the air temperature 10 cm above the prevailing snow surface. These measurements began in February. He estimated the temperature difference between the shelter and a point 10 cm above the snow surface for the months preceding February. The snow surface temperature itself was estimated from the 10 cm values. The corrections are small compared with the marked variation in air temperature during a year but, Georgi points out that the estimates of snow-surface temperatures are improved by applying them.* Georgi's estimated monthly averages of snow-surface temperature at Eismitte are listed with observed air temperature data in Table I.

No data are available to adjust the U.S.A.F. data to obtain snow-surface temperatures. However, it will be assumed that negligible error is made if Georgi's corrections are applied. The monthly averages for 2-100 are listed in Table II.

Analysis. Sorge (1935, pp. 232-236) showed that the snow-surface temperatures of Table I can be represented by

---

*Measurements by Nyberg (1938) indicate that the increase of temperature with height, in the 1st 10 cm above the snow surface, is an order of magnitude greater than estimated by Georgi (footnote added in proof reading).

Table I

Monthly mean temperatures at Eismitte* (°C)
(1930-1931)

Month	Air temp in the instrument shelter	Correction according to Georgi	Air temp 10 cm over the snow surface (rounded off)	Correction (estimated)	Temp of the snow surface
Aug	-17.7	0°	-17.7	0	-17.7
Sept	-22.1	-0.5°	-22.6	0	-22.6
Oct	-35.6	-1°	-36.6	-0.1	-36.7
Nov	-43.1	-1.5°	-44.6	-0.2	-44.8
Dec	-38.8	-1.5°	-40.3	-0.2	-40.5
Jan	-41.7	-2°	-43.7	-0.3	-44.0
Feb	-47.5	-1.75°	-49.0	-0.2	-49.2
Mar	-39.4	-1.00°	-40.4	-0.1	-40.5
Apr	-31.0	+0.12°	-50.9	0	-50.9
May	-20.1	+0.85°	-19.5	+0.1	-19.2
June	-15.3	+0.86°	-14.4	+0.1	-14.5
July	-10.8	-0.12°	-10.9	0	-10.9
Average	-30.2		-30.85		-30.94

*Eismitte of 1930-31 was the French Station Centrale of 1949-51 and Station 5-40 of this study.

Table II

Air temperature data for Station 2-100, Greenland

Month	Air temperature-°C 1953	1954	1955	1956	Average	Georgi's correction	Temp at snow surface
1 Jan	-	31.67	36.11	36.83	34.8	-2.3	-37.1
2 Feb	-	30.56	31.11	35.67	32.4	-1.95	-34.4
3 March	-	33.89	34.44	35.22	34.5	-1.10	-35.6
4 Apr	-	23.89	30.67	26.72	27.1	+0.12	-27.0
5 May	-	16.11	16.44	19.50	17.3	+0.93	-16.4
6 June	-	8.89	8.33	-	8.61*	+0.96	- 7.6
7 July	-	6.11	8.22	-	7.16*	-0.12	- 7.3
8 Aug	8.33	7.22	12.00	-	9.17	0.0	- 9.2
9 Sept	20.00	**	18.94	-	19.44*	-0.5	-19.9
10 Oct	28.89	25.56	18.22	-	24.20	-1.1	-25.3
11 Nov	35.00	27.78	31.72	-	31.50	-1.7	-33.2
12 Dec	41.67	38.33	36.78	-	38.90	-1.7	-40.6
Average		-22.5	-23.6		-23.8		-24.4

* Based on data from 2 years only.

** Average of 1953 and 1955 data was used for Sept 1954.

the first two terms of a Fourier series, i.e.:

$$f(t) = \sum_{n=o}^{2} \left(P_n \cos nt + q_n \sin nt \right),$$

$$= P_o + P_1 \cos t + q_1 \sin t + p_2 \cos 2t + q_2 \sin 2t \qquad (1)$$

Equation 1 may be rewritten as a series involving cosine terms only,

$$f(t) = P_o + a_1 \cos(t - A_1) + a_2 \cos(2t - A_2) \qquad (2)$$

where the constants between equations 1 and 2 are related as follows:

$$a_1 = \sqrt{P_1^2 + q_1^2} \quad , \qquad A_1 = \tan^{-1} \frac{q_1}{P_1}$$

$$a_2 = \sqrt{P_2^2 + q_2^2} \quad , \qquad A_2 = \tan^{-1} \frac{q_2}{P_2}$$

The data from Station 2-100 (Table II) can also be represented by equations 1 and 2.

Values of the constants in equation 2 for the data of Tables I and II are summarized in Table III.

The phase angles are expressed in terms of angular degrees with 30 degrees set equal to 1 month and t = 0 on 15 July, so the phase angles in Table III give maximum values for the

Table III

Values of constants in equation 2

	5-40 Sorge's values	5-40* Sorge's values corrected	2-100 Average of 3 years data	2-100 1954 values only
P_o °C	-31.0	-31.0	-24.4	-23.2
P_1 °C	17.46	17.46	16.1	15.40
q_1 °C	- 1.63	- 1.63	- 0.552	- 0.948
P_2 °C	2.6	2.6	2.47	2.68
q_2 °C	- 1.6	- 1.6	- 0.197	- 0.317
a_1 °C	17.54	17.54	16.11	15.41
a_2 °C	3.03	3.05	2.48	2.70
A_1	-6°15'	-5°20'	-1°58'	-3.52°
A_2	-27°50'	-31°35'	-4°34'	-6.75°

*Numerical errors are present in Sorge's values a_2, A_1 and A_2, these are slight and do not affect his results.

year and half-year waves as follows:

Date of maximum value

Station	Year wave	Half-year wave
5-40	10 July	1 July
2-100 (3 yr average)	13 July	13 July
2-100 1954 data	12 July	12 July

In general the annual temperature variation on the snow surface has the same phase throughout the north-south extent of the region considered in this paper, i.e., 70°N to 77°N. It reaches its maximum within ± 2 days of 12 July. The existing data suggest that the maximum occurs slightly earlier in the south than in the north. The maximum deviation from mean annual temperature is nearly the same over the region but, according to the available data, it is about 10% greater at 70°N than at 77°N latitude.

Seasonal temperature variation below the snow surface

Data. The temperature profiles of Figure 33 show the seasonal temperature variation below the snow surface at Stations 1-0, 2-0, 2-50, 2-100, 2-120, and 2-200 in north Greenland. Similar curves for Station 5-40 (Eismitte of 1930-1931) were presented by Sorge (1935).

It may be seen that profiles measured at the same station

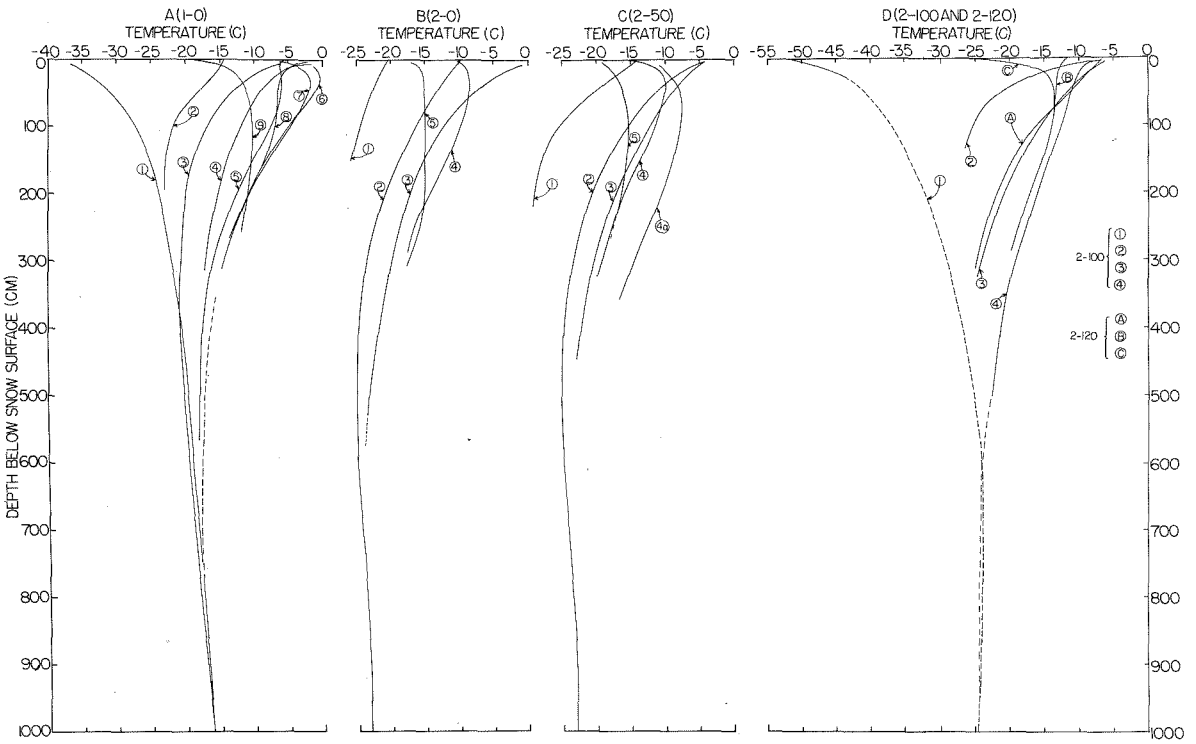

Figure 33.--Temperature profiles at Stations 1-0, 2-0, 2-50, 2-100, and 2-120.

Station			
1-0	1	3 March	1954[a]
	2	19 May	1955
	3	3 June	1954[a]
	4	6 July	1953
	5	18 July	1953
	6	17 August	1952
	7	18 August	1954[a]
	8	19 August	1953
	9	21 Sept	1953
2-0	1	22 May	1955
	2	21 June	1954
	3	27 July	1953
	4	21 Aug	1952
	5	19 Sept	1953

Station			
2-50	1	24 May	1955
	2	9 July	1954
	3	4 Aug	1953[b]
	4	21 Aug	1953[b]
	4a	21 Aug	1953[b]
	5	18 Sept	1953
2-100	1	? March	1954[c]
	2	28 May	1955
	3	7 July	1954
	4	26 Aug	1953
2-120[d]	A	1 July	1952
	B	30 Aug	1952
	C	3 Sept	1952

[a]From measurements by L. H. Nobles.

[b]Curve 4 was measured in undisturbed snow 50 m from the pit of 4 August; 4a was measured 1 m from the test wall of the 4 August pit.

[c]Curve 2 based on observations in the winter by G. E. Frankenstein and the mean annual value at the deep pit.

[d]Curve A measured by H. Bader within 1 mile of the 1954 Survey area pit B. Curves B and C were obtained at 2-120, 1952. The elevations are nearly equal at these locations (See Figs. 1 and 2).

in different years, but at about the same time of year are remarkably similar. For example, the curves measured on 17 August 1952, 19 August 1953, and 18 August 1954, at station 1-0 are practically indistimguishable below 160 cm. It is assumed that this annual reproducibility of temperature profiles implies that the ice sheet climate is sufficiently constant to permit comparison between temperature profiles, measured in four different years, as if they were all from the same year. Thus, at Station 2-0 (Fig. 33) the measurements made at nearly the same time of month in May, 1955; June, 1954; July, 1953; August, 1952; and September, 1953, illustrate a part of the annual cycle.

To evaluate temperature as a variable on the ice sheet its distribution at a given time must be known. As a parameter in defining facies temperatures should be measured in the upper 3 to 5 m during the peak of the melt season. It has not been possible to obtain simultaneous measurements over a large area of the ice sheet,but temperature profiles obtained in August are available for most of the north (77°N) and south (70°N) legs of the traverse, i.e., 0-0 to 4-0 and 5-0 to 5-230 (Figs. 34a, b). These curves illustrate the altitudinal variation in firn temperature, during late summer, in the most familiar form, i.e., temperature plotted against depth. However, to locate facies boundaries it is useful to represent the above data as isotherms in the top 4 to 5 m of firn with altitude as the abscissa. Table IV and

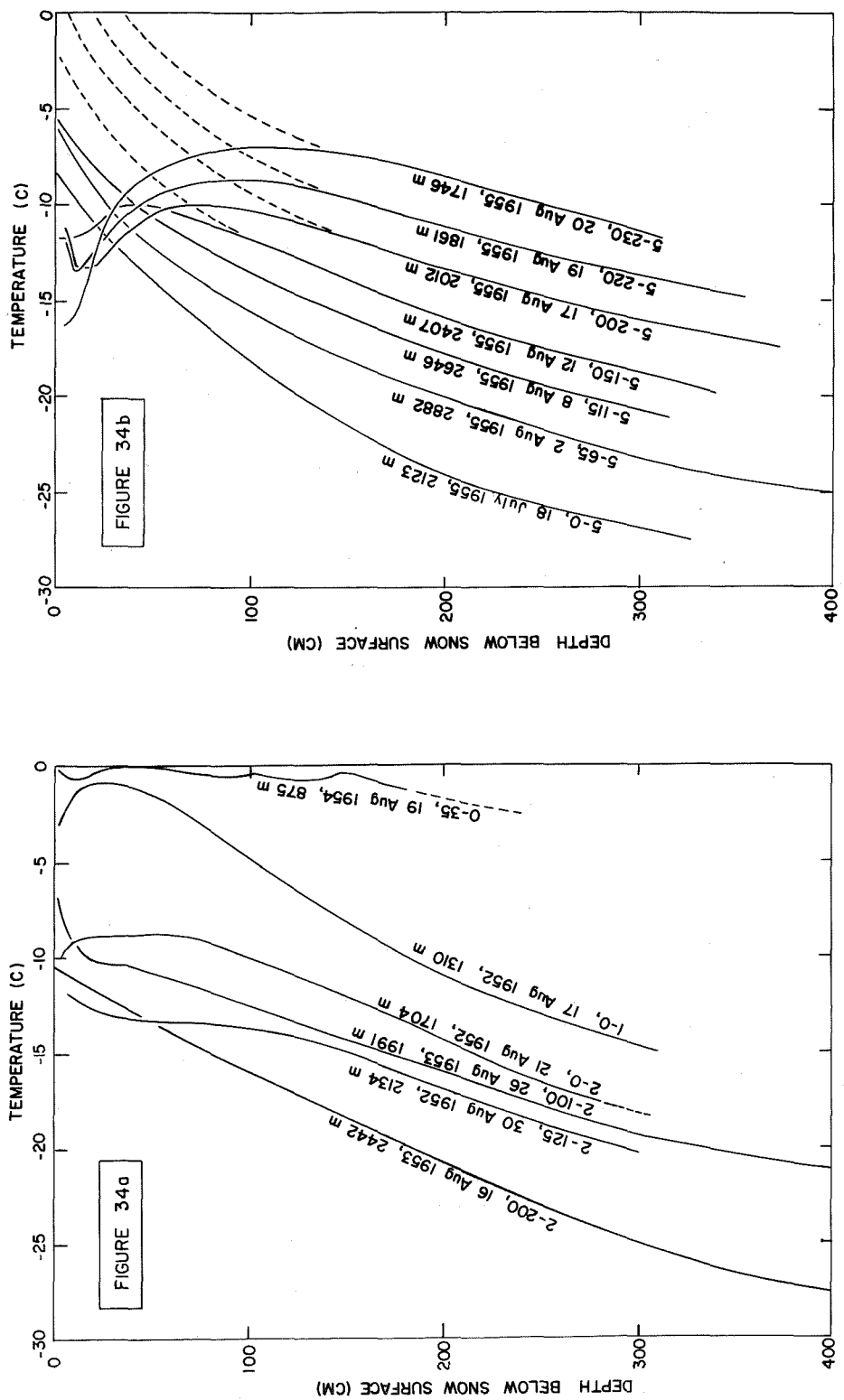

Figure 34.--Temperature profiles measured in late summer on the west slope of the Greenland ice sheet.

a.--Measurements over a 1560 m (5120 ft) range of altitude at 77.0±0.3°N Latitude.

b.--Measurements over a 1380 m (4530 ft) range of altitude at 70.4±7°N Latitude.

-105-

Table IV

Location of isotherms during peak of the melt season at:
(A) 77.0±0.3°N and (B) 70.4±0.7°N

Station	Elevation (m)	Date	Depth below snow surface (cm) 0°C	-5°C	-10°C	-15°C	-20°C	-25°C	-30°C
A									
2-200	2442	15-8-53	- -	- -	- -	80	184	304	- -
2-180	2387	15-8-53	- -	- -	0	100	200	- -	- -
2-160	2313	14-8-53	- -	- -	20	120	215	- -	- -
2-140	2228	14-8-53	- -	- -	24	120	219	- -	- -
2-120	2140	11-8-53	- -	- -	35	140	250	- -	- -
2-120	2134	30-8-52	- -	- -	- (35)	140	290	- -	- -
2-100	1990	26-8-53	- (0)*	- (10)	25 (45)	170	330	- -	- -
2-30	1887	23-8-52	- (0)	- (30)	60 (70)	170	-	- -	- -
2-0	1704	21-8-52	- (5)	50	100	212	370	- -	- -
1-0	1302	17-8-52	- (30)	100	184	320	- -	- -	- -
1-0	1302	18-8-54	- (35)	100	184	-	- -	- -	- -
0-35	914	16-7-53	180 (220)						
0-35	914	19-8-54	170						
B									
5-0	3123	18-7-55	- -	-	13	70	130	230	420
5-20	3072	20-7-55	- -	-	-	85	150	270	
5-40	3005	23-7-55	- -	-	6 (5)	75	165 (170)	290	
5-65	2882	2-8-55	- -	4	30 (25)	100	205	380	
5-90	2763	6-8-55	- -	4	18 (20)	125	250		
5-115	2646	8-8-55	- -	- (4)	40	135	270		
5-140	2466	10-8-55	- -	- (10)	60	165	340		
5-150	2407	12-8-55	- (0)	- (10)	50 (70)	180	340		
5-160	2342	13-8-55	- (0)	2 (10)	10-80 (85)	190	- (400)		
5-170	2283	14-8-55	- (0)	- (10)	50 (85)	15/205	- (400)		
5-180	2206	15-8-55	- (0)	- (15)	60 (85)	220			
5-190	2146	16-8-55	- (5)	- (25)	65 (100)	230			
5-200	2012	17-8-55	- (10)	- (30)	80 (110)	255			
5-210	1963	18-8-55	- (10)	- (40)	50/105 (115)	0/300			
5-220	1861	19-8-55	- (20)	- (50)	40/160 (180)	355			
5-230	1746	20-8-55	- (30)	- (90)	30/155 265	13			
French Camp VI	1598	28-8-50	- -	(-5.8°C) 500	800	4000			

*Extrapolated values indicate depths at peak of melt season (see p. 107), all extrapolated values are enclosed in parentheses. The extrapolated values are plotted in Figure 35 and the unadjusted values are plotted in Figure 38.

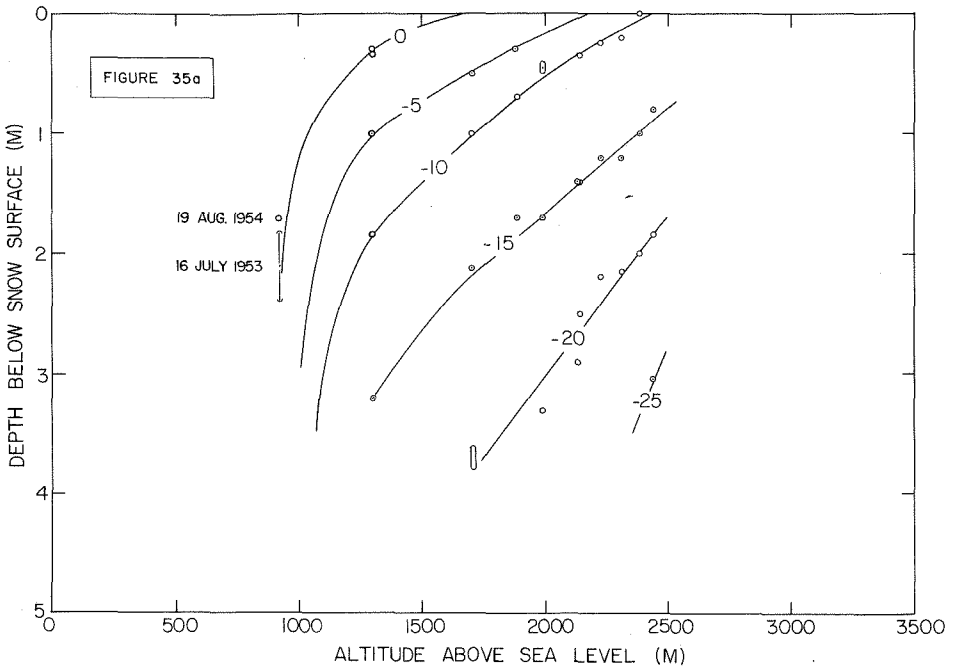

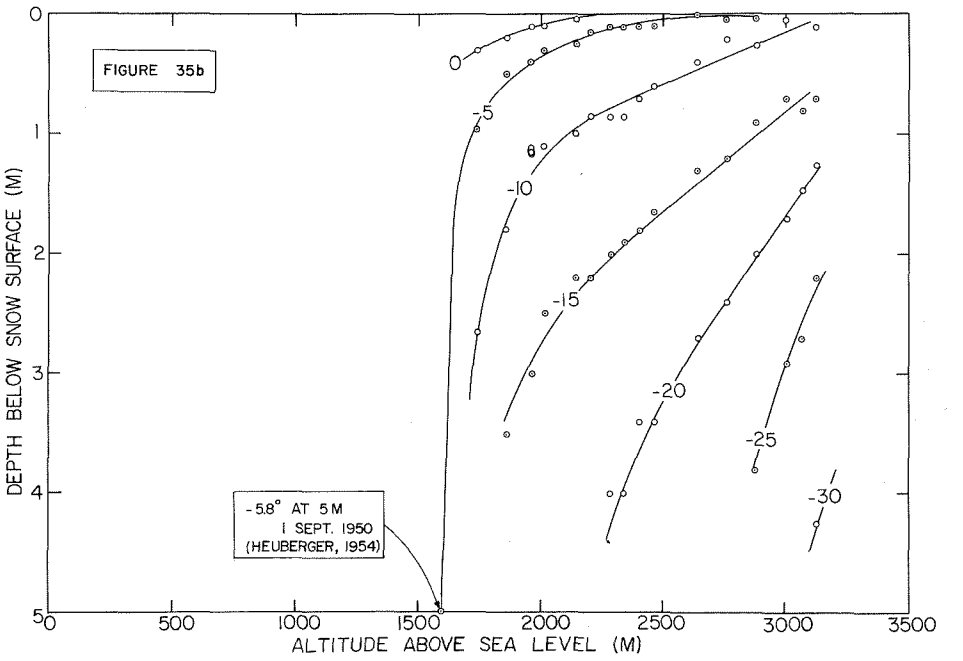

Figure 35.--Isotherms in the upper 5 m on the west slope of the Greenland ice sheet during the peak of the melt season. Data points are from Table IV.

a. 77.0±0.3°N Latitude

b. 70.4±0.7°N Latitude

Figures 35a, b, summarize the data in this form. The main goal of this representation is to show the maximum penetration of isotherms during the melt season. Clearly, the top 1-2 m of some temperature profiles are measurably influenced by the fall cooling wave. In such cases a reasonable estimate of temperatures during the peak of the melt season may be obtained by extrapolation as shown in Figure 34b. The amount of melt evidence in the upper layers, together with the shape of July profiles, is used to guide the extrapolation. All extrapolations are indicated in Table IV.

Analysis. Sorge (1935, pp. 236-263) carried out a detailed mathematical analysis of the annual temperature variation with depth at Eismitte (Station 5-40). He assumed that heat is transferred in the snow and firn purely by conduction and used the function:

$$f(z,t) = R_o e^{-z\sqrt{\frac{\pi}{T\alpha}}} \cos\left(\frac{2\pi t}{T} - z\sqrt{\frac{\pi}{T\alpha}}\right) , \qquad (3)$$

where

R_o is the amplitude* of temperature on the snow surface.

T is Period (in our problem the period is 1 year for the year wave and one-half year for the half-year wave).

---

*Sorge uses the term "halbamplitude" for R_o but from the equation he means "amplitude" which is the half range. The use of "halbamplitude" for amplitude and "amplitude" for range is inconsistent in his paper. The term "amplitude" means half range except on pages 237, 240, 246, 257, and 259.

α is the thermal diffusivity of firn.

$R_z = R_o e^{-z\sqrt{\frac{\pi}{T\alpha}}}$ gives the amplitude of the temperature variation at the depth z.

The term "$z\sqrt{\frac{\pi}{T\alpha}}$" gives the phase angle at the depth z.

The temperature variation on the snow surface is expressed as the sum of two cosine terms. Therefore the temperature function at any depth may be obtained by substituting each of these surface functions separately into equation 3 and adding the results. This can be done as soon as values for α, the thermal diffusivity, are known. Sorge (1935, pp. 237-239) points out that it is not correct to compute α by making a least squares analysis of the observed temperature variations, because the snow surface is not constant, as it always receives new accumulation, and the value of α itself is not constant over the depth range considered. A functional relationship between α and firn-density was experimentally determined, and values of α obtained from it were used to compute the temperature variations with depth. The computed and observed temperatures agreed closely; this fact was interpreted as additional proof of the relation between α and ρ. The density profiles from Stations 2-100 and 5-40 are so close that negligible error is made if Sorge's values of α are used in analyzing* the

---

*This type of analysis does not give the complete picture because heat is also transferred in the upper layers by

annual temperature depth relations at 2-100.

Computed annual temperature variations at the snow surface and at several depths below the snow surface are plotted in Figure 36.

Maximum computed deviations from the mean annual value in the top 16 m of firn at Stations 5-40 and 2-100, presented in Table V, show two features immediately:

(a) The firn temperature 10 m below snow surface is never more than 0.3°C from the mean annual value.

(b) If the mean annual temperature is -20°C or greater, the snow surface will be occasionally exposed to melting temperatures for a period of at least one month.

The occurrence of melting on the snow surface has been neglected in the analysis. Therefore, the analysis may give positive temperatures for the snow surface at some locations. All positive values must be considered to be 0°C. They cause the actual mean annual temperature to be higher than computed.

Temperature values obtained at depths shallower than 10 m deviate from the mean annual value by more than 0.3°C. However, a correction for the deviation from mean value at a given date and depth can be computed from equation 3. This is done in Appendix II; no depths less than 3 m were used in an attempt to minimize the effects of convection (see pp. 118-119).

---

convection. The effects of this are discussed on pages 118-119, but first an analysis of temperature variations below the snow surface will be carried out using equation 3.

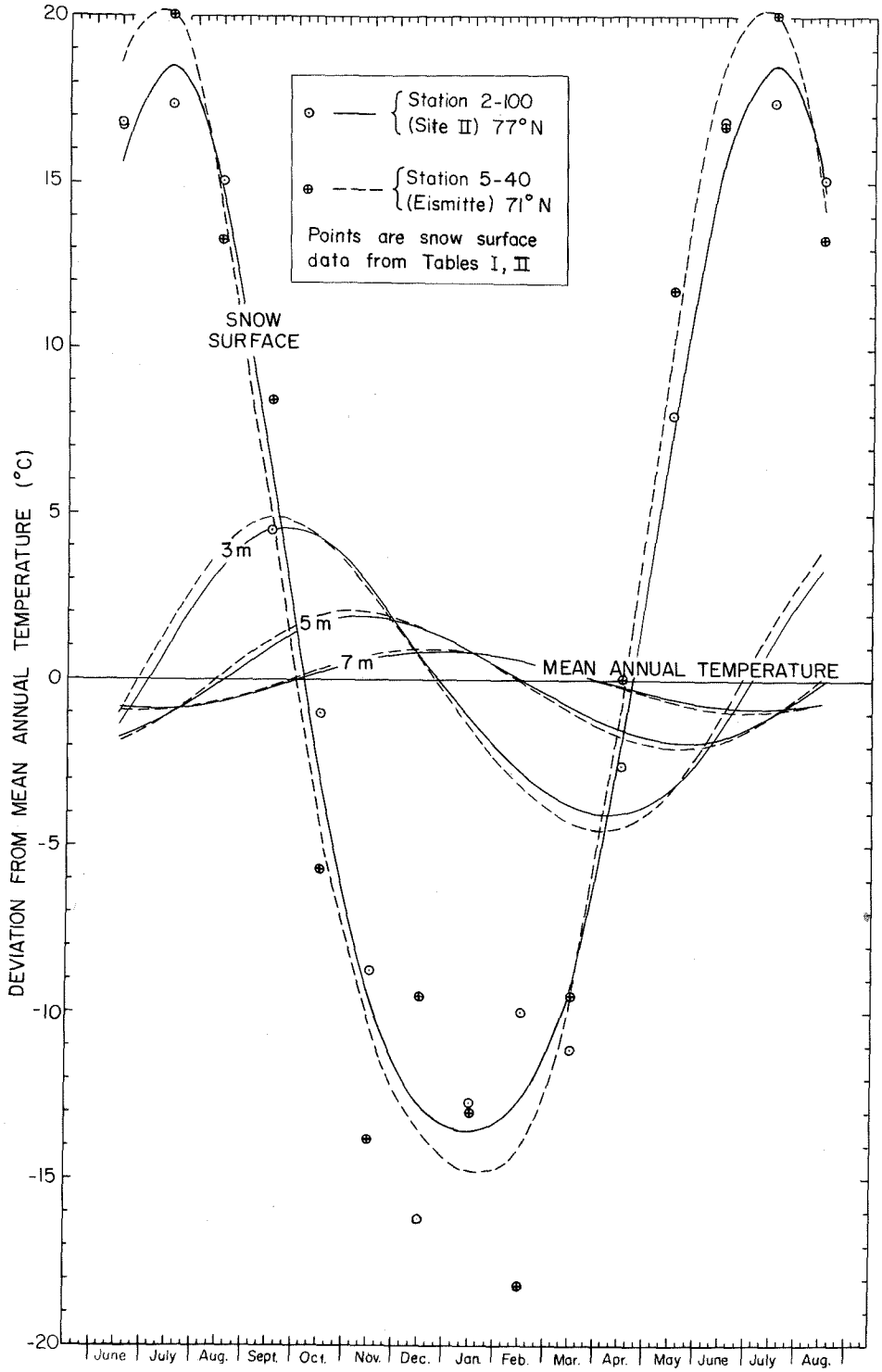

Figure 36.--Annual temperature variations at the snow surface and at depths 3, 5, and 7 m below the surface. Curves for the snow surface were computed from equation 2 with values of constants from Table III. Curves for depths below the surface were computed from equation 3. Data points are from the snow surface at Station 5-40 (Eismitte Table I); and Station 2-100 (Table II).

Table V

Maximum theoretical deviation (°C) from mean annual temperature

Depth below snow surface (m)	71°N Station 5-40	77°N Station 2-100
0	20.59	18.59
1	12.73	11.51
2	8.00	7.28
3	5.13	4.66
4	3.33	3.03
5	2.20	2.00
6	1.46	1.34
7	0.983	0.899
8	0.667	0.609
9	0.464	0.414
10	0.310	0.284
11	0.216	0.198
12	0.143	0.132
13	0.102	0.094
14	0.071	0.065
15	0.048	0.044
16	0.034	0.031

Distribution of mean annual temperature on the ice sheet

The data of Appendix II, plotted against altitude in Figure 37 suggest the possibility of mapping the distribution of mean annual temperature on the ice sheet, because they indicate the rate of change of temperature with altitude and latitude.

Altitude gradient. The altitude gradients in Figure 37 can be related to processes in the atmosphere* by assuming that the air in contact with the snow surface has the same temperature as the snow. The altitude gradient is nearly 1°C/100 m at 70° and 77°N; this is essentially the magnitude of the dry-adiabatic rate of temperature change for vertically moving air. It is important to note that these gradients refer to the rate of change of temperature measured along the surface of the ice sheet (or a parallel surface 10 m below the snow surface) and are not to be confused with the meteorological "lapse-rate" which refers only to the vertical temperature gradient $(\frac{dT}{dz})$ in the free atmosphere. The lapse rate is not generally applicable to air temperature measurements made at different elevations along the surface of the earth, because horizontal variations in air masses may be encountered. This is especially true in Greenland because the lapse rate over the entire ice sheet is usually positive as a result of strong inversions; whereas the rate of change

*A summary of the meteorological concepts and terms involved in this discussion is given in Appendix I.

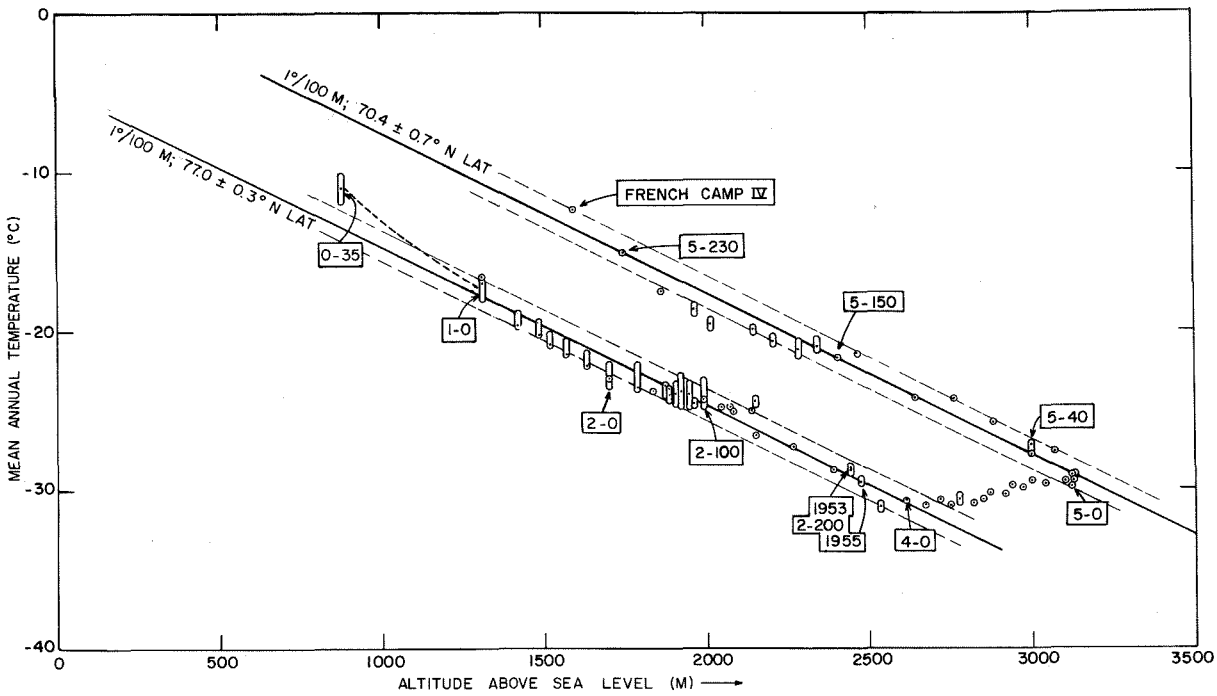

Figure 37.--Mean annual temperature plotted against altitude on the west slope of the Greenland ice sheet. The error in temperature values varies from ± 0.5 to 1.0°C (Appendix II). The absolute altitude values are known to within about ± 30 m; but the relative error between stations is less than this. The altitude gradient at 77 and 70°N is approximately 1°C/100 m whereas the altitude and latitude effects nearly cancel each other on the north-south leg between Stations 4-0 and 5-0. The dashed lines indicate a ± 1°C range around the gradient at 77 and 70°N.

of temperature along the surface (Fig. 37) is close to or even greater than the dry-adiabatic rate.

In continental arctic regions and especially over snow surfaces, strong inversions are commonly formed as the ground is cooled by net outgoing radiation (Wexler, 1936). Typical inversions in polar continental air often extend 1 or 2 km above the earth's surface and are in turn overlain by a nearly isothermal layer; the normal negative lapse rate is generally not found below 2 km in winter. The result of this temperature distribution is an extremely stable stratification of air. A high density layer (with negligible vertical motion within it) about 500 m thick, covers the ice sheet and flows under the influence of gravity. This is the origin of the commonly observed katabatic winds.

The west slope of the ice sheet between 70° and 77°N is subject to winds from all directions, but two predominate; (1) katabatic winds from the southeast, and (2) cyclonic storm winds from the southwest. The katabatic winds are warmed according to the dry adiabatic rate as they descend along the surface of the ice sheet. The storm winds, composed of saturated air masses, cool at a rate considerably less than dry adiabatic as they rise along the surface of the ice sheet. If the gradients in Figure 37 are caused primarily by the movement of air over the snow surface, the implication is that the prevailing winds are katabatic. This agrees with observation, but does not lend support to the concept of a

glacial anticyclone.* It merely states that cyclonic storm winds, which nourish the ice sheet, do not significantly upset the thermal regimen of the upper firn layers. Instead, they produce minor perturbations in the thermal equilibrium controlled by the nearly constant drainage of cold air from the interior, the katabatic winds.

The above discussion is based on the assumption that temperature gradients along the snow surface are controlled entirely by adiabatic processes in the air moving over the surface. The effects of radiation are assumed constant over the region considered, and the analysis is not applicable in the soaked facies because of abundant melt.

Three factors in addition to the ascent of moisture-laden storm winds on the ice sheet, will cause the vertical temperature gradient recorded at a constant depth below the snow surface to deviate from the dry-adiabatic rate: (1) More efficient cooling of the snow surface by radiation occurs at higher elevations because the water vapor content of the air is lowest there. This tends to make the gradient along the snow surface larger than adiabatic. (2) Relatively more melt occurs at the lower of any two positions considered.

---

*Hobb's theory of the "glacial anticyclone" was based largely on the observed drainage of cold air radiating outward from the highest elevations. This is not adequate basis for his anticyclone theory. An excellent review of the meteorological data on Greenland and a critical appraisal of the glacial anticyclone theory may be found in Dorsey (1945), Matthes (1946), and Matthes and Belmont (1950).

This also makes the gradient along the snow surface larger than adiabatic. (3) The air of katabatic winds has greater ability to absorb moisture from the snow at the lower of any two elevations because its temperature is higher. This produces relatively more cooling by latent heat transfer at the lower elevation and tends to make the gradient less than adiabatic. However, the rate at which moisture is removed depends on wind speed; and, of two positions at the same elevation, the one with most wind action will have the lower snow temperature because of the greater heat loss in the desication process.

Deviations from the dry-adiabatic gradient observed during late summer at 77°N (Fig. 34a) may be evaluated in the light of the meteorological processes outlined above. Of the data in Figure 34a, those at 3 m depth are least dependent on local, short-duration meteorological perturbations; and, if only these values are used, the vertical temperature gradient between Stations 1-0 and 2-200 is 0.91°C/100 m. The gradient varies from one trail segment to the next as shown in Table VI.

The maximum deviations from the adiabatic gradient occur in the trail segments which terminate at 2-0; and they are attributed mainly to the wind action on the ridge crest (p. 65). Between positions 1-0 and 2-0 there is a significant difference in the amount of summer melting, and the maximum gradient is observed in this segment of the trail.

Table VI

Rate of temperature decrease with elevation along the surface, from measurements at 3 m below snow surface during summer at 77°N

Location	Elevation difference (m)	ΔT(°C)	Gradient °C/100 m
1-0 to 2-200	1139	10.4	0.91
1-0 to 2-0	402	3.3	0.82
2-0 to 2-100	286	1.5	0.52
2-100 to 2-200	451	5.6	1.24

This may be accounted for if the firn temperatures at 1-0 are higher than their "adiabatic value" because of melt action, while those at 2-0 are lower because of desication. Between 2-0 and 2-100, the difference in melt evidence is not great and the minimum gradient observed over this interval may be entirely due to desication at 2-0.

The overall gradient, from 1-0 to 2-200, is slightly less than adiabatic in late summer (0.91°C/100 m), but slightly greater when mean annual values are considered (1.05°C/100 m). Although these departures from the adiabatic gradient are not large, they are in the right direction because: (1) thermal control exercised by katabatic wind is weakest in summer, (2) heat loss by radiation is maximum during the winter, and (3) penetration onto the ice sheet by moisture-laden storm winds, with gradients only half as great as the

dry adiabatic, is most frequent in summer. This probably occurs because the high pressure area over the interior moves farther south in winter, tending to let only the very large storms penetrate deeply.

Vertical air temperature gradients measured during June and July, 1912 in south (66 to 67°N latitude) Greenland (DeQuervain and Mercanton, 1925, pp. 153-156) were greater than dry-adiabatic during times of strong outgoing radiation, approaching the dry-adiabatic while föhn (katabatic) winds prevailed, and less than half of the dry-adiabatic gradient during stormy or overcast days. These observations, combined with the observed gradient of mean annual temperature in the firn which is greater than the dry-adiabatic gradient, indicate that strong cooling by radiation is a prevailing mean annual condition which is accompanied by deep inversions and produces the katabatic winds.

Some uncertainty exists in the mean annual temperature values obtained by applying equation 3 to measurements, because convection was not considered. Air moves through the upper layers of the snow pack, and the associated convection is several times more effective in transporting heat than is conduction (Bey, 1951). The effects of convection decrease with depth and were minimized, in preparing Appendix II, by using no data from less than 3 m below the snow surface. All temperatures computed in Appendix II are probably within a degree of the value at 10 m, according to check-points existing

at stations where 10 m data are available.

Figure 38 compares observed isotherms (uncorrected data of Table IV) with those computed from equation 3 using an assumed altitude gradient of 1°C/100 m. It is clear that the fall cooling cycle has progressed more rapidly than indicated by the conduction model. The 0 and -5°C isotherms have been completely removed from the snow by mid August and the -10°C isotherm is well above its computed position. The difference between measured and computed values is attributed to convection and decreases with depth as expected.

Sorge (1935, p. 246) observed that maximum temperatures occurred earlier than computed down to 7 m below the snow surface, being 10-14 days early at 6-7 m. He attributed this deviation to convection caused by air circulation in the tunnel connecting the Eismitte living quarters with the glaciology pit. The presence of the tunnel undoubtedly influenced his measurements, but, air circulation through the porous snow alone causes noticeable convection as illustrated by Figure 38.

Latitude gradient. The latitude gradient may be obtained from two independent sets of data. First, from measurements on the ice sheet itself (Fig. 37) and second, from sea-level meteorological stations on the west coast of Greenland. Mean annual temperatures on the ice sheet are known with greatest accuracy at Stations 2-100 and 5-40. They indicate the

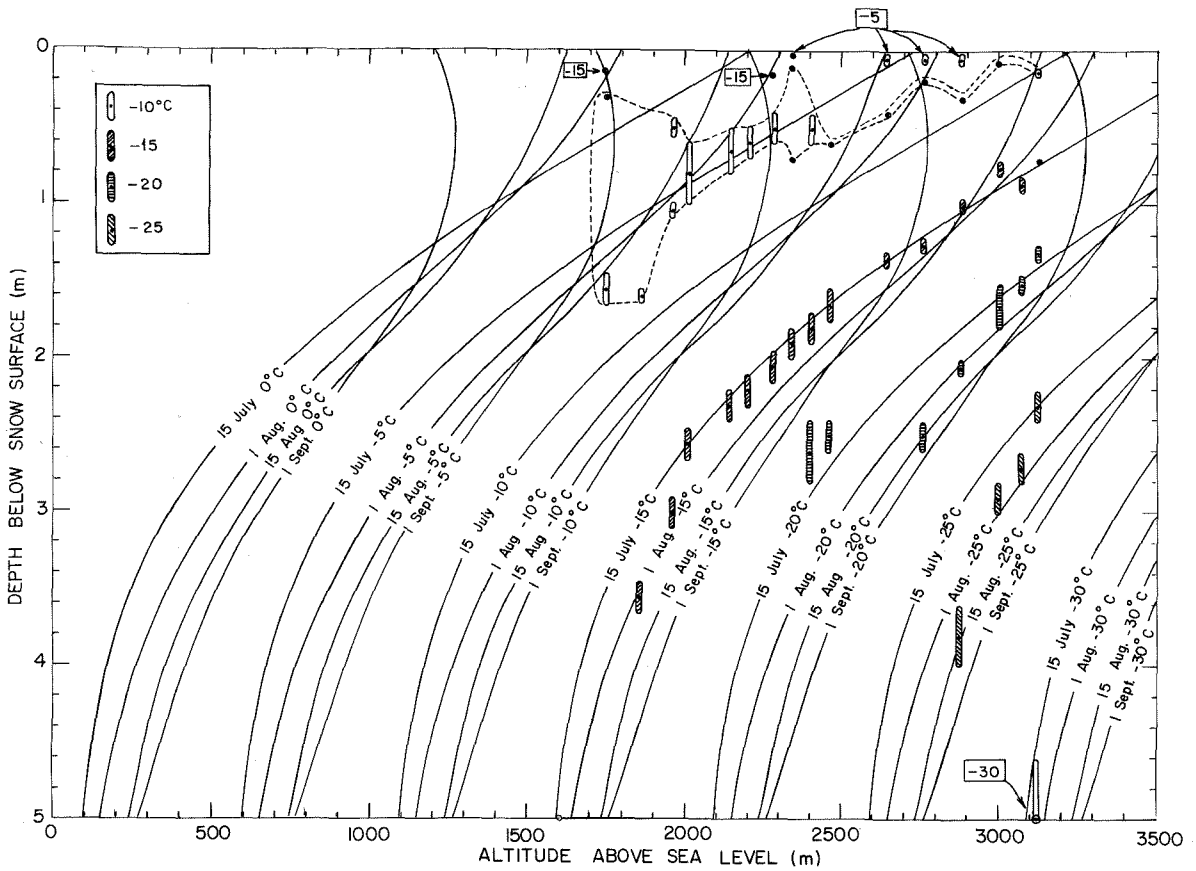

Figure 38.--Isotherms computed from equation 3 for 15 July, 1 August, 15 August, and 1 September using an assumed altitude gradient of 1°C/100 m. Data points are observed values from Table IV. Equation 3 is based on the assumption that all heat is transferred through the snow by conduction. However, it is clear that the fall cooling cycle has progressed more rapidly than predicted by the conduction model. The 0 and -5°C isotherms have been completely removed from the snow by mid-August and the -10°C isotherm is well ahead of its computed position. The difference between measured and computed values is attributed to convection and decreases with depth as should be expected (see page 118). The depth range (see data sheets) of each temperature value is indicated by the vertical extent of the line enclosing the data point.

following values:

71°N latitude; -28.0°C at 3000 m,

77°N latitude; -24.5°C at 2000 m.

If the altitude gradient of 1°C/100 m is used, the resulting latitude gradient is 1.08°C per degree latitude.

Meteorological records from Ivigtut, Godthaab, Jakobshavn, and Upernavik are nearly continuous from about 1875 to present. These stations, together with those recently established at Thule (1946) and Alert, (Ellesmere Island, 1950) provide information over a range of 21.5 degrees of latitude. They are all less than 32 m above sea level and may be regarded as equal in altitude for the present discussion. Records from these stations are summarized in Table VII and Figures 39a and b. The average air temperature has increased especially since about 1920. Therefore, values shown for Thule and Alert (since 1946) correlate with the upper limit of data points obtained farther south (Fig. 39b).

The latitude gradient, expressed in °C per degree latitude, is 0.8 from Ivigtut to Upernavik, 1.4 from Upernavik to Thule, and 1.0 from Thule to Alert. The gradient measured north of Upernavik is closest to that observed on the ice sheet. This is probably because the sea north of Upernavik is covered by ice and snow during the major portion of the year, thus making the environment more continental than it is farther south.

Summary. A simplified model of the distribution of mean

Table VII

Mean annual air temperature data*

	Ivigtut (61.2°N)		Godthaab 64.2°N		Jakobshavn 69.2°N		Upernavik 72.8°N		Thule 76.5°N		Alert 82.5°N	
Decade	A	B	A	B	A	B	A	B	A	B	A	B
1871-1880	(1)	1.2	(5)	-1.4	(8)	-4.6	6	-8.2	-	-	-	-
1881-1890	(10)	0.2	(8)	-2.5	(7)	-6.0	10	-9.3	-	-	-	-
1891-1900	(10)	0.6	(3)	-1.6	(10)	-6.3	7	-8.5	-	-	-	-
1901-1910	(10)	0.6	(8)	-2.0	(10)	-5.3	10	-8.3	-	-	-	-
1911-1920	(8)	1.4	(10)	-1.6	(7)	-5.7	10	-8.4	-	-	-	-
1921-1930	(8)	1.4	(10)	-0.7	(7)	-3.7	10	-6.8	-	-	-	-
1931-1940	(10)	1.7	(10)	-0.5	(10)	-3.3	6	-6.4	-	-	-	-
1941-1950	(10)	2.0	(10)	-0.6	(7)	-4.0	7	-6.1	4	-11.3	-	-
1951-1960	-	-	-	-	-	-	-	-	4	-11.7	7	-17.9

A: Number of years for which data are available in the stated decade.
B: Average annual air temperature (°C) in the stated decade.

*Data from: Danish Meteorological Institute, U.S. Weather Bureau, U.S. Air Force Air Weather Service, and Canadian Department of Transport, Meteorological Branch.

The data in Table VII are summarized in Figures 39a and b. The increase in temperature since early in the present century (Ahlmann, 1953) is readily apparent.

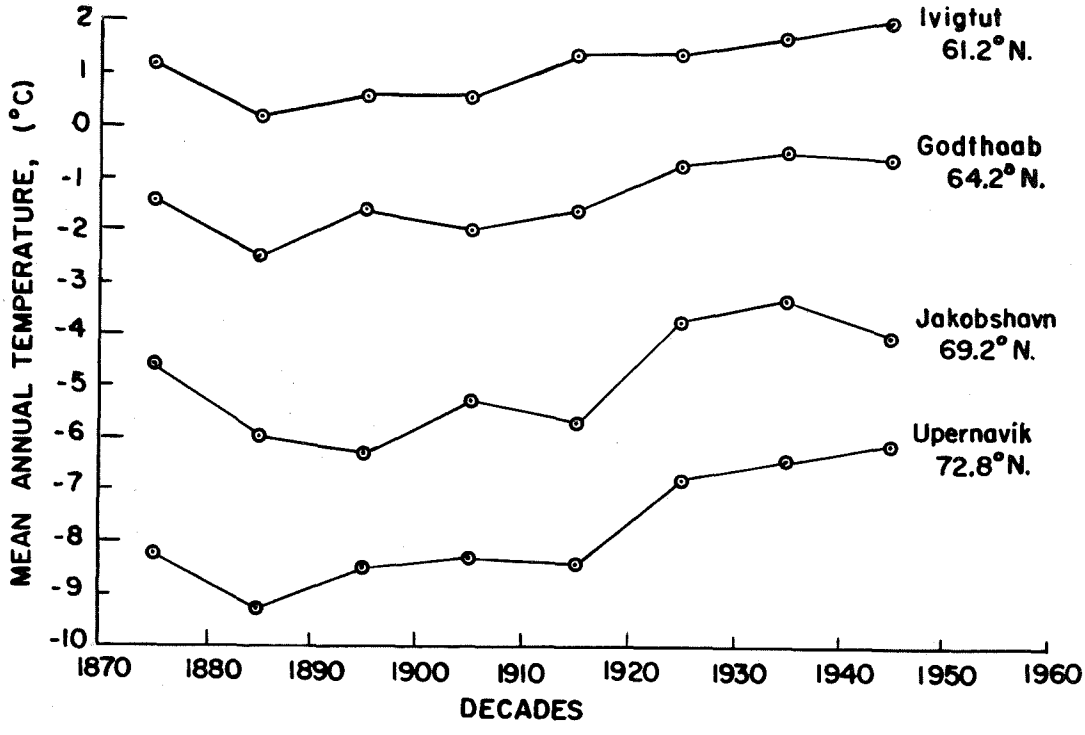

Figure 39a.--Mean annual temperature plotted against time for stations on the west coast of Greenland (Data from Table VII).

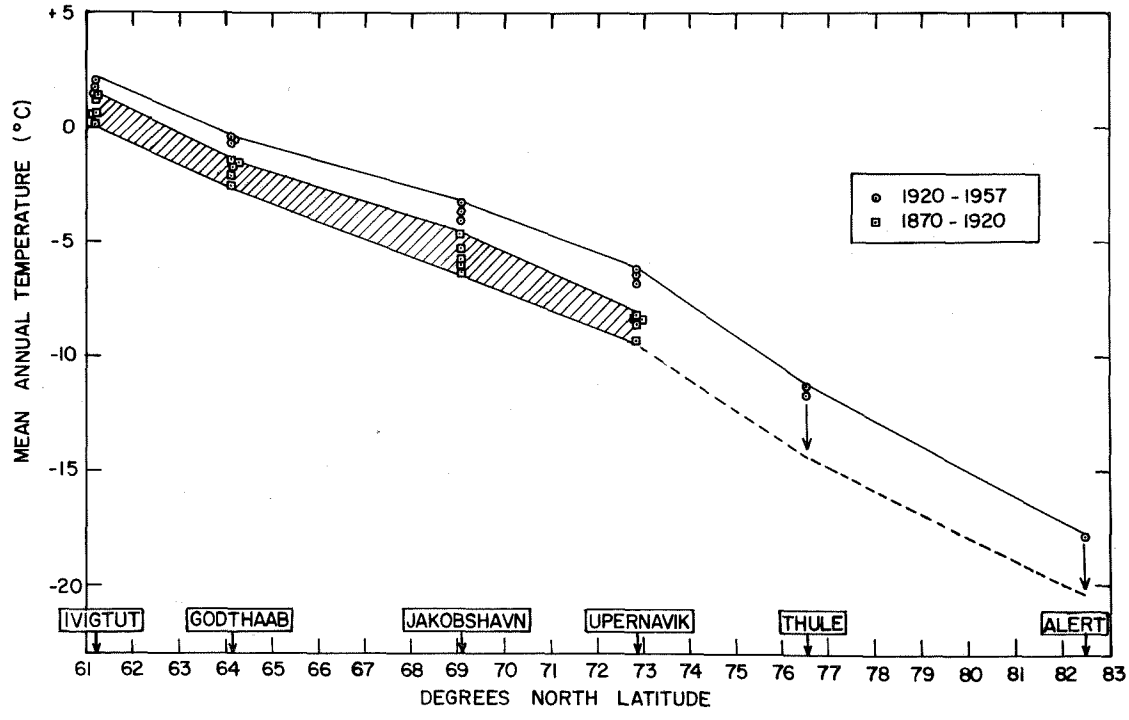

Figure 39b.--Mean annual temperature plotted against latitude along the west coast of Greenland (Data from Table VII).

annual temperature (i.e., the temperature measured 10 m below snow surface at any time of year) may be summarized as follows:

(1) The altitude gradient is based on the assumption that the prevailing meteorological environment of the ice sheet is a strong cooling by radiation, producing a temperature inversion and nearly steady drainage of dense air by katabatic winds. The air is warmed as it descends along the ice sheet at the dry-adiabatic rate of about 1°C per 100 m. This process in the air controls the altitude gradient of temperature, measured 10 m below the snow surface, above the saturation line.

(2) The latitude gradient of temperature is based on the measurements at Stations 2-100 and 5-40 and, as pointed out on page 121, this gives a latitude gradient of 1.08°C per degree latitude. An isotherm map of mean annual temperatures, constructed with these gradients, is presented in Figure 40, with data points indicated.

At least two qualifications* concerning the temperature distribution model are in order. First, deviations from the altitude gradient are to be expected where mean annual temperature is higher than about -15°C because of downward percolating melt water. Such areas include the entire soaked facies and possibly the lowest extreme of the percolation facies. Data are not available to show the variation in the

---

*These qualifications are more significant south of 69°N than they are farther north.

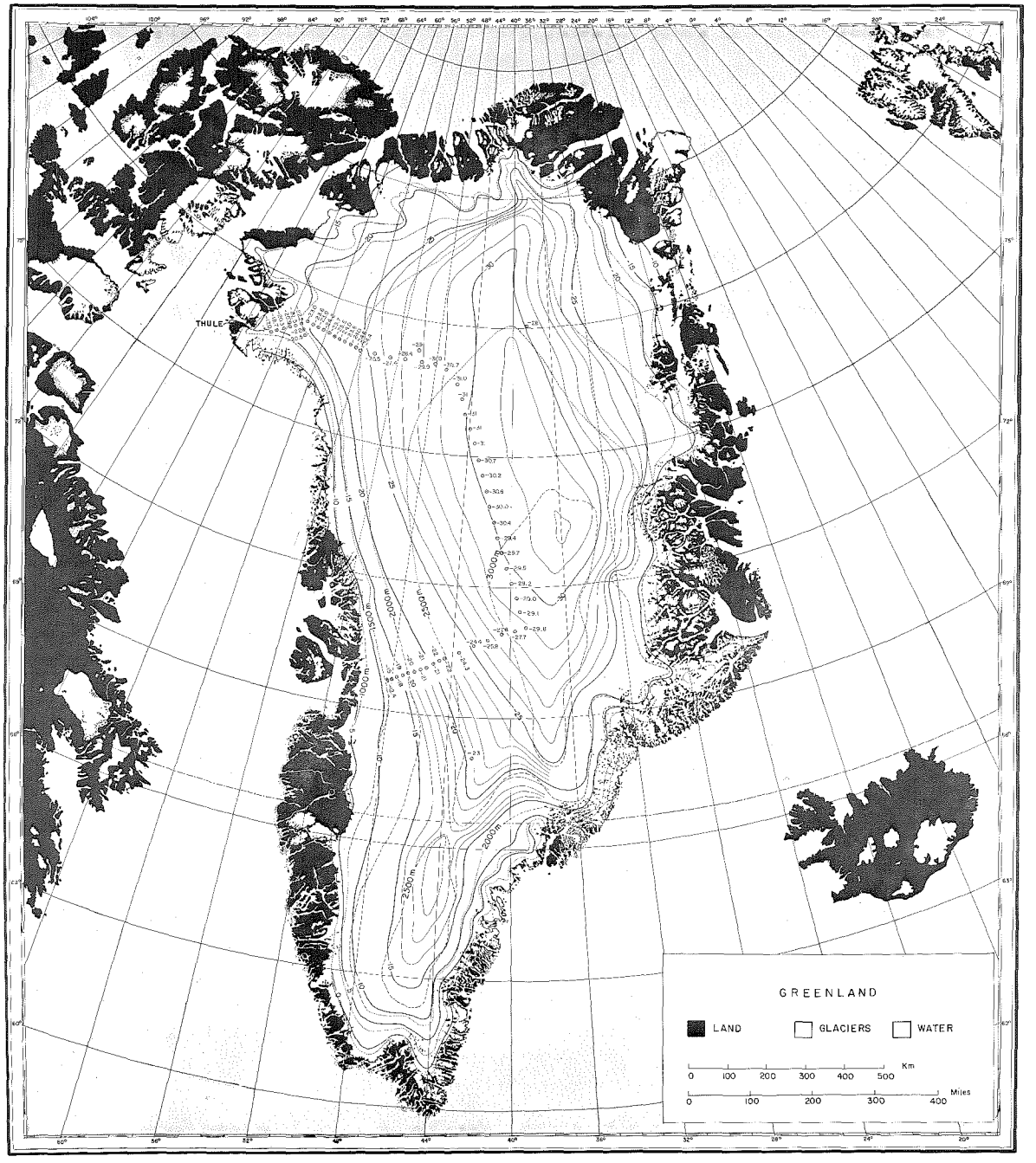

Figure 40.--Isotherms of mean annual temperature computed from the altitude gradient of 1°C/100 m and the latitude gradient of 1°C per degree latitude (see p. 124). Data points are from Appendix II, except for the value at Northice (Bull, 1956) and the one for HIRAN Station 29 (Bader, 1956).

altitude gradient of temperature across the saturation line, and no attempt was made to correct for this in constructing Figure 40.

The latitude gradient may be 0.1 to 0.2 units too high south of 69°N latitude because, the proximity of open water on either side of the ice sheet in this region tends to make the climate more maritime than it is farther north. Sea-level stations indicate that the latitude gradient is lower in south than in north Greenland (Fig. 39b) but, in the absence of data from the ice sheet itself no attempt was made to correct for this in Figure 40.

Facies in terms of temperature data

Snow and firn are soaked to the depth of the 0°C isotherm. This soaked layer includes the entire annual increment of accumulation at altitudes below 1070 ± m (about 3500 ft) at 77°N, and below 1550 ± m (about 5100 ft) at 70°N (Figs. 35a, b). By definition, these positions locate the saturation line.

In terms of temperature the dry-snow line is not as sharply defined as the saturation line or the firn line. It is the uppermost limit of observable melt, yet, traces of melt are found at least once in about 20 years high in the dry-snow facies. For sake of definition, the dry-snow line is placed at the highest altitude where the average -5°C isotherm intersects the snow surface; therefore, it is always above the -25°C isotherm of Figure 40. It lies at about 2150 ± m (7050ft)

at 77°N latitude and 3000 ± m (9850 ft) at 70°N latitude.

Hardness

Ram hardness number

The ram hardness number "R" represents the resistance to penetration which a given snow layer offers to the cone of the penetrometer as it moves through that layer. The mechanism of this penetration is complex, and involves both compressional and shearing stresses. These details are ignored and R is regarded simply as a resisting force, and, for convenience, it is presented as kg-force on the data sheets. The correlation between density and Rammsonde (or "ram hardness") profiles is generally good (see data sheets).

A discussion of equations used to evaluate R is given by Haefeli (Bader, et al., 1939, p. 128-132). He outlines "three different ways" of computing R. These "three different ways" actually involve a single approach to the problem, and effects produced by bouncing of the hammer are ignored. Haefeli's equations 30 and 31 are equations 6 and 7 below.

R is computed by equating the work done on the snow, as the cone moves through it, to the energy given up by the falling hammer and the descending penetrometer. If we ignore all impacts after the first one, i.e., neglect the effects of bouncing, we have:

$$R\,\Delta z = Mgh\alpha + (M + m)g\,\Delta z \qquad (4)$$

where Δz = the amount of penetration produced by one fall of the hammer,

M = mass of hammer,

m = mass of penetrometer,

h = height of fall of hammer,

g = acceleration of gravity, and,

α = the fraction of energy still in the system after the first impact.

$$\alpha = \frac{(M - \epsilon m)^2 + Mm(1 + \epsilon)^2}{(M + m)^2}$$

where ϵ = the coefficient of restitution,

$0 \leqq \epsilon \leqq 1$.

For convenience we set:

$Mg = P$ = the weight of the hammer, and

$mg = Q$ = the weight of the penetrometer.

Then,

$$\alpha = \frac{(P - \epsilon Q)^2 + PQ(1 + \epsilon)^2}{(P + Q)^2}, \text{ and}$$

$$R = \frac{Ph}{\Delta z}\alpha + P + Q \qquad (5)$$

The value of R is dependent upon the value of ϵ. If $\epsilon = 1$, the collision between hammer and penetrometer is completely elastic; if $\epsilon = 0$ it is completely inelastic. These extremes are:

(a) if $\epsilon = 1$, then $\alpha = 1$ and

$$R_{max} = \frac{Ph}{\Delta z} + (P + Q) \qquad (6)$$

(b) if $\epsilon = 0$, then $\alpha = \frac{P}{P + Q}$ and

$$R_{min} = \frac{P^2 h}{\Delta z(P + Q)} + (P + Q) \qquad (7)$$

To simplify and standardize the application of the Rammsonde it is assumed that $\epsilon \cong 1$ and equation 6 is used exclusively.

Continuity of strata

The reproducibility of ram hardness profiles where strata are continuous has been observed repeatedly in Greenland (Benson, 1959) and was clearly demonstrated by Haefeli (Bader, et al., 1939). Thus, once the physical properties of firn layers are recorded in pits, the Rammsonde may be used to determine lateral continuity of strata in a particular region.

Integrated ram hardenss profiles

The direct comparison of profiles is useful in correlating individual strata between pit stations. However, one may observe significant differences in the range of hardness values between the different regions (see the data sheets). It is desirable to examine the nature of the variation in hardness between the facies, but, the direct comparison of

many profiles from a large area would clearly be cumbersome for this purpose. It is necessary to reduce the data on each profile to a few significant values which can be more easily compared. One such reduction is effected by integrating the profiles.

The ram hardness number is expressed in units of force. When it is integrated over a depth interval the resulting quantity is the work done on the snow as the penetrometer moves through the stated interval.* In practice, this integration is performed by multiplying each depth increment, Δz by its hardness number, R and adding these values from $z = 0$, at the snow surface, to any desired depth. The intervals Δz do not approach zero, nor does the number of intervals increase indefinitely; yet, it is convenient to regard the summation as an "integral" and to examine $\int_0^z R dz$ as a function of z. The total work done by the penetrometer in moving from the snow surface to a stated depth z_i may be written as

$$R_i = \int_0^{z_i} R dz.$$

For convenience the values z_i are taken at 1-m intervals.

---

*The ram hardness number is expressed in units of Kg-force. Thus, the integrated Rammsonde profile has units of Kg-f cm. These are converted into joules by the following relations:

1 Joule = 10.2 Kg-f cm

1 Kg-f cm = 0.098 Joule

The maximum depth of ram profiles from the snow surface is 4 m. Therefore, a maximum of four values (R_1, R_2, R_3, and R_4) may be obtained from each profile and they are cumulative values by definition.

The use of overlapping profiles at pit stations is justified to eliminate discontinuities at a single deep-pit (Benson, 1959). However, such composite profiles cannot be used to compute the four R values because, by definition, these values measure the work required to penetrate from the snow surface to a given depth. Furthermore, one often desires to use ram profiles made at locations where there is no pit. If these are to be compared with pit-station ram profiles it is essential that all of the measurements be made in the same way.

Integrated ram data for six 1953 stations are presented in Figure 41. The measurements were made during the melt season. At Station 0-20, the very low values in the upper 2 m, together with the rapid increase below 3 m are typical features of the soaked facies. The low initial values are due to the weakness of water-soaked firn. The rapid increase below 3 m results from the abundance of ice layers, lenses, and glands at depth. Ram profiles in the soaked facies often cannot be carried as deep as 4 m, because R_4 generally exceeds 5000 joules. The spread in R values between Station 1-0 and the other stations in the percolation facies (2-0, 2-50, and 2-100) is caused by the relatively

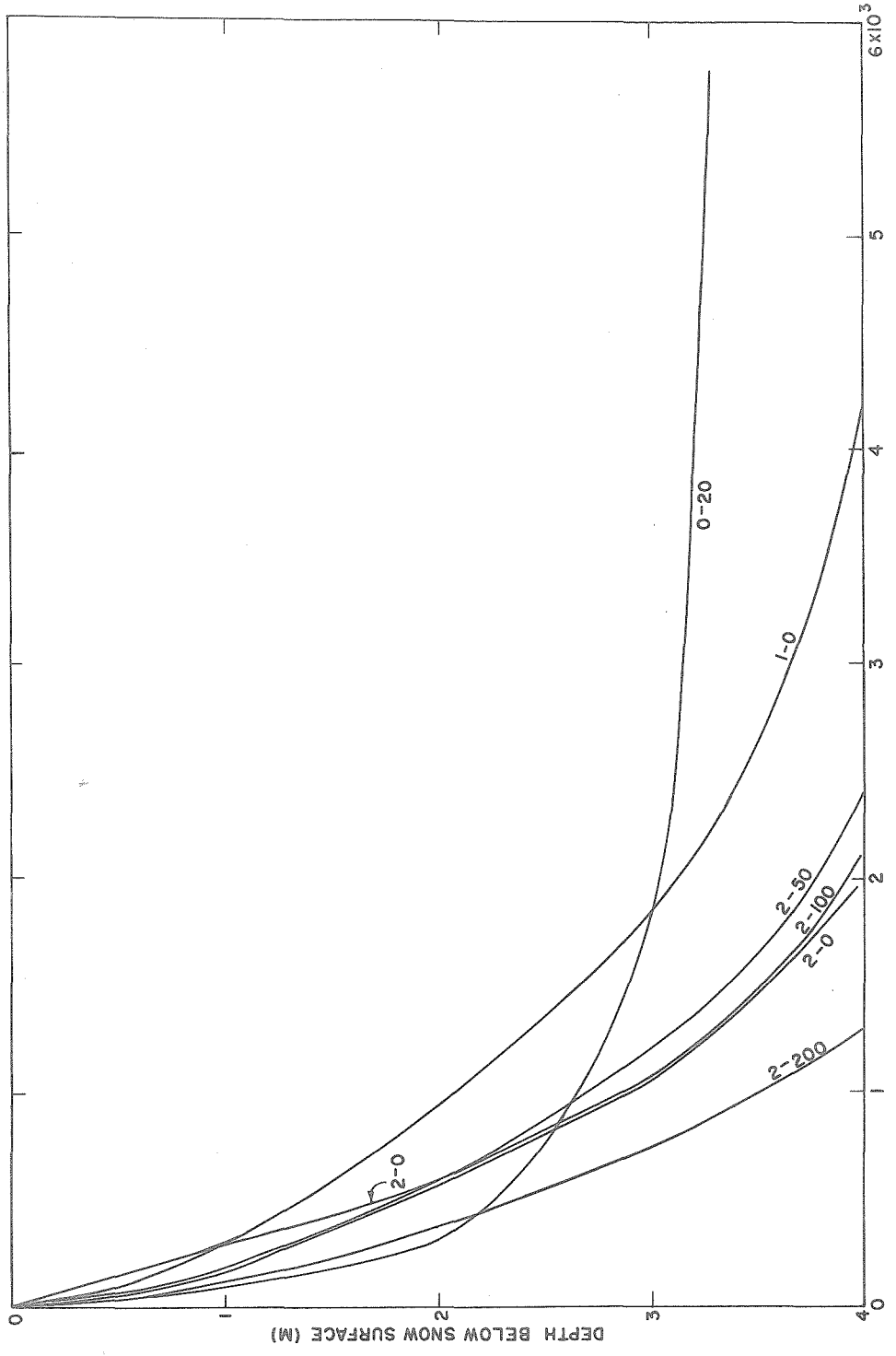

Figure 41.--Integrated ram hardness plotted against depth for six of the 1953 stations. The measurements were made at the peak of the melt season.

greater amount of iced firn and icy layers at 1-0. Station 1-0 is near the lower end of the percolation facies. The R values decrease rapidly with increased elevation inland from 1-0. As an example, it may be noted that R_4 does not exceed 3000 joules after position 1-15 has been passed. Station 2-200 is the only example shown of the dry-snow facies, but it is representative.

Temperature dependency of ram hardness

The R values of each station in 1953, 1954, and 1955 are plotted in Figure 42. The R values are progressively greater from 1953 to 1955. This is a temperature effect. The 1953 expedition "SOLO" crossed the saturation line in mid-July, in 1954 "CRYSTAL" crossed it in late May, and in 1955 "JELLO" crossed it in mid-May. The strength of ice is dependent upon temperature (Butkovitch, 1954), and this may be expected to affect the ram resistance of a snow pack.

The temperature variation of R_1 in the percolation and dry-snow facies is shown in Figure 43. The percolation facies is subdivided into an upper and lower part. The greater variation at lower altitudes in the percolation facies reflects the increase in melt action. At temperatures near the melting point the ram-resistance is low, but at temperatures below the melting point the increase in ram-resistance is roughly proportional to the amount of melt-

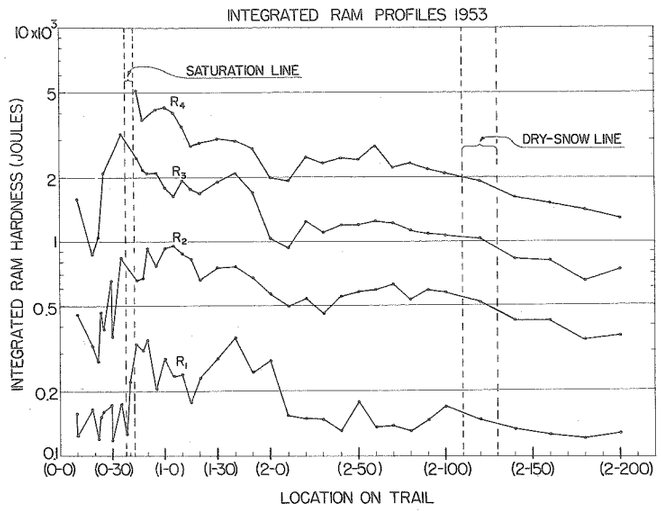

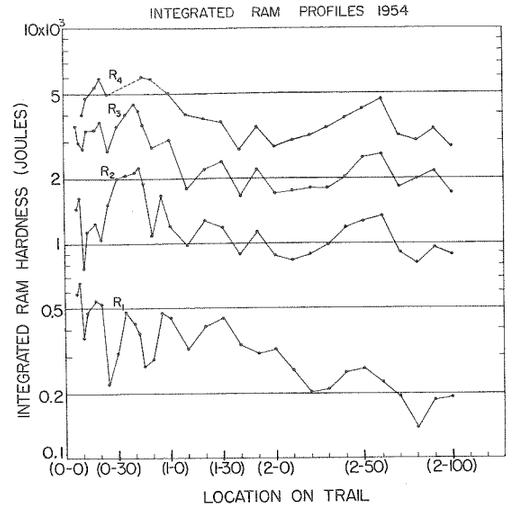

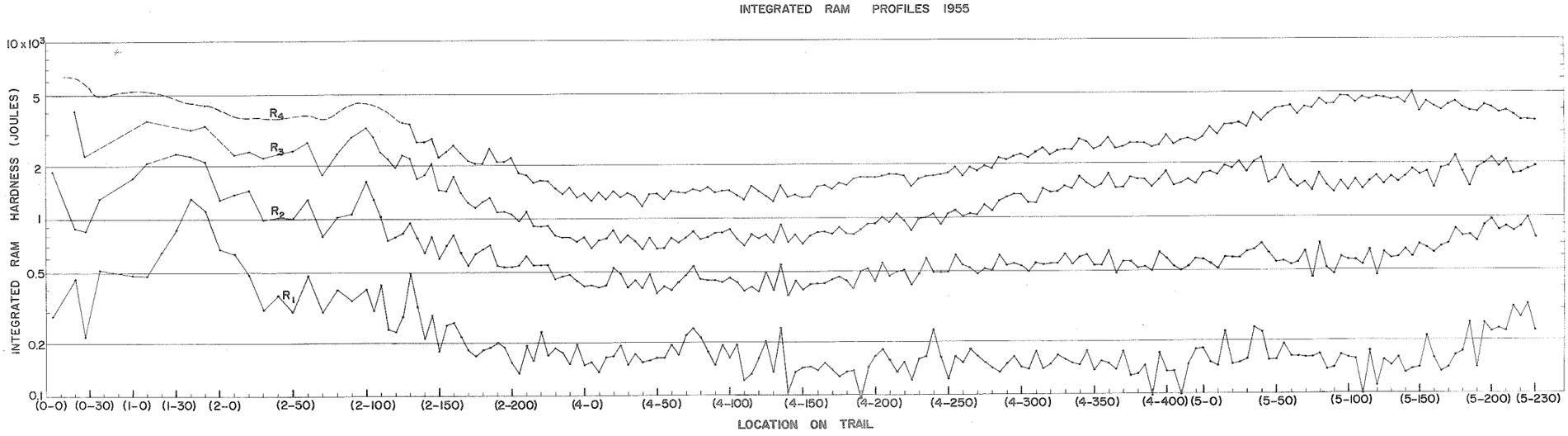

Figure 42.--Integrated ram hardness values plotted against position on the trail for the years 1953, 1954, and 1955. R_1 represents the work done by the Rammsonde in penetrating from the snow surface to a depth of 1 m; similarly, R_2 represents the work to penetrate from the snow surface to a depth of 2 m, etc. (see p. 130). In 1953 the measurements were made during the peak of the melt season and the saturation line stands out clearly because soaked snow is easier to penetrate than non-soaked snow. In 1954 and 1955 the saturation line was traversed prior to the melt season so no discontinuity was observed (see p. 137). The increase in R_i values from 1953 through 1955 is a temperature effect (see p. 133 and Fig. 43).

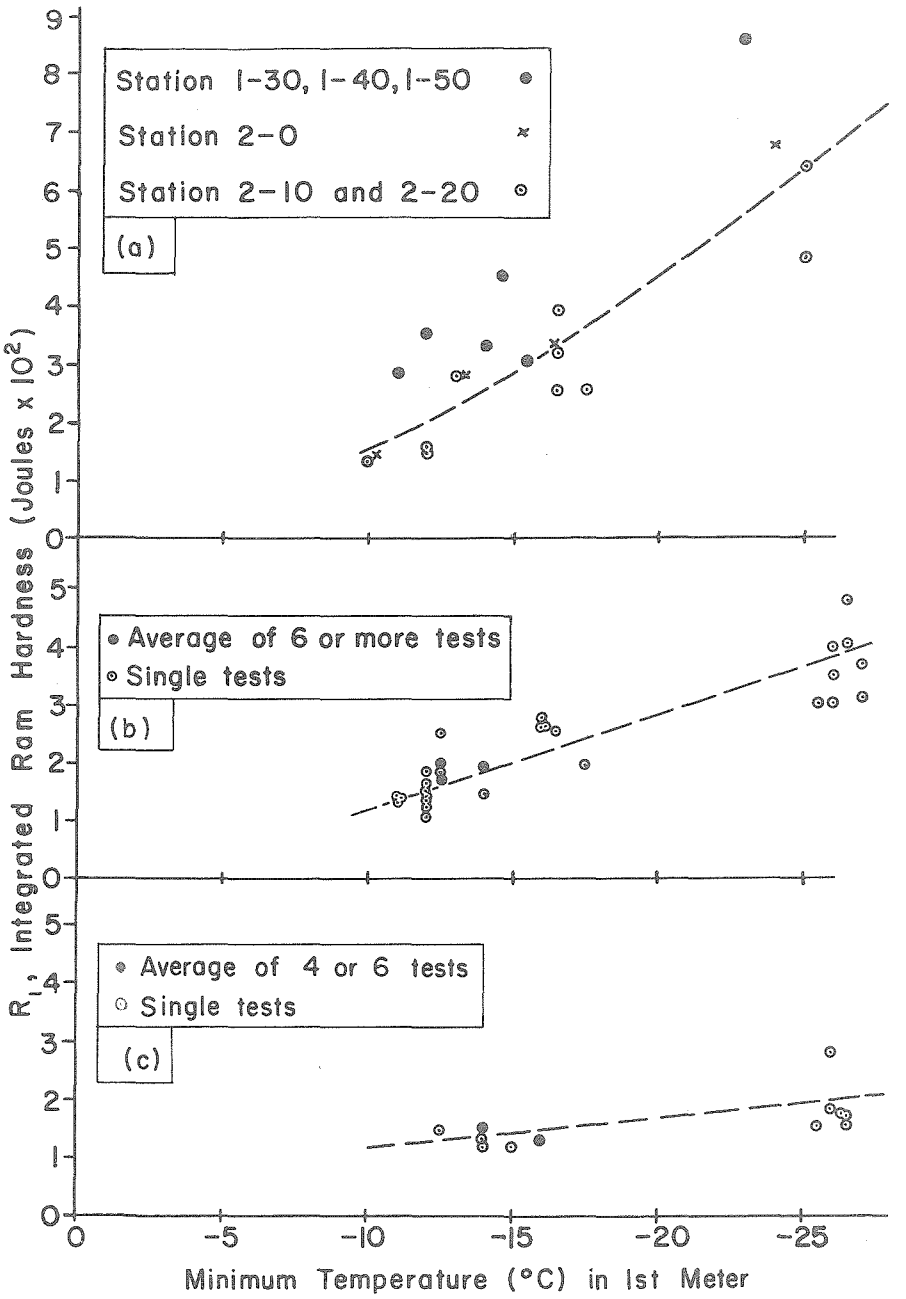

Figure 43.--R_1 plotted against minimum temperature in the 1st meter:

a. Percolation facies below 1850 m at 77°N.
b. Percolation facies above 1850 m at 77°N.
c. Dry-snow facies.

bonding between grains. The variation, as well as the range, of R, in the dry-snow facies is low because the snow and firn rarely attain temperatures as high as -5°C, and melt-bonding between grains is minimal. The values of R_{2-1} and R_{3-2}, i.e., the work required to penetrate the second and third meters respectively, when plotted against their minimum temperatures show results similar to those of Figure 43 but with more scatter of the data points.

Where significant soaking occurs the variation of R_1 values with temperature must be considered separately. For example, at 0-35 the top meter of firn has 3 very different physical manifestations, it may consist of:

(1) New snow prior to the melt season (at this time the top meter of snow may be nearly identical from the edge of the ice sheet to the dry-snow line);

(2) Completely wetted snow during the height of the melt season (at this time R_1 has its minimum value and the difference between soaked and non-soaked facies is readily apparent); and,

(3) Iced firn in the fall and early winter (at this time the value of R_1 is extremely high).

Temperature coefficients for R within a given facies are easiest to recognize in the first meter, i.e., in the R_1 values. The rate of increase in the value of R_1 with the minimum temperature in the top meter may be summarized as follows:

	Temperature coefficient for R_1	
	Kg-f cm/°C	Joule/°C
Dry-snow facies	30	3
Upper* percolation facies	170	17
Lower* percolation facies	320	31

*Above or below 6000 ft (1830 m) at 77°N lat.

Facies in terms of hardness data

In 1953 the measurements were made during the melt season and the discontinuity in R_1 near 0-40 locates the saturation line (Fig. 42a). The low values on the left were obtained in the soaked facies while the upper meter was wet. The higher values on the right are from the percolation facies. Therefore, between 0-0 and 1-0, the saturation line may be placed at an altitude of about 1050 m (3500 ft) in agreement with the analysis of the isotherms in Figure 35a. From ram data, the saturation line may be located without digging pits. In 1954 and 1955 the measurements were made before melting had occurred, and, accordingly, there is no discontinuity between the soaked and percolation facies.

The dry-snow line is not uniquely determined by Rammsonde data. In general, the values R_i are lowest in the dry-snow facies, but the limiting values at the facies margin are temperature dependent. For example, in August 1953 the R_4 value was less than 2000 joules above the dry-snow

line. In May 1955 the R_4 value was less than 3000 joules above the dry-snow line (Fig. 42).

Density

Variation in density as a stratigraphic parameter was discussed in Chapter III. Here attention is focused on the gross changes in density with depth and, especially with differences between the depth-density curves of different facies.

Depth-density data

Average density values for each meter are plotted against depth in Figure 44. Data are from Greenland, with the exception of those from the Upper Seward Glacier, Yukon Territory, Canada (Sharp, 1951), and from the Snow Dome of Mt. Olympus. The latter glaciers are temperate and the data are from the soaked facies of each.

The data from 2-100 and from Eismitte (Sorge, 1935, p. 134) show that the slope of the depth-density curve decreases below a depth of 8 to 10 m. These stations lie in the upper extreme of the percolation facies. In the soaked facies the change in rate of densification occurs at shallower depths (at about 4-5 m in the Seward Glacier). It is also clear from Figure 44 that the range of firn density decreases as we move upward from the soaked through the dry-snow facies; and that the rate of increase of density with depth is greater

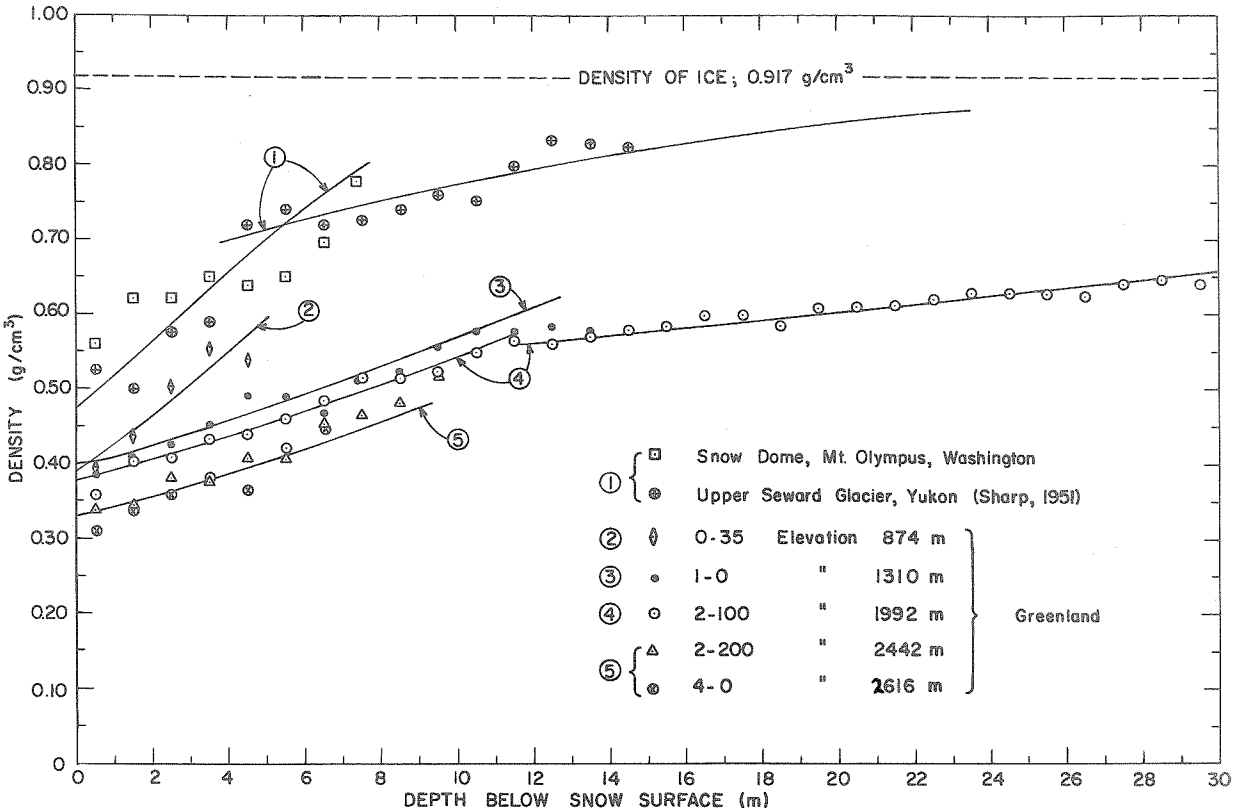

Figure 44.--Depth-density curves. Each point represents the average density over a depth interval of 1 m. Data are averages of 2 years measurements from snow surface to 4 m at 0-37, to 6 m at 1-0, and to 10 m at 2-100; all other points are based on single observations. Curves in this figure were computed from equation 14. The values of constants (see also equation 9 and Fig. 49) are as follows:

Station	Depth* range	ρ_o	ν_o	K	m
Seward Glacier and Mt. Olympus	$0 < z < z_c$	0.475	2.12	0.859	37.5×10^{-4}
	$z_c < z < \infty$	0.640	1.56	-0.405	12.0×10^{-4}
Greenland:					
0-35	$0 < z < z_c$	0.390	2.56	1.651	37.5×10^{-4}
1-0	$0 < z < z_c$	0.395	2.53	1.599	16.0×10^{-4}
	$z_c < z < \infty$	0.695	1.44	-0.820	4.3×10^{-4}
2-100	$0 < z < z_c$	0.378	2.65	1.779	16.0×10^{-4}
	$z_c < z < \infty$	0.500	2.00	0.652	4.3×10^{-4}
2-200 (1953) 4-0 (1955)	$0 < z < z_c$	0.330	3.03	2.357	18.0×10^{-4}

*z_c is defined on p. 157 .

in the soaked facies than in non-soaked facies.

Summer melting of firn increases the rate of densification, and the difference in amount of melt above and below the saturation line is expressed by a grouping of the depth-density curves. Data from a 1000-mile traverse in the percolation and dry-snow facies all lie within the range defined by the 1-0 and 4-0 curves. Station 0-35, only 23 miles from 1-0, has significantly higher density values and a greater rate of densification with depth; it lies in the soaked facies.

The decrease in density with elevation observed in the non-soaked facies results in part from the corresponding decrease in temperature. Melt is negligible at high elevations and the primary cause of densification is the load of snow which is added annually. But, because the strength of ice increases as temperature decreases the colder firn is more able to resist the compressive stresses of the overburden. This reduces the rate of densification.

Depth-load data

If firn density could be expressed as a function of depth, i.e., $\rho = \rho(z)$ one could obtain the load at any depth "Z" by integrating $\rho(z)$ from snow surface; $\sigma = \int_0^z \rho \, dz$. Without knowing $\rho(z)$ the integration may be approximated by a summation. This has been done for all stations and the results are summarized in Figure 45.

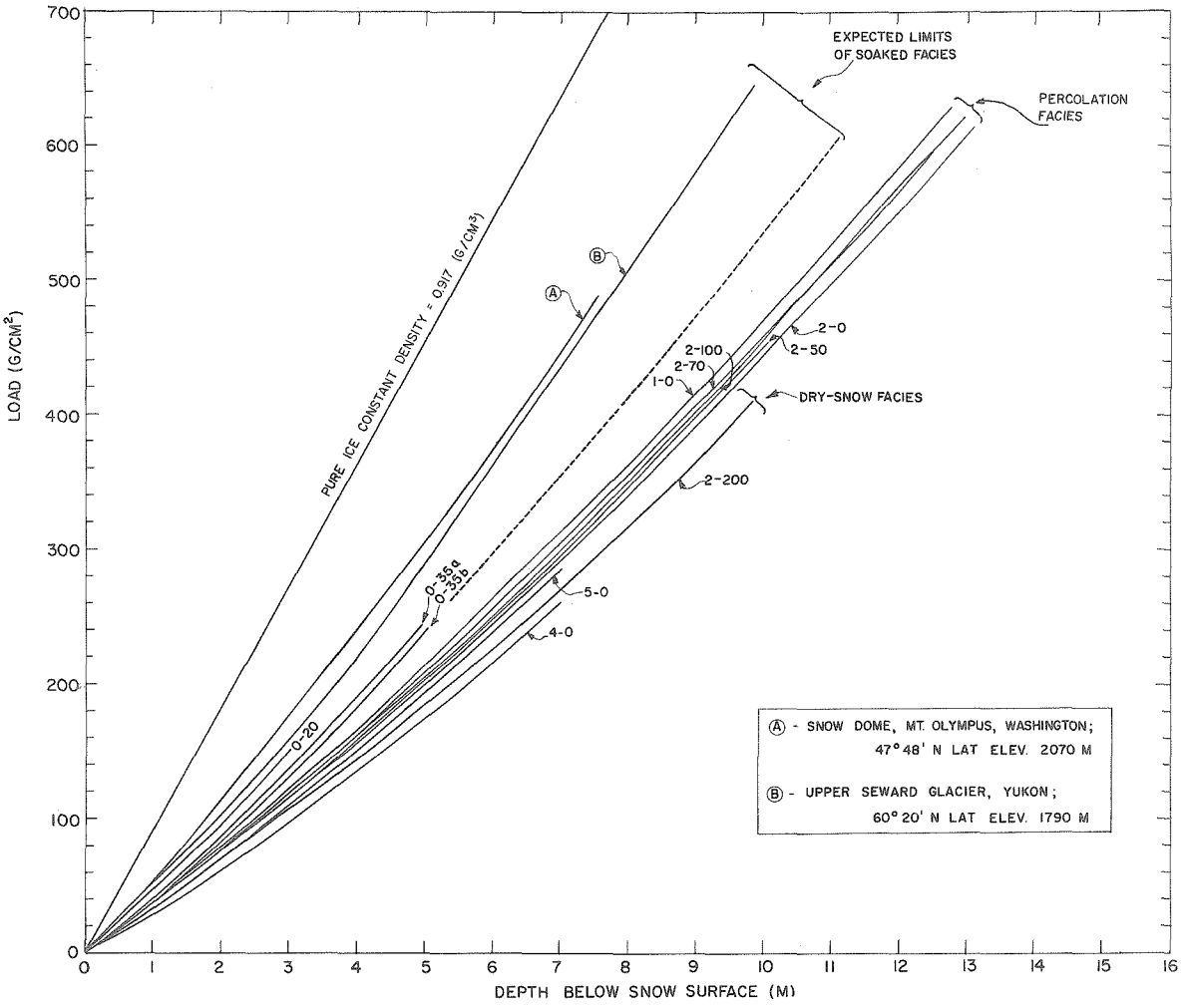

Figure 45.--Depth-load curves. Curves from the soaked facies lie between those shown for Snow Dome, Mt. Olympus, Washington and Station 0-35, of this study.

Curves 0-20 and 0-35a are based on measurements of July 1953 when the firn was completely soaked. Curve 0-35b is from data obtained before melting occurred in the Spring of 1954.

All curves from the percolation facies lie within the region bounded by the curves 1-0 and 2-0.

All curves from the dry-snow facies lie within the region bounded by the curves 4-0 and 5-0.

The curve for pure ice represents the limiting case.

A tentative grouping of curves according to facies is indicated but more data are obviously desirable in the soaked facies. Except for the data from Seward Glacier and Mt Olympus the contribution of ice masses in the firn was neglected in computing the depth-load curves of Figure 45. This was done because the irregular and discontinuous shapes of the ice masses make it difficult to get an exact measure of their water equivalent. Depth-load curves which include estimates of the water equivalent of ice masses have been computed and they differ from the curves of Figure 45 as follows:

Station	Depth range (m)	Average excess of load values with estimate of the water equivalent of ice masses over those without such estimates
0-35	0-6	7%
1-0	0-14	4%
2-0	0-14	2%
Stations above 6000' elev at 77°N lat 2-20 to 2-200	0-14 (max)	less than 1%

The inclusion of estimates for the water equivalent of ice masses increases the differences between facies shown in Figure 45. It also removes the 2-0 curve from its apparently

anomalous position* on the lower boundary of the percolation facies and places it between the curves for 2-50 and 2-100. The differences between curves bounding the facies are:

Facies	Difference between load curves bounding the facies at depth of 5 m below snow surface	
	Without estimates for water equivalent of ice masses (Fig. 45)	With estimates for water equivalent of ice masses
Soaked and percolation	11%	16%
Percolation and dry-snow	2.5%	4%

The gaps between groups of curves are significant because curves measured in pits dug within 100 m of each other in consecutive years are reproducible to within an error of about 1%. Table VIII summarizes the reproducibility of depth-load curves from the four stations which had pits deeper than 4 m in both 1953 and 1954. The average difference is 0.63%.

The load at a depth of 5 m below snow surface is shown

*The desicating effect of wind in summer and fall may account for the fact that firn density and hardness values (neglecting ice layers) at 2-0 are lower than those measured at higher and lower altitudes in the percolation facies; in fact they are the lowest recorded in any deep pit of the percolation facies (see Figs. 42a and 45). This could be due to the extraction of sufficient moisture from the snow to offset some of the densification produced by summer melting. The minimum accumulation in the 2-0 region allows the fall cooling process to affect a greater part of the annual layer here (perhaps the entire layer) than at positions with more accumulation.

Table VIII

Reproducibility of depth-load curves at the stations which had pits deeper than 4 m in both 1953 and 1954. The 1954 pits were dug within 100 m of the 1953 pits at each station

Station	Depth (m)	Load (g/cm^2)		% Difference	
		1953	1954		
1-0	4	166.88	166.15	0.43	Average of 12 measurements = 0.63%
2-0	4	155.06	155.76	0.45	
2-50	4	159.15	160.24	0.68	
2-100	4	159.86*	161.73	1.16*	
1-0	6	264.06	264.97	0.34	
2-0	6	243.03	245.38	0.96	
2-50	6	250.03	247.48	1.02	
2-100	6	250.41*	251.02	0.24*	
1-0	8	n.d.	362.96	--	
2-0	8	338.49	339.75	0.37	
2-50	8	351.12	346.07	1.44	
2-100	8	350.32	350.76	0.13*	
1-0	10	n.d.	470.18	--	
2-0	10	n.d.	444.04	--	
2-50	10	n.d.	450.38	--	
2-100	10	453.53*	455.08	0.34*	

n.d. No data

*The 1953 data at 2-100 included 13 cm of fresh snow (average density = 0.21 g/cm^3) which caused its top 13 cm to contain 1.28 cm less water than that of 1954 (see data sheets). The value 1.28 g/cm^2 was added to the first 13 cm of 1953 data to adjust for this.

for each station in Figure 46. At some stations a range of load value is indicated; the lower value represents the load computed by omitting ice masses, and the upper value includes an estimate for the contribution of ice masses to the load. The difference between load values computed with and without estimates for the ice masses is negligible where only one value is shown.

Facies boundaries are indicated in Figure 46. The saturation line was clearly crossed in the north near Station 0-35. It was not crossed in the south although it lies very close to Station 5-230. The firn line is separated from the saturation line on the Thule peninsula by nearly 40 miles because of the gradual increase in elevation there. In the vicinity of Disko Island the firn line and saturation line are much closer to each other because of the steeper surface slope. They probably are within 5 miles of each other.

The dry-snow line shows more clearly in the north because the traverse crosses normal to it. In the south the traverse ran nearly parallel to the dry-snow line in the vicinity of 5-0. If a westward course had been taken at Station 4-325, the transition between the dry-snow and percolation facies would have looked like it does between 2-100 and 2-200.

Facies in terms of density data

The density data form the most complete basis for subdivision of the ice sheet, and glaciers in general, into facies.

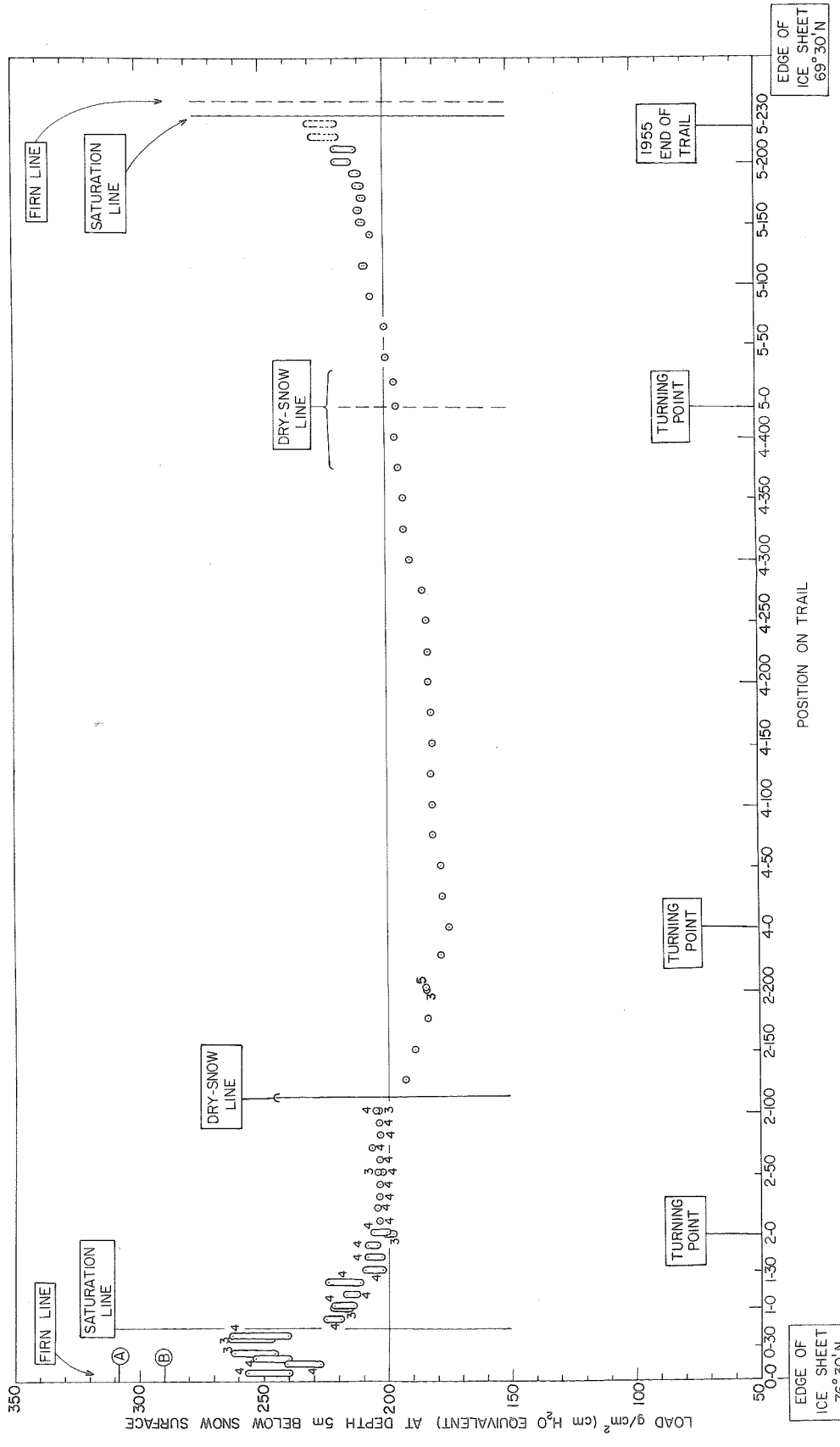

Figure 46.--Load, in cm H_2O, at a depth of 5 m below the snow surface along the traverse in Figure 1. Facies boundaries are indicated. The points A, and B on the left margin indicate the upper extreme of the soaked facies.

A - Snow Dome, Mt. Olympus, Washington, 47°48'N Latitude
Elevation 2070 m (Measured by Benson in 1957).

B - Upper Seward Glacier, Yukon Territory, 60°20'N Latitude
Elevation 1790 m (Sharp, 1951).

Temperature and hardness data will also locate the saturation line but the dry-snow line is more subtle, and is best defined, at present, in terms of density. The relation between density and facies is summarized as follows:

(a) Firn density decreases from soaked to dry-snow facies as shown in Figure 44 and in the following summary:

Facies	Average density in the upper 5 m (g/cm^3)
Soaked facies	Greater than 0.500
Percolation facies	0.430 to 0.390
Dry-snow facies	Less than 0.375

(b) The load at a given depth decreases from soaked to dry-snow facies as shown in Figure 45 and in the following summary:

Facies	Load 5 m below snow surface (g/cm^2)
Soaked facies	240-300 and above
Percolation facies	200-225
Dry-snow facies	175-200

Glacier Facies--a Classification of Glaciers

The definition of boundaries between diagenetic facies, in terms of the measurements described above, provides the

basis for a quantitative classification of glaciers. This "facies classification" does not require that Ahlmann's useful distinction between temperate and polar glaciers be abandoned. A temperate glacier exhibits only the two facies below the saturation line, whereas one or both of the facies above the saturation line are present on polar glaciers. However, the consideration of glacier facies goes beyond Ahlmann's classification in that it permits quantitative subdivision of large glaciers which span the entire range of environments from temperate to high-polar.

If the strata could be observed from top to bottom, in a glacier with all facies present, we would find that: (1) all of the material had been soaked, at one time or another, below the saturation line, (2) layers which had and had not been soaked would alternate between the saturation line and the dry-snow line, and (3) no soaked layers would be observed above the dry-snow line (Fig. 15).

Some glaciers exhibit all facies whereas others have only those at one end of the spectrum. Data from ice shelves in the Ross Sea area (Wade, 1945) and from the Weddell Sea area at Maudheim (Schytt, 1954) indicate that the firn line and the saturation line lie below sea level; in these areas the glaciers exhibit only the percolation and dry-snow facies. At the opposite extreme, the saturation line lies above the highest point on temperate glaciers which exhibit only the soaked and ablation facies.

The main advantages of this classification are: (1) it extends and refines Ahlmann's geophysical classification without abandoning its major point, (2) the use of the facies concept is familiar to all geologists and glaciologists and emphasizes the fact that glaciers are rock units, and (3) the classification is quantitative and areal in extent, with the facies boundaries defined by simple physical measurements.

Characteristics of the glacier facies may be summarized as follows:

(1) The ablation facies extends from the edge, or snout, of the glacier to the firn line. The firn line is the highest elevation to which the snow cover recedes during the melt season.

(2) The soaked facies becomes wet throughout during the melting season and extends from the firn line to the uppermost limit of complete wetting, the saturation line. The saturation line is the highest altitude at which the 0°C isotherm penetrates to the melt surface of the previous summer.

(3) The percolation facies is subjected to localized percolation of melt water from the surface without becoming wet throughout. Percolation can occur in snow and firn of sub-freezing temperatures with only the pipe-like percolation channels being at the melting point. A network of ice glands, lenses, and layers forms when refreezing occurs. This facies extends from the saturation line to the dry-snow line. Negligible soaking and percolation occur above the dry-snow line.

(4) The dry-snow facies includes all of the glacier lying above the dry-snow line.

The saturation line gives rise to discontinuities in temperature, density, and Rammsonde data, and may also be located by examination of melt evidence in firn strata. It is as sharply defined as the firn line; but the dry-snow line, although determined by the same methods, is a 10- to 20-mile wide zone of transition in Greenland.

Location of the facies boundaries, i.e., the firn line, saturation line, and dry-snow line, will change with changes in climate; therefore, they may serve as long-term climatic indicators. The altitude of facies boundaries depends on latitude and on meteorological factors similar to those which govern the altitude of the snow line (Matthes, 1942, pp. 157-161). On glaciers the snow line is the firn line, herein defined as a facies boundary. In particular, the altitude of the firn line and of the saturation line but not of the dry-snow line, is dependent on the amount of annual accumulation. This follows directly from definition because, the complete stripping away or the complete soaking of an annual layer depends among other things, on its thickness, whereas the presence or absence of detectable melt does not.

The variation of facies boundaries with altitude and latitude on the west slope of the Greenland ice sheet is shown in Figure 47. The descent of the firn line and the saturation line at 75°N is due to the increase in accumulation on the

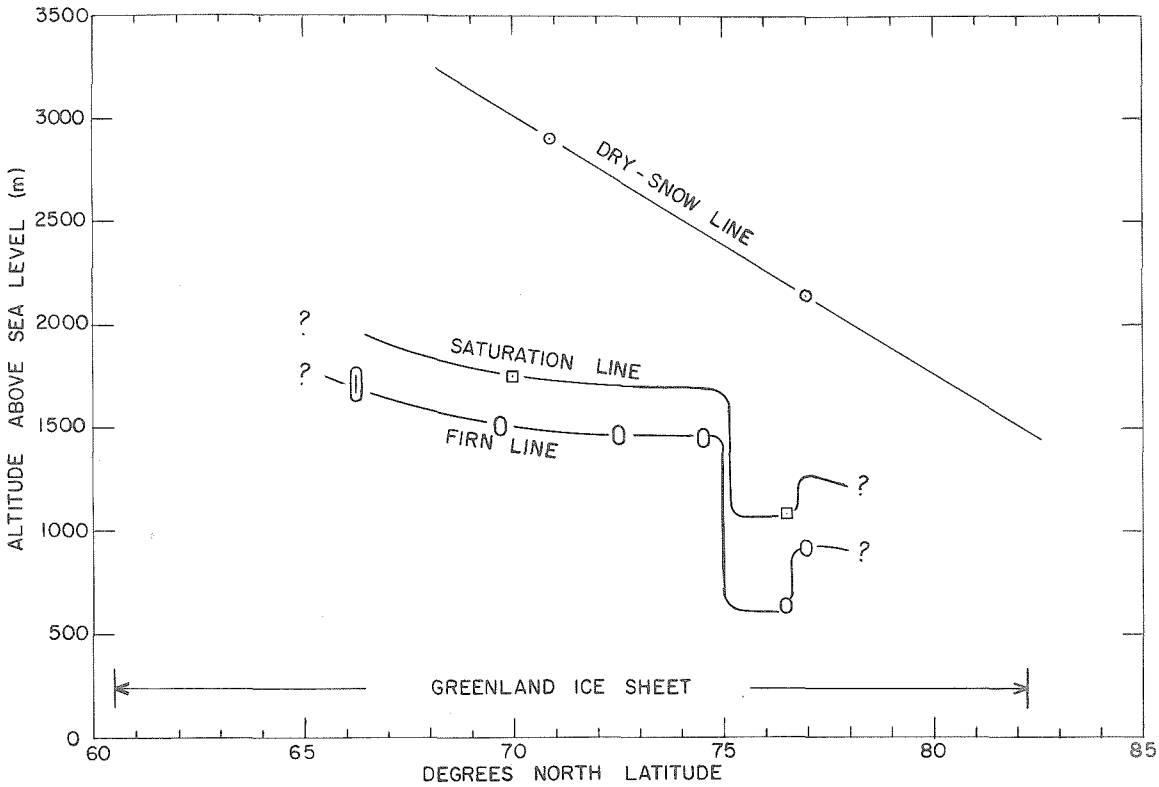

Figure 47.--The variation of facies boundaries with altitude and latitude on the west slope of the Greenland ice sheet. The descent of the firn line and saturation line at 75°N is due to the increase in accumulation on the south slope of Thule Peninsula (Fig. 30). On the north side of Thule Peninsula these lines rise again. The dry-snow line is independent of accumulation. Data points obtained during this study except for the firn line observations at:

66°16'N Mint Julep (Schuster, 1954)
69°42'N Heuberger (1954)
72°30'N Koch and Wegener (1930)
74°30'N Belknap (1934)

south slope of Thule peninsula. On the north slope of this peninsula these lines rise again. The dry-snow line has a constant slope of 1.15 m/km, and crosses the 3000 m elevation at 70°N latitude. The distribution of diagenetic facies on the Greenland ice sheet is shown in Figure 48.

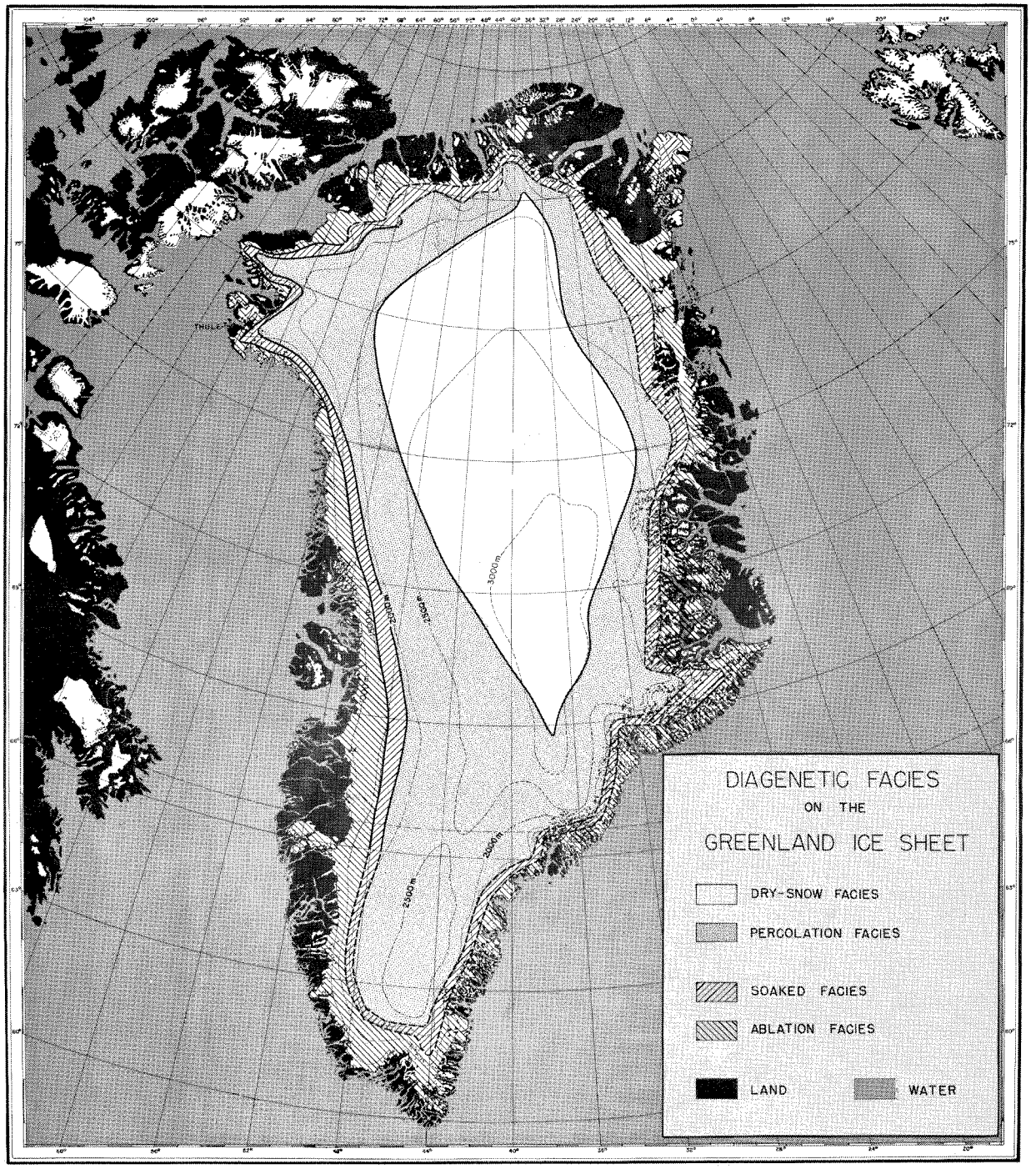

Figure 48.--Distribution of facies on the Greenland ice sheet. The location of facies boundaries is most certain along the west side of the crest between 66 and 79°N. Away from this region, the dry-snow line may be extrapolated with the greatest confidence because it is independent of accumulation. The dry-snow line on this map was drawn along the intersection between a plane, sloping 1.15 m/km to the north, and the surface of the ice sheet. Location of the firn line and saturation line in south and east Greenland is highly speculative.

CHAPTER V

DENSIFICATION OF SNOW AND FIRN

Load-Volume Relationship

The depth-density curve is linear over the depth range of 10 to 50 m, but non-linear above and below. This has made it difficult to derive a simple functional relationship between depth and density. As stated by Landauer (1959)*
". . . So far we have not been able to express this relationship in any simple yet accurate way." Actually, there is no a priori reason why depth should be a significant variable. Compressive stresses on the firn increase with depth, but because the firn density is not constant, we cannot replace the load at a given depth by the depth itself. In an attempt to get an analytic expression for the phenomenon of densification, load rather than depth is used as the independent variable. In place of firn density as the dependent variable, its reciprocal (specific volume) is used, with the assumption that it approaches the value for pure ice (1.09 cm^3/g) as a limit. The use of volume rather than density enables us to think directly in terms of changes in volume produced by changes in applied stress.

To obtain a first approximation some simplifying assumptions are made. First, where melt is negligible it is assumed

---

*Also see the discussions in SIPRE Technical Report 20 and Research Report 26.

that the only cause of densification is the load of overlying snow and firn. It is further assumed that this load is applied at a constant rate of "A" g/cm^2 per year and that an equal amount of material is lost each year by flow at depth within the metamorphic member of the ice sheet. Thus, within the sedimentary member of the ice sheet a steady-state system exists with firn moving downward as it becomes densified, while the depth-density curve remains invariant with time as stated by Sorge's law (Bader, 1954) and as shown in Table VIII. Along with these assumptions the existence of a vertical pressure gradient is recognized in the ice sheet. Within the metamorphic member unbalanced horizontal components of stress result in flow; however, this aspect of the problem is neglected here. It is also assumed that the ice composing the firn grains remains at constant density;* and as a direct result of this the observed volume changes in firn are solely due to the elimination of pore space. The rate at which pore space may be eliminated with increase in load, under the assumed steady-state conditions, must be related in some manner to the amount of pore space present; the simplest possible relation between these quantities is a linear one. The implications of this simplest of assumptions, expressed

---

*This assumption is reasonable because the maximum pressure at the base of the ice sheet does not exceed 300 atmospheres and this produces a total density increase of the order of 0.005 g/cm^3.

in equation 8, are investigated below:

$$\frac{dv}{d\sigma} = -m(v - v_i) \qquad (8)$$

where ρ = firn density

σ = load

$v = \frac{1}{\rho}$ = specific volume of firn

v_i = specific volume of ice (1.09 cm^3/g)

$(v - v_i)$ = the volume of pore space in the firn, and

the parameter "m" depends on the mechanism of compaction.

Equation 8 may readily be solved for v in terms of σ to obtain:

$$v = v_i + (v_o - v_i)\, e^{-m\sigma} \qquad (9)$$

where v_o is the specific volume when $\sigma = 0$. Depth-density data for Station 2-100, and several other stations* expressed in terms of specific volume and load are compared with equation 2 in Figure 49. The data of station 2-100 will be discussed in detail because they are the most complete.

---

*Points A (0.82 g/cm^3 at 60 m depth) and B (0.88 g/cm^3 at 100 m) from Maudheim (Schytt, 1954, p. 238) also appear to be compatible with equation 9 falling near the curves drawn for 1-0 and 2-100. The range of density values recorded at Maudheim suggests that they should fit the facies described here somewhere between 1-0 and 2-100, i.e., midway in the percolation facies.

At station 2-100, the change in rate of densification, apparent at a depth of 10 meters below snow surface in Figure 44, is more pronounced in Figure 49. For convenience, the depth at which this discontinuity occurs is called the "critical depth,", z_c, and the load, density, specific volume, porosity, void ratio, and temperature values measured at this depth will be referred to as the critical values, σ_c, ρ_c, v_c, n_c, ϵ_c, and T_c, respectively.

The slope of the load-volume curve is given by equation 8 both above and below z_c but, the parameter "m" above z_c is nearly 4 times greater than it is below. Specifically, the constants used for equation 9 at Station 2-100, in Figure 49 are:

Load values (g/cm^2)	m (cm^2/g)	v_o (cm^3/g)
$0 < \sigma < 455$	16.0×10^{-4}	2.65
$455 < \sigma < \infty$	4.3×10^{-4}	2.00

The abrupt change in rate of densification seen in the 2-100 data is also present in data from other stations shown in Figure 49. It is clear in the data from Upper Seward Glacier (Sharp, 1951), even though they violate the original assumption that melt is negligible. The beginning of the change shows at 1-0.

It is proposed that the main reason for the abrupt change in rate of densification is a change in the basic mechanism of densification. It is assumed that in the

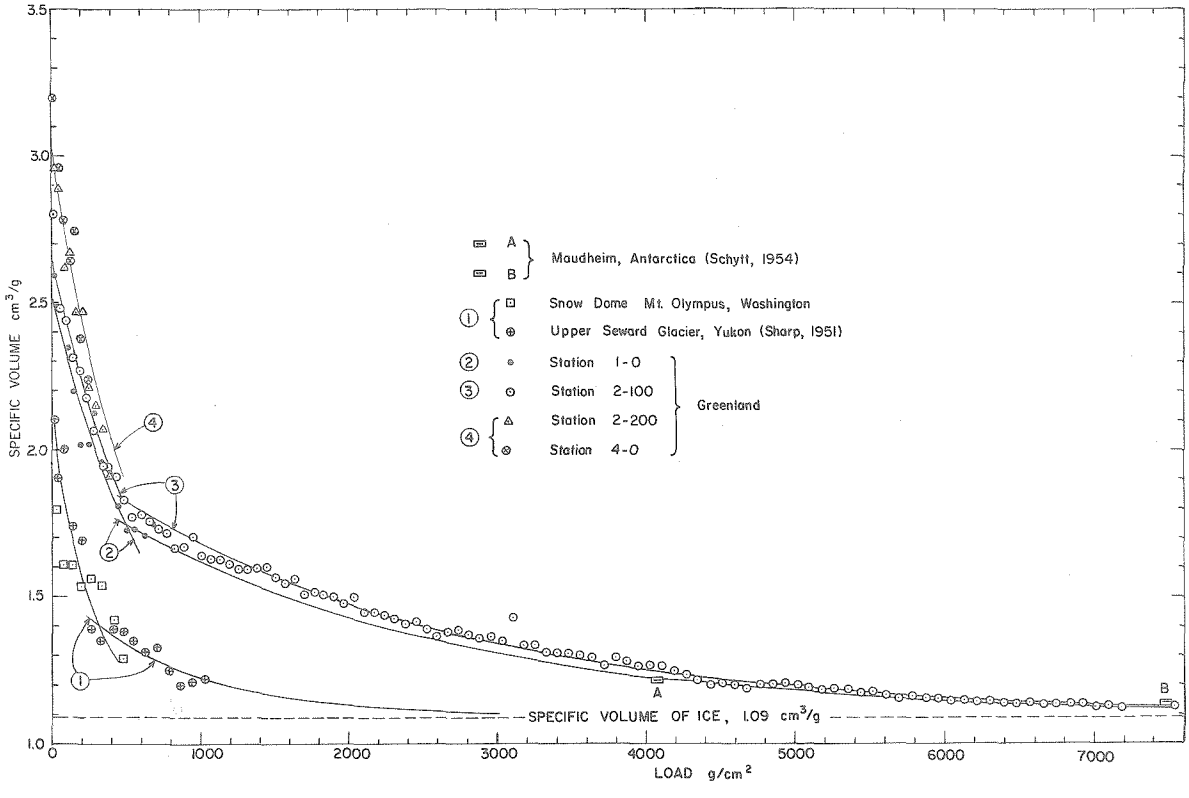

Figure 49.--Specific volume plotted against load. Computed curves are from equation 9

$$v = v_i + (v_o - v_i)e^{-m\sigma} \qquad (9)$$

with values of the constants given on p. 139.

Points A and B are from Maudheim, Antarctica (Schytt, 1954, p. 238).

complete absence of melt, densification proceeds, above z_c, primarily by packing of the ice grains comprising snow. The minimum porosity that can be attained experimentally by this mechanism alone is about 40% (i.e., snow density of about 0.55 g/cm^3). This lies between the values for loosest (47.6%) and closest (26.0%) theoretical packing of spheres.

> ". . . it is found experimentally that assemblages of spheres, or even sand particles, will have porosities averaging about 40 per cent in spite of careful efforts to induce closer packing, and even though the predominant array in the assemblage is rhombohedral with a porosity of only 26 per cent" (Muskat, M. The Flow of Homogeneous Fluids Through Porous Media. McGraw-Hill, 1937, page 13).

This agrees well with the critical values on load-volume curves measured where melting is slight or absent. The observed values of critical porosity at 2-100, 2-200, and 1-0 range between 36.7 and 43.3% as shown in Table IX.

An extreme example of the packing process is commonly observed in the sudden collapse* of depth-hoar and other "soft layers" of relatively low density. Such layers are common in the upper 7 m (see data sheets and Figs. 6a, b, and 8). They constitute flaws which are first to deform under

---

*The actual collapse of soft layers is frequently observed when one walks in an undisturbed area, and when pit digging begins. Sometimes the effect is spectacular.

During an airdrop at 2-120 on 29 August, 1952, a barrel broke out of its parachute harness and penetrated more than

the compressive stress of the overburden. The density profiles on data sheet 5 clearly shows the effect of this; the soft layers, common above 7 m, have been practically eliminated below 10 m.

When the critical density is reached compaction by grain packing is no longer possible and the loss of this mechanism of densification is signified by a marked reduction in the rate of densification (Fig. 49). Compaction beyond the critical density brings other mechanisms into predominance; grains change size and shape by growing together to relieve stress, and as load increases plastic deformation of the grains also increases. Basically, densification is the elimination of pore space. As pore space is eliminated there is also a reduction in the amount of intercommunicating pore space, and therefore in permeability. When all pores are isolated, the measurable air permeability vanishes and snow or firn becomes glacier ice by definition.

---

2 m below the snow surface. A sudden settling of weak layers spread from the point of impact and was accompanied by a startling sound. Similar examples, not started by man, were recorded by Sorge (1933, p. 340) . . .

> "Several times we heard and felt a kind of earthquake: on 2 October, 1930, at 01.20 a.m.; on 19 February 1931, at 06.55 a.m. (Middle Greenland Time). We called it "Firnstoss" (Firnpush or Firncrash). It consisted of a noise approaching rapidly; then followed a large crash; and then the noise ran away. Our mercury barometer, which had been hung in a separate ice cave at a depth of 6 to 8 feet, was caught and got nearly broken. The layers were compressed by one inch."

The distinction between material above and below the critical point is based on a change in the primary mechanism of densification, which reflects a structural change, and produces the discontinuity in the load-volume curves. On the other hand, the transition from snow, or firn, to glacier ice is gradual and the distinction between the two materials is based solely on the loss of measurable air permeability. It appears that changes occur in most physical properties at the critical density. Because of this, Anderson and Benson (1959) use the critical density as a physical distinction between "old snow" and "firn" since there is no such distinction at present. The steady-state relationship between $\frac{dv}{d\sigma}$ and v at Station 2-100 is plotted in Figure 51.

The critical values vary from one location to the next as shown in Table IX and Figure 50. The data appear to satisfy the following equation:

$$\rho_c = \rho_{cl} + (\rho_{co} - \rho_{cl})e^{ST_c} \qquad (10)$$

where $\rho_{cl} = 0.50$ g/cm^3,

$\rho_{co} = 0.73$ g/cm^3,

$S = 0.07$ C^{-1}, and

T_c = critical temperature (a negative quantity).

This empirical equation provides a quantitative description of the relation between critical temperatures and densities defined here, and has some interesting implications. First, as T_c approaches the melting point, ρ_c approaches its maximum value, ρ_{co}. Secondly, as T_c decreases without limit, the value of ρ_c also decreases, but approaches a lower limit, ρ_{cl}. Thus, it appears that the minimum critical density is about 0.50 g/cm^3 regardless of how low the temperature may be.

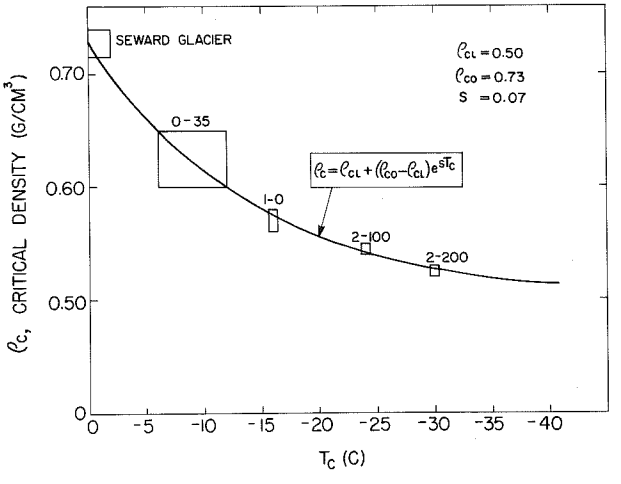

Figure 50.--Critical density vs critical temperature.

Table IX

Critical values observed on Seward Glacier and in Greenland

Station	z_c (m)	v_c cm^3/g	ρ_c g/cm^3	n_c porosity %	T_c(°C)
Seward Glacier*	4.5 ± .5	1.35-1.40	0.715-0.74	22.0 to 19.3	0 to -2
0-35	5 to 46	1.54-1.67	0.60-0.65	34.6 to 29.1	-9 ± 3
1-0	10	1.73-1.78	0.56-0.58	38.9 to 36.7	-16 ± 0.5
2-100	10	1.82-1.86	0.54-0.55	41.1 to 40.0	-24 ± 0.5
2-200	10	1.88-1.92	0.52-0.53	43.3 to 42.2	-30 ± 0.5

*From Sharp (1951).

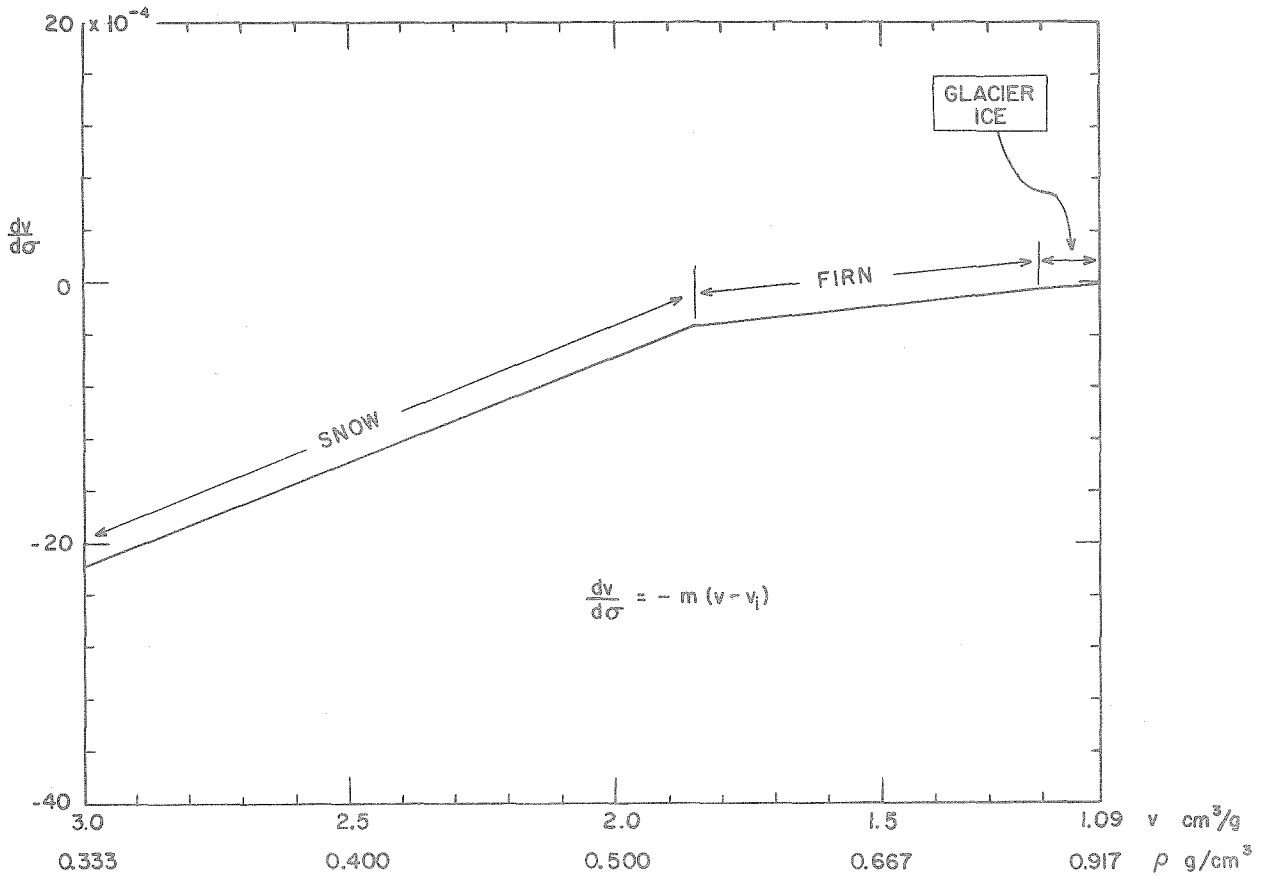

Figure 51.--Relation between $\frac{dv}{d\sigma}$ and v at Station 2-100.

It must be noted that, although Figure 50 shows the observed relationship between critical density and temperature, the relation between these variables is not simple because temperature changes have many ramifications. A very important temperature-dependent factor is the amount of melt water, which is especially notable on Seward Glacier and at 0-35, of minor importance at 1-0, negligible at 2-100, and completely absent at 2-200. Average grain size decreases from left to right in Figure 50 and this is primarily a temperature effect. Strength of ice increases with decreasing temperature and decreases the rate of densification. The rate of accumulation is roughly an inverse function of temperature. The latter two factors combine to make the age of the material at the critical density increase from left to right. These factors are all involved in the abscissa "T_c" which is the most significant critical value to correlate with critical density.

Even though melting occurs the discontinuity at the critical point still reflects the same change in densification process. The presence of "free water" in the snow permits closer packing than can be obtained by packing dry snow. For example, if dry snow can be compacted to a minimum porosity of 39% it would be expected that 39% free water added to the snow would lead to complete densification (i.e., the final product when frozen would be impermeable ice). Actually, in such a case, complete densification requires only about 29%

free water (Anderson and Benson, 1959) because the presence of water in the snow has allowed tighter packing, partly by lubrication of the grains. As a result of this, locations on glaciers where melt occurs have lower values of critical porosity than locations where no melt occurs. However, this effect is merely superimposed on the primary mechanism of densification by packing above z_c,

Assume that the minimum critical porosity obtained by packing dry snow is n_{co}%. Then the reduction of pore space caused by melt action at any location will be given by

$$(n_{co} - n_c)\% \ ,$$

where n_c is the critical porosity at the given location. If n_{co} = 41% then an estimate of the reduction of pore space by melt water at the critical depth at stations shown in Figure 50 is:

Seward Glacier	19 to 22%
0-35 Greenland	6 to 12%
1-0 "	2 to 4%
2-100 "	0 to 1%
2-200 "	0%

On this basis the following estimates are made of the reduction of pore space by melt action in the various facies:

Facies	Reduction of pore space by melt action at z_c
Ablation	approaches 100%
Soaked	6 to 25%
Percolation	1 to 4%
Dry-snow	less than 1%

Depth-Density Relationship

An explicit relationship between depth and density may be obtained from equation 8 after making the following substitutions:

$$v = \frac{1}{\rho} \quad , \quad dv = -\frac{d\rho}{\rho^2}$$

$$\sigma = \int_0^z \rho \, dz \quad , \quad \text{and } d\sigma = \rho \, dz .$$

Then equation 8 becomes

$$\frac{d\rho}{dz} = m\rho^3\left(\frac{1}{\rho} - \frac{1}{\rho_i}\right) = m\rho^2\left(\frac{\rho_i - \rho}{\rho_i}\right) = m\rho^2 n \qquad (11)$$

$$\text{where } n = \text{porosity} = \frac{\rho_i - \rho}{\rho_i} .$$

Equation 11 may be integrated to obtain the depth-density relationship as follows:

$$\frac{d\rho}{dz} = m\rho^2\left(\frac{\rho_i - \rho}{\rho_i}\right) \tag{11}$$

$$\int_0^z \frac{m}{\rho_i}\, dz = \frac{m}{\rho_i}\, z = \int_{\rho_o}^{\rho} \frac{d\rho}{\rho^2(\rho_i - \rho)} \tag{12}$$

Integration of the right hand side of equation 12 may be carried out by expanding it into partial fractions to obtain:

$$z = -\frac{1}{m\rho_i}\left[\frac{\rho_i}{\rho} + \ln\left(\frac{\rho_i - \rho}{\rho}\right)\right]_{\rho_o}^{\rho} \tag{13}$$

Equation 13 may be put in the following symmetric form by adding the constant term $\frac{1}{\rho_i^2}$:

$$z = -\frac{1}{m\rho_i}\left[\frac{\rho_i - \rho}{\rho} + \ln\frac{\rho_i - \rho}{\rho}\right]_{\rho_o}^{\rho} \tag{13a}$$

When the limits of integration are subsituted in equation 13a we obtain:

$$z = \frac{1}{m\rho_i}\left[K - (\epsilon + \ln\epsilon)\right], \tag{14}$$

where $K = \frac{\rho_i - \rho_o}{\rho_o} + \ln \frac{\rho_i - \rho_o}{\rho_o} = \epsilon_o + \ln \epsilon_o$,

$\epsilon = \frac{\rho_i - \rho}{\rho}$ = void ratio for firn of density ρ , and

$\epsilon_o = \frac{\rho_i - \rho_o}{\rho_o}$ = void ratio for firn of density ρ_o.

Curves obtained by plotting equation 14 are shown in Figure 52.

It is of interest to examine the nature of the depth-density curve as revealed by the derivatives $\frac{d\rho}{dz}$ and $\frac{d^2\rho}{dz^2}$.

The first derivative is given by equation 11 which states that the change in density with depth is proportional to the product of porosity and the square of the density.

The second derivative is:

$$\frac{d^2\rho}{dz^2} = m \frac{d}{dz}\left(\rho^2 - \frac{\rho^3}{\rho_i}\right)$$

$$= m^2 \left(2\rho - \frac{3\rho^2}{\rho_i}\right)\left(\rho^2 - \frac{\rho^3}{\rho_i}\right). \qquad (15)$$

Several interesting points about the curvature of the depth-density curve revealed by equation 15 are summarized below:

(a) $\frac{d^2\rho}{dz^2} = 0$ when $\rho = \frac{2}{3}\rho_i \cong 0.61$ g/cm^3,

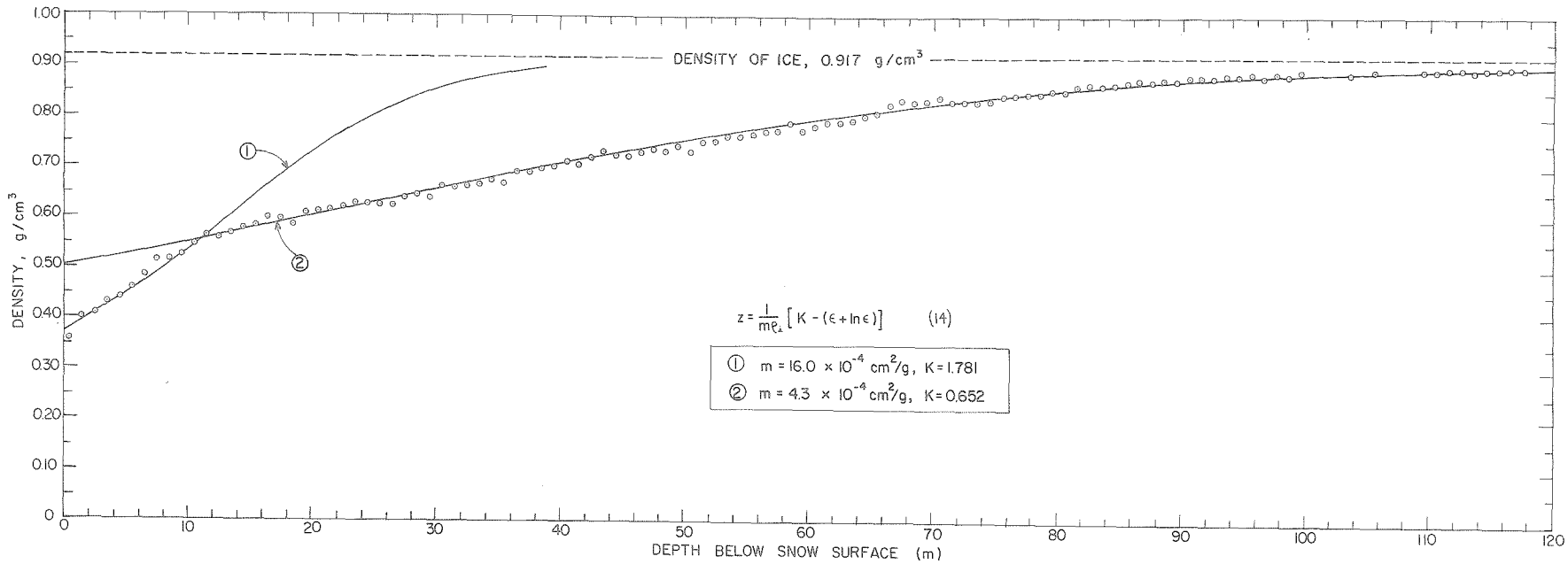

Figure 52.--Depth-density relationship at Station 2-100. Curves were computed from equation 14 with values of constants as indicated. The data points were obtained by averaging the writer's measurements made in 1953, 1954 and 1955 in the upper 14 m with measurements made by SIPRE personnel at the deeper depths.

(b) $\frac{d^2\rho}{dz^2} > 0$ when $\rho < \frac{2}{3}\rho_i$ and

(c) $\frac{d^2\rho}{dz^2} < 0$ when $\rho > \frac{2}{3}\rho_i$.

The point of inflection at $\rho = \frac{2}{3}\rho_i$ is independent of the value of the parameter "m," but is a direct consequence of the functional relationship assumed in equation 8.

The overall curvature of the depth-density curve is slight; therefore, the existence of a point of inflection at $\rho = \frac{2}{3}\rho_i$ demands that the curve be nearly linear for some distance on either side of $\rho = \frac{2}{3}\rho_i$. The point of inflection with the second derivative being positive for $\rho < \frac{2}{3}\rho_i$ and negative for $\rho > \frac{2}{3}\rho_i$, shows clearly in Figure 52.

A physical reason for the existence of a point of inflection is that the model does not allow negative densities. Thus, from a purely mathematical point of view, the depth-density curve obtained from the steady-state assumption expressed in equation 8 is asymptotic to zero density as z approaches $(-\infty)$, and asymptotic to the density of pure ice as z approaches $(+\infty)$; with $z = 0$ at the snow surface. This depth-density curve explicitly includes a nearly linear relation between depth and density in the depth range $10 < z < 50$ m, and this agrees well with observation.

CHAPTER VI

CLIMATOLOGICAL IMPLICATIONS

Introduction

Knowledge of weather and climate in the polar regions is fragmentary. During the past 10 years significant increases in arctic meteorological data for the western hemisphere have resulted chiefly through the efforts of the late Charles J. Hubbard; yet, the overall picture is not complete. Many phenomena of arctic climatology are hemispherical in extent, but Greenland constitutes a special problem because of its extensive ice cover (see Hare, 1951, pp. 961-963). Some climatological results of this study have been presented above, i.e., the distributions of gross annual accumulation (Fig. 30), mean annual temperature (Fig. 40), and diagenetic facies (Fig. 48). The purpose of this chapter is to discuss several implications which were not directly involved in the above discussion.

It is significant that as late as 1950 the erroneous "glacial anticyclone theory" was still prevalent (in the U.S.) to the extent that Matthes (1946) and Matthes and Belmont (1950) devoted papers to its refutation. After extensive review of recent meteorological data from Greenland Matthes concluded:

> "that there is no evidence of a virtually permanent 'glacial anticyclone' centered over the Greenland ice sheet. On the contrary, there is consistent evidence from all parts of Greenland that the weather over the ice sheet is controlled by alternating cyclonic and anticyclonic movements. Cyclonic activity is most intense in southern Greenland and weakest in northern Greenland. The entire ice sheet is supplied with snow brought by rising maritime air masses, not by air descending from the upper trosphere" (Matthes, 1946, p. 324).

The results of the present study are completely compatible with Matthes' conclusions; and they contribute quantitative information on the amount and distribution of precipitation for part of the ice sheet.

Katabatic Winds and Accumulation

If a staunch proponent of the glacial anticyclone were found today, he might argue that "the maximum accumulation shown at low elevations, near the margin of the ice sheet (Fig. 28), is due to katabatic winds which sweep the snow outward from the interior." This is not a valid argument because, although the katabatic winds prevail (p. 114), they are weaker and cause much less drifting of snow than do the storm winds. This is known by direct observation of the drifts which form around objects, such as huts or piles of barrels, in the course of a year. Such drifts are always lined up with the storm winds which come from the southwest and erosion-deposition features from the prevailing katabatic winds are merely superimposed on them. Thus, the distribution

of accumulation shown in Figure 28 exists in spite of, not because of, the katabatic winds.

Rather than adding to the net accumulation at a given point, the katabatic winds may actually detract from it. The ability of the air to hold moisture increases markedly as it moves from the cool, dry interior toward the warmer coastal areas. As an example, saturated air at 0°C contains 3.5 times more water by weight than saturated air at -15°C. Thus, katabatic winds, originating over the interior highlands of the ice sheet, absorb moisture as they descend, especially in summer months, and leave the shores of Greenland with a net increase in water vapor. This is similar to the process which acts over the United States as outlined by Holzman (1937, p. 38):

> "The principal amount of moisture returned to the atmosphere by continental evaporation is absorbed by continental, or dry, air masses that are generally incapable of immediately releasing their moisture and that pass off continental areas with large gains in moisture."

Therefore, desert regions like Inglefield Land are dry not only because they lie in precipitation shadows, but also because much of what they do receive is "blotted up" and carried off by the katabatic winds.

Annual Heat Exchange

Consider a column of unit cross-section extending from

snow surface to the depth of 10 m. By definition, Q is the amount of heat required to raise the temperature of this column of firn to the melting point. The maximum and minimum values of Q, Q_{max}, and Q_{min}, occur during winter and summer respectively. Q, sometimes called "cold content," is computed by summing increments ΔQ over depth increments Δz (taken to be 20 cm each for convenience). Then

$$\Delta Q = mcT$$

where

m = the mass in grams of the 20 cm^3 volume

T = the average temperature, and

c = 0.5 cal/m°C

A summary of data obtained in the top 5 m in late summer is shown in Figure 53. Except for the spacing between curves of the soaked and non-soaked facies, the cold content increases fairly smoothly with elevation. The environmental difference existing between points lying well above the firn line is shown by the fact that the curve for Q_{max} at 1-0 (not shown) is about the same as that shown for Q_{min} at 2-200. Thus, the amount of heat required to melt the upper layers of snow at 2-200 in summer is the same as that required at 1-0 in winter. Values of Q_{min} (to 10 m) for several positions are:

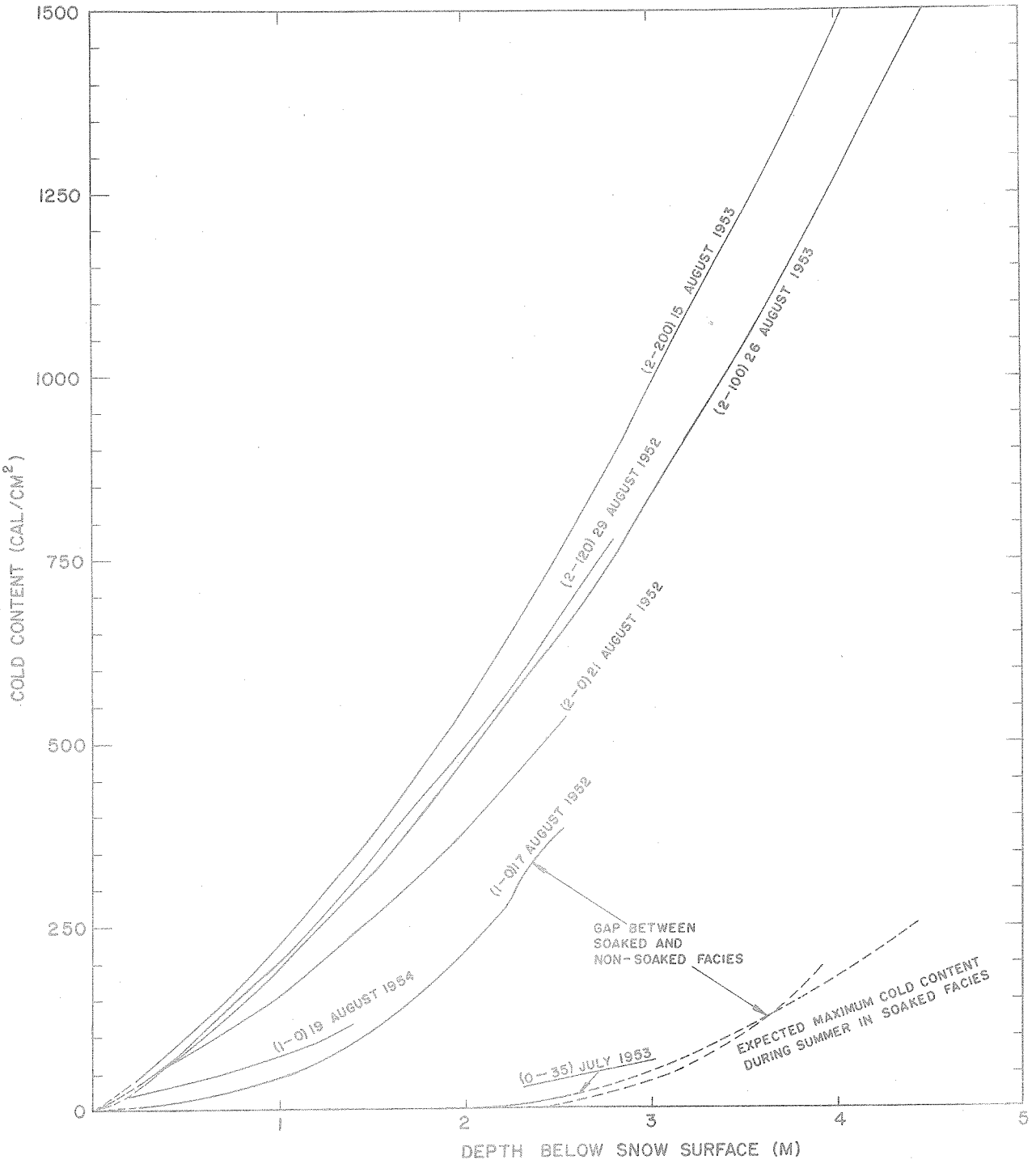

Figure 53.--"Cold content" in the top 5 m during the peak of the melt season at 77°N. The cold content is defined as the amount of heat (in calories) required to raise a unit column of snow to the melting point.

Position	Q_{min}, Calories	
Seward Glacier	0.0	x 10^{-3}
0-35	1.0 to 2.0	»
1-0	3.5	»
2-100	4.7	»
2-200	6.0	»

Q_{min} may prove useful as a climatic index for glaciers, being zero for a truly temperate glacier.

The amount of heat exchanged annually between the top 10 m of firn and the atmosphere is denoted by ΔH. If heat exchanges associated with phase transformations are ignored,

$$\Delta H = Q_{max} - Q_{min} .$$

At 77°N lat ΔH remains essentially constant, within 10%, even though measured in different temperature ranges at different altitudes as summarized below:

	Date	Q, calories	ΔH, calories
1-0	3 March, 1954	4856	1382
1-0	17 August, 1952	3474	
2-100	Feb-March, 1954	6285	1543
2-100	26 August, 1953	4742	

The 10% difference between ΔH at 1-0 and 2-100 is in the right direction to indicate more melt at 1-0, and sufficient to completely melt a 5 cm layer of snow of density 0.40 gm/cm^3. This is not an unreasonable estimate for the difference in melting between 1-0 and 2-100.

The Balance of the Greenland Ice Sheet

Bauer (1955) discussed the present-day balance of the Greenland ice sheet and came to the conclusion that it was in negative balance, i.e., more material is being lost than gained. Bauer's estimate is based on the following:

(1) The assumption was made that the firn line separates the regions of accumulation and ablation. He then estimated the firn line for each of the USAF World Aeronautical Charts.

(2) Loewe's (1936) estimates were accepted for the mean ablation (110 cm H_2O per year) and for the mean accumulation (31 cm H_2O per year) for the entire ice sheet.

(3) An estimate was made of the total discharge of icebergs from glaciers.

Bauer used a firn line 4000 ft (1220 m) for the Smith Sound and Humbolt Glacier maps. This is definitely too high because pits at 4000 ft in this area are well above the firn line; indeed, they are above the saturation line. It is also known that the firn line does not separate the regions of ablation and accumulation in Greenland because of the formation

of superimposed ice (Schuster, 1954; Schytt, 1955, pp. 52-57). Thus the stated figure for total ablation area is too high.

Bauer's ablation area is reduced by 32,000 km^2 if the average altitude of the firn line is placed at 3000 ft (915 m) north of 76°N, except on the south slopes of Thule and Inglefield peninsulas where it is known to lie at about 2300 ft (700 m). The amount of area transferred from the ablation to the accumulation area on each of the maps involved is as follows:

World Aeronautical Chart		Area km^2	
#20	Smith Sound	13,000	19,000 west slope
#19	Humbolt Glacier	6,000	
# 8	Robeson Channel	0,000	
# 9	Independence Fjord	3,500	13,000 east slope
#18	Germania Land	9,500	
	Total	32,000	

The average accumulation value of 31 cm H_2O for the entire ice sheet is too low. Planimetric measurements of the areas between accumulation contour lines on the 1:5,000,000 map of Figure 30 give an overall average accumulation value of 34 cm H_2O as summarized in Table X and Figure 54.

From the work reported herein, no comments can be made about Bauer's estimate for the amount of discharge of ice-

Table X

Distribution of gross accumulation on the Greenland ice sheet

A = Annual accumulation (cm H_2O) Range	Surface area km^2	Surface area %	Annual accumulation (cm H_2O)
5 - 10	138,000	7.8	0.58
10 - 20	397,000	22.4	3.36
20 - 30	314,000	17.7	4.42
30 - 40	267,000	15.0	5.25
40 - 50	259,000	14.6	6.57
50 - 60	197,000	11.1	6.10
60 - 70	91,000	5.1	3.32
70 - 80	51,000	2.9	2.18
80 - 90	40,000	2.3	1.96
greater than 90	20,000	1.1	1.04
	1,774,000	100.0	34.78

The total area of the ice sheet obtained from these measurements is 2.8% greater than that obtained by Bauer on the 1:1,000,000 map. Bauer's figure is more accurate than the one obtained here from the 1:5,000,000 map. Therefore, the average annual accumulation value of 34.78 cm H_2O should be reduced by 2.8% to give 33.86, or to the nearest cm, 34 cm H_2O.

The areal distribution of precipitation on the ice sheet is plotted below:

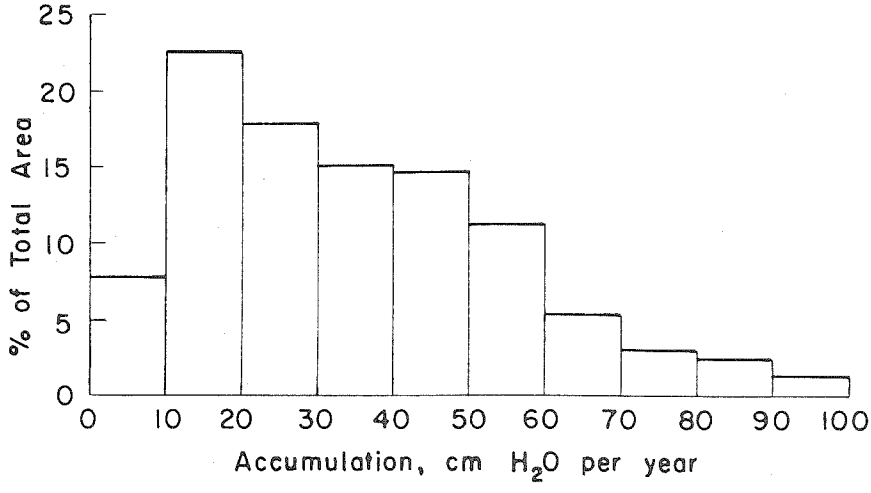

Figure 54.--The areal distribution of gross accumulation on the Greenland ice sheet.

bergs by glaciers. His value is accepted as being the best available estimate. Loewe's estimate of average gross ablation is also accepted here in the absence of sufficient data to apply a correction. His quoted value of 110 cm H_2O per year refers to net ablation; therefore, the addition of 3 cm H_2O per year to gross accumulation, as determined above, reduces his net ablation by the same amount to give 107 cm H_2O per year. The three* attempts to determine the balance of the Greenland ice sheet are summarized in Table XI.

I would estimate, as did Loewe (1936) that the Greenland ice sheet is in balance with present-day climate, or that it is so close to being in balance that our present methods of measuring the variables involved cannot show significant deviations one way or the other.

---

*Based on observations from his 1912 expedition, DeQuervain concluded that the balance of the ice sheet was positive. He dealt with the west slope only so he did not estimate the magnitude of the positive balance but generalized that the ice sheet was maintaining itself at present and was not strictly a relic of the past.

Table XI

Balance of the Greenland ice sheet

	Loewe (1936)	Bauer (1955)	Present study
Area:			
Accumulation zone (km^2)	1,380,000	1,439,800	1,471,800
Ablation zone (km^2)	270,000	286,600	254,600
Total ice sheet (km^2)	1,650,000	1,726,400	1,726,400
Average Annual Rates:			
Accumulation (cm H_2O/year)	31	31	34
Ablation (cm H_2O/year)	110	110	107
Net Values:			
Accumulation (km^3 H_2O/year)	425	446	500
Ablation (km^3 H_2O/year)	295	315	272
Excess of accumulation over ablation (km^3 H_2O/year)	130	131	228
Discharge of icebergs from glaciers (km^3 H_2O/year)	150	215	215
Balance (km^3 H_2O/year)	-20	-84	+13

APPENDIX I

STRATIGRAPHY, METEOROLOGY AND GLACIOLOGY

This appendix presents certain terms and concepts from stratigraphy, meteorology, and glaciology used in this paper. However, it also indicates specific applications of these fields to studies of the Greenland ice sheet.

Stratigraphy

Formation

> "The formation is the fundamental unit in the local classification of rocks. Like other categories of rock units, the formation is a genetic unit, defined by objective criteria observable in the local stratigraphic column. Formations should be established with boundaries that may be readily traced in the field and represented on geologic maps to best express the geologic development and structure of the area.
>
> "In most cases, formations should be distinguished as much as possible on the basis of lithologic unity--dominantly shale or dominantly sandstone, for instance--or repeated interlamination of two or more lithologies, as shale and limestone. Occasionally, however, a formation may contain a great variety of rock types, and such heterogeneity may itself distinguish the unit from more homogeneous units above and below.
>
> "A formation is a genetic unit and represents a response to an environment, or a series of related environments, and such environments must be limited geographically as well as temporally. Therefore, there are limits to the geographic extent of formations, and the same name should be applied only over the area in which the lithology maintains a degree of unity.

> "Formation names are binomial, usually consisting of a geographic name followed by a descriptive lithologic term (St. Louis limestone), the latter being uncapitalized" (Krumbein and Sloss, 1951, p. 27).

In view of the above statements the Greenland ice sheet (also the Antarctic ice sheet, the Vatnajokull ice cap, and most other glaciers) is unique as a formation in several respects. Its boundaries are unmistakably traced in the field. Lithologically, it is monomineralic; perhaps its closest competitor for purity is the St. Peter sandstone which, in size, however, is only a fraction of the ice sheet. From the genetic standpoint it most certainly represents a response to an environment.

Diagenesis. The term "diagenesis" is used here in reference to the processes involved in transforming snow (the loose sediment) into firn (the sedimentary rock). The diagenetic environment is defined as follows:

> "The diagenetic environment is the environment of post-depositional change. It extends an indefinite distance downward from the depositional interface. The nature of the diagenetic environment and the rapidity of the post-depositional changes depend upon the medium of deposition and the kind of sediment being deposited" (Krumbein and Sloss, 1951, p. 213).

On the ice sheet the depositional interface is the snow surface and the diagenetic environment extends downward from it for an unspecified distance, but includes most of the sedimentary member.

Facies

> "'Sedimentary facies' is defined as any areally restricted part of a definite stratigraphic unit which exhibits characters significantly different from those of other parts of the unit" (Moore, 1949, p. 32).

Facies in the Greenland ice sheet are based on differences in extent of melt action, and are produced by diagenetic processes.

Meteorology

Adiabatic processes. If a parcel of air is raised or lowered in the free atmosphere, it will expand or be compressed. No significant error is introduced by considering this process to be purely adiabatic. If the air is dry (not saturated with water vapor) its rate of temperature change will be approximately 1°C/100m (0.98°C/100m), regardless of whether the movement is upward or downward. This is called the "adiabatic rate" or "dry-adiabatic rate." If the element of air is saturated with water vapor its cooling rate on ascent will be less than adiabatic because heat is added to the air by condensation of water vapor. It may be half of the dry adiabatic rate of cooling. Descent of the air mass, on the other hand, will always produce the dry-adiabatic rate of warming regardless of the original moisture content.

Lapse rate. The term "lapse rate" is applied to the observed variation in air temperature with elevation. It

pertains to vertical temperature gradients in the free atmosphere only. It is not generally applicable to air temperature measurements made at different elevations along the surface of the earth, because horizontal variations in air masses may be encountered. The normal lapse rate is about -0.65°C/100m, the negative sign indicating that temperature decreases with increasing elevation. If the lapse rate happens to coincide with the adiabatic rate of temperature change for dry air, the air is said to have a "dry adiabatic lapse rate." In continental Arctic regions and especially over snow surfaces, strong "inversions" (i.e., Temperature increasing with height) are common (Wexler, 1936). Lapse rates less than adiabatic and especially those occurring in inversions are called "stable lapse rates." They result in the most stable stratification of air, vertical motions being strongly inhibited.

Inversions. At night, when short-wave solar radiation is absent, the snow surface radiates like a black body for all wave lengths. The atmosphere radiates with black body intensity only in certain bands of the spectrum, which are mainly due to water vapor. Also, the air loses energy both upward and downward but the snow surface radiates upward only. As a result of these conditions the snow surface will be in equilibrium with the air above when its temperature is lower than that of the air. This is the basic cause of inversions.

In the high latitudes of Greenland the process is effective even in summer because the sun never rises high above the horizon and much of its short wave energy is reflected by the snow surface. (Even though snow acts like a black body for terrestrial long wave radiation, it has a high albedo for solar radiation.) Polar maritime air shows normal lapse rates; however, Wexler (1936) has shown how it is transformed into polar continental air as it moves over a snow-covered continent. Therefore, an inversion will develop over the ice sheet regardless of the source of the air mass.

Glaciology

Firn line. The firn line is defined as "the highest level to which the fresh snow cover on a glacier's surface retreats during the melting season" (Matthes, 1942, p. 161).

Glacier classification. The classification of glaciers proposed by Ahlmann (1948) has been well received. It is a three-fold classification: (a) morphological, (b) dynamic, and (c) geophysical. Of these, the "morphological classification" is the most quantitative. Greenland may be discussed according to these classifications as follows:

Morphological: In Ahlmann's morphological classification the Greenland and Antarctic ice sheets are included under the heading:

> "A. Glaciers extending in continuous sheets, the ice moving outwards in all directions: (1) Continental glacier or inland ice, covering a very large area" (Ahlmann, 1948, p. 61).

Recently Bauer (1955) constructed the normal-area distribution curve, according to Ahlmann's convention, for the Greenland ice sheet. He found that it fits very well in the Ahlmann classification, and adds that this is the first classification which successfully includes the Greenland ice sheet.

Dynamic: An attempt to discuss Greenland's ice sheet according to an overall dynamic classification would be complex. The span of latitude is nearly 23°, 75% of which is above the Arctic Circle. This results in wide variation between local regimens and the rate of flow varies from fast in the south to slow in the north.

Geophysical: Ahlmann's geophysical classification divides glaciers into two broad groups, temperate and polar; the latter is further subdivided into high-polar and sub-polar. The most recent statement of this classification follows:

> "I. Temperate glaciers consist of crystalline ice formed by fairly rapid recrystallization of the annual surplus of solid precipitation due to great quantities of fluid water. Throughout these glaciers the temperatures correspond to the melting-point of the ice, except in winter time, when the top layer is frozen to a depth of not more than a couple of meters. The glaciers of Scandinavia and the Alps are included in this group.

> "II. Polar glaciers consist, at least in their higher and upper parts, of hard crystalline firn formed by slow recrystallization of the annual surplus of accumulated solid precipitation. The temperature of the glacier is negative even in summer down to a certain depth. These polar glaciers can be subdivided into:
> (a) High-polar glaciers, which consist, at least in their accumulation areas, of crystalline firn with temperatures below freezing-point to a considerable depth. Even in summer the temperature in the accumulation area is so low that as a rule there is no melting accompanied by formation of water.
> (b) Sub-polar glaciers, which in their accumulation areas consist of crystalline firn down to a depth of some 10 to 20 m. In the summer the temperature allows surface melting accompanied by the formation of fluid water" (Ahlmann, 1948, p. 66).

Ahlmann considers that most of the Antarctic together with the interior portions of the Greenland ice sheet are high-polar types. He recognizes more diversity in Greenland than in the Antarctic.

> "At lower levels, where both the winter and the summer temperatures are higher than at 'Eismitte', the Greenland inland ice is of sub-polar nature, and its outlet glaciers are temperate, at least in the lower latitudes" (Ahlmann, 1948, p. 67).

If truly temperate outlet glaciers exist in Greenland they are most likely limited to the extreme south.

Snow and ice as rock units. The concept of snow and ice as rock units certainly is not new (Grout, 1932; Seligman, 1936; Bader, et al, 1939; Flint, 1947). Grout mentions ice as one of the few examples of monomineralic deposits which attain the necessary dimensions to be properly classed as rocks. According to rock-type the following classification may be used.

1. Snow--sediment
2. Firn--sedimentary rock
3. Glacier ice--sedimentary and/or metamorphic rock
4. Lake ice--crystallization from melt } "igneous" rocks
5. Sea ice--crystallization from solution } "igneous" rocks

The difference between firn (also called neve) and glacier ice is best expressed in terms of permeability. Firn has intercommunicating pore spaces, while glacier ice is impermeable, i.e., the pore spaces are sealed from each other. The transformation from firn to glacier ice occurs at density values of 0.82 to 0.84 g/cm^3. (Perutz and Seligman, 1939; Schytt, 1954).

Temperate glaciers have received considerable treatment in the sense of being bona fide metamorphic rocks. However, firn as a stratified sedimentary rock has received little formal treatment. Ahlmann (1935, 1936, 1940, 1949) emphasized the importance of such studies and pioneered in the field.

APPENDIX II

MEAN ANNUAL TEMPERATURE

Observed temperature data are corrected to mean annual values in this appendix by use of equation 3. These computations do not take convection into account. However, the effects of convection were minimized by excluding all measurements made in the upper 3 meters of snow (see pages 118-119).

At some stations a range of temperature values is listed for a given depth and date. The actual temperature should lie within the indicated range.

In some cases, two values of the temperature correction are listed. This is done mostly where temperature data were obtained during August when differences between computed temperature corrections are greatest (Fig. 36).

The error in mean annual temperature values is between $\pm$ 0.5 and $\pm$ 1.0.

Depth (cm)	Date	Observed temp.	Correction	Mean annual temp.	Average	
			Station 1-0			
300	18-8-52	-14.5	-3.75	-18.2	-18.2	-17.0±0.5
300	18-7-53	-16.0	-2.0	-18		
300	3-6-54	-20.5	+2.25	-18.2		
400	22-7-53	-17.0	0	-17	-17.6	
400	4-6-54	-20.5	+2.35	-18.2		
500	22-7-53	-18.0	+0.8	-17.2	-17.6	
500	4-6-54	-20.0	+1.9	-18.1		
600	22-7-53	-18.3	+1.0	-17.3	-17.7	
600	4-6-54	-19.5	+1.3	-18.2		
700	7-6-54	-18.5	+0.8	-17.3	-17.3	
800	7-6-54	-18.0	+0.35	-17.6		
900	7-6-54	-17.5	+0.15	-17.3		
1000	7-6-54	-17.0	+0.03	-17.0		
1100	7-6-54	-16.5	-0.06	-16.6	-16.6	
1200	7-6-54	-16.5	-0.08	-16.6		
			Station 1-10			
300	15-6-54	-21.0	+1.3	-19.7		
			Station 1-20			
300	16-6-54	-21.5	+1.2	-20.3		
			Station 1-30			
300	17-6-54	-22.0	+1.1	-20.9		
			Station 1-40			
300	18-6-54	-22.5	+1.0	-21.5		
			Station 1-50			
300	19-6-54	-23.0	+0.85	-22.2		
(300)	19-5-55	-27.0	+3.0	-24.0[a]		
	"	(-26)	+3.0	(-23.0)		
			Station 1a-10			
300	19-5-55	-27.0	+3.0	-24.0		
			Station 1a-20			
300	20-5-55	-25.5	+3.0	-22.5		

Depth (cm)	Date	Observed temp.	Correction	Mean annual temp.	Average	
			Station 2-0			
300	21-8-52	-18.0	-3.9	-21.9	-22.5	-23.0
300	27-7-53	-20.0	-2.5	-22.5		
300	20-6-54	-24.0	+0.75	-23.2		
400	27-7-53	-22.0	0	-22.0	-22.6	
400	20-6-54	-25.0	+1.75	-23.2		
500	27-7-53	-23.0	+0.6	-22.4	-22.8	
500	20-6-54	-25.0	+1.7	-23.3		
600	27-7-53	-24.0	+0.95	-23.0	-23.3	
600	20-6-54	-25.0	+1.35	-23.6		
1132	24-6-54	-22.6	-0.2	-22.8	-22.8	
1675	24-6-54	-23.0	-0.3	-23.0	-23.0	
			Station 2-10			
300	25-6-54	-24.0	+0.25	-23.8	-23.6	
400	25-6-54	-25.0	+1.50	-23.5		
650	25-6-54	-23.0	+1.1	-21.9[b]		
			Station 2-20			
300	26-6-54	-24.0	+0.2	-23.8	-23.9	
400	26-6-54	-25.5	+1.4	-24.1		
500	26-6-54	-25.5	+1.55	-24.0		
900	26-6-54	-24.0	+0.25	-23.8		
			Station 2-30			
300	28-6-54	-24.5	-0.05	-24.6	-24.2	
400	28-6-54	-25.5	+1.35	-24.2		
500	28-6-54	-26.0	+1.50	-24.5		
600	28-6-54	-25.75	+1.30	-24.4		
1100	1-7-54	23.75	+0.02	-23.8		
1500	1-7-54	23.5	-0.03	-23.5		
			Station 2-40			
300	4-7-54	-24.5	-0.70	-23.8	-23.7	
400	4-7-54	-25.0	+1.0	-24.0		
800	5-7-54	-24.0	+0.55	-23.4		

Depth (cm)	Date	Observed temp.	Correction	Mean annual temp.	Average	
			Station 2-50			
300	6-8-53	-20.5	-3.1	-23.6	-24.1	-23.5
300	21-8-53	-19.5	-3.9	-24.4		
300	18-9-53	-19.0	-4.7	-23.7		
300	9-7-54	-23.5	-1.15	-24.6		
(300)	24-5-55	-27.5	+2.75	(-24.8)[a]		
400	6-8-53	-22.5	-0.8	-23.3	-23.7	
400	9-7-54	-25.0	+0.8	-24.2		
900	7-8-53	-23.2	+0.45	-22.8	-22.8	
1000	10-7-54	-23	+0.2	-22.8		
			Station 2-60			
300	11-7-54	-23.5	-1.3	-24.8	-24.0	
400	11-7-54	-25.0	+0.5	-24.5		
500	11-7-54	-25.0	+1.2	-23.8		
800	12-7-54	-24.0	+1.1	-23.9		
1000	12-7-54	-23.25	+0.2	-23.05		
			Station 2-70			
300	24-8-52	-19	-4.0	-23	-23.6	-23.8
300	24-8-52	-18.5	-4.0	-22.5		
300	16-7-54	-23.5	-1.8	-25.3		
400	16-7-54	-25.0	+0.4	-24.6	-24.4	
500	16-7-54	-25.5	+1.0	-24.5		
600	16-7-54	-25.0	+1.0	-24.0		
800	16-7-54	-24.5	+0.6	-23.9	-23.5	
1400	16-7-54	-23.25	-0.05	-23.3		
			Station 2-80			
300	19-7-54	-23.0	-2.0	-25.0	-24	
800	19-7-54	-23.75	+0.65	-23.1		
			Station 2-90			
300	20-7-54	-22.5	-2.1	-24.6	-24.6	
700	21-7-54	-25.5	+0.9	-24.6		
			Station 2-100			
300	26-8-53	-19.2	-4.2	-23.4	-24	
300	7-7-54	-24.0	-0.95	-24.9		
300	23-7-54	-21.5	-2.3	-23.8		

Depth (cm)	Date	Observed temp.	Correction	Mean annual temp.	Average
			Station 2-100 (cont)		
400	26-8-53	-21.2	-1.85	-23.0	-23.7
400	23-7-54	-24.2	-0.1	-24.3	
500	26-8-53	-22.5	-0.4	-22.9	-23
10m	all year	-24.3 ±0.2			-24
35.45 37.55 47.5		-24.4			-24.4
			Station A		
300	6-8-54	-21.75	-3.1	-24.8	-24.9
(400)	6-8-54	(-24.0)	-0.85	-24.8[a]	
			Station B		
300	9-8-54	-21.5	-3.25	-24.8	-24.9
(400)	9-8-54	(-24.0)	-1.0	-25.0	
			Station 2-120		
300	11-8-53	(-21.5)	-3.5	(-25.0)	-24.7
300	30-8-52	-2.0	-4.25	-24.2	
300	30-8-52	-20.5	-4.25	-24.8	
300	1-7-52	-25	-0.25	-25.2[c]	
			Station 2-125		
300	30-5-55	-29	+2.4	-26.6	26.6
(400)	30-5-55	-29	+2.4	-26.6[a]	
			Station 2-150		
300	1-6-55	-29.75	+2.4	-27.4	-27.4
			Station 2-175		
300	2-6-55	-30.75	+2.3	-28.4	-28.4
			Station 2-200		
300	15-8-53	-25.0	-3.6	-28.6	(-28.7)
400	16-8-53	-27.0	-1.8	28.8	
300	4-6-55	-32.0	+2.1	-29.9	-29.6
400	4-6-55	-31.5	+2.3	-29.2	

Depth (cm)	Date	Observed temp.	Correction	Mean annual temp.	Average
			Station 2-225		
300	7-6-55	-32.0	+1.9	-30.1	-31.1
400	7-6-55	-32.0	+2.2	-29.8	
800	7-6-55	-31.0	+0.4	-30.6	
			Station 4-0		
300	10-6-55	-32.5	+1.7	-30.8	-30.7
400	10-6-55	-33.0	+2.1	-30.9	
			Station 4-25		
300	12-6-55	-32.5	+1.5	-31.0	-31.0
400	12-6-55	-33.0	+2.0	-31.0	
			Station 4-50		
300	15-6-55	-31.75	+1.25	-30.5	-30.7
400	15-6-55	-32.5	+2.00	-30.5	
800	16-6-55	-31.5	+0.5	-31.0	
			Station 4-75		
300	17-6-55	-32.0	+1.05	-31.0	-31
400	17-6-55	-32.5	+1.90	-30.6	
800	18-6-55	-31.75	+0.5	-31.2	
			Station 4-100		
300	19-6-55	-31.25	+0.85	-30.4	-30.6
400	19-6-55	-32.0	+1.80	-30.2	
800	20-6-55	31.75	+0.5	-31.2	
			Station 4-125		
300	21-6-55	-31.5	+0.65	-30.8	-30.9
400	21-6-55	-32.5	+1.7	-30.8	
800	22-6-55	-31.5	+0.5	-31.0	
			Station 4-150		
300	23-6-55	-31.0	+0.45	-30.6	-30.6
400	23-6-55	-32.0	+1.6	-30.4	
800	24-6-55	-31.25	+0.55	-30.7	
			Station 4-175		
300	25-6-55	-30.25	+0.25	-30.0	-30.2
400	25-6-55	-31.00	+1.50	-30.5	
800	26-6-55	-30.75	+0.55	-30.2	

Depth (cm)	Date	Observed temp.	Correc-tion	Mean annual temp.	Average
			Station 4-200		
300	27-6-55	-30.25	+0.1	-30.2	-30.3
400	27-6-55	-31.5	+1.4	-30.1	
800	28-6-55	-31.2	+0.55	-30.6	
			Station 4-225		
300	30-6-55	-29.5	-0.25	-29.8	-29.8
400	30-6-55	-31.0	+1.25	-29.8	
			Station 4-250		
300	2-7-55	-29.5	-0.5	-30.0	-30.0
400	2-7-55	-30.5	+1.1	-29.4	
800	3-7-55	-31.0	+0.55	-30.4	
			Station 4-275		
300	5-7-55	-28.5	-0.75	-29.2	-29.4
400	5-7-55	-30.5	+1.0	-29.5	
800	7-7-55	-30.0	+0.58	-29.4	
			Station 4-300		
300	8-7-55	-28.75	-1.0	-29.8	-29.7
400	8-7-55	-30.5	+0.8	-29.7	
			Station 4-325		
300	10-7-55	-28.5	-1.2	-29.7	-29.5
400	10-7-55	-30.0	+0.7	-29.3	
800	11-7-55	-30.0	+0.6	-29.4[a]	
			Station 4-350		
300	12-7-55	-28.5	-1.5	-30.0	-29.5
400	12-7-55	-30.0	+0.6	-29.4	
700	13-7-55	-30.0	+0.9	-29.1	
			Station 4-375		
300	14-7-55	-27.75	-1.65	-29.4	-29.0
400	14-7-55	-29.75	+0.5	-29.2	
(500)	14-7-55	-30.0	+1.1	-28.9[a]	
700	15-7-55	-29.5	+0.9	-28.6	
			Station 4-400		
300	16-7-55	-28.0	-1.75	-29.8	-29.2
400	16-7-55	-29.5	+0.4	-29.1	
700	17-7-55	-29.5	+0.9	-28.6	

Depth (cm)	Date	Observed temp.	Correction	Mean annual temp.	Average
			Station 5-0		
300	18-7-55	-27.0	-1.95	-29.0	-29.8
400	18-7-55	-29.0	+0.25	-28.8	
700	19-7-55	-29.75	+0.9	-28.8	
			Station 5-20		
300	20-7-55	-26.0	-2.1	-28	-27.7
400	20-7-55	-27.5	+0.1	-27.4	
			Station 5-40		
300	23-7-55	-25.0	-2.25	-27.2	-27.2
400	23-7-55	-27.0	-0.1	-27.1	
1000	15-6-31	-28.4	+0.06	-28.3[d]	
1000	Aug 1950	-27.35	+0.3		(27.8)
		-27.20	+0.3	-27.0[d]	
		-27.50	+0.3		
2000	Aug 1950	-27.01	+0.01	-27	
10000	" "	-27.78		-27.8	
			Station 5-65		
300	2-8-55	-23.5	-3.0	-26.5	-25.8
400	2-8-55	-25.0	-0.7	-25.7	
700	5-8-55	-26.0	+0.75	-25.2	
			Station 5-90		
300	6-8-55	-22.0	3.1	-25.1	-24.35
300	6-8-55	-22.0	-3.3	-25.3	
400	6-8-55	-23.5	-1.0	-24.5	
700	7-8-55	-24.0	+0.75	-23.2	
			Station 5-115		
300	8-8-55	-21.0	3.4	-24.4	-24.3
"			3.2	-24.2	
			Station 5-140		
300	10-8-55	-19.5	-3.1	-21.6	-21.6
300	10-8-55	-19.5	-3.6	-22.1	
(700)	10-8-55	-22.0	+0.7	-21.3[a]	

Depth (cm)	Date	Observed temp.	Correction	Mean annual temp.	Average	
			Station 5-150			
300	12-8-55	-18.5	-3.7	-22.2	-21.8	
"	"	"	-3.0	-21.5		
			Station 5-160			
300	13-8-55	-18.0	-3.75	-21.75	-21.5	-21.1
"	"	"	-3.25	-21.25		
(400)	13-8-55	-19.0	-1.4	-20.4	-20.7[a]	
"	"	-19.0	-1.0	-20.0		
"	"	-20.0	-1.4	-21.4		
"	"	-20.0	-1.0	-21.0		
			Station 5-170			
300	14-8-55	-18.0	-3.8	-21.8	-21.5	-21.3
"	"	"	-3.3	-21.3		
(400)	14-8-55	-20.0	-1.95	-22.0	-21.2[a]	
"	"	-20.0	-1.1	-21.1		
"	"	-19.5	-1.95	-21.4		
"	"	-19.5	-1.1	-20.6		
			Station 5-180			
300	15-8-55	-17.0	-3.9	-20.9	-20.6	-20.8
"	"	-17.0	-3.3	-20.3		
(700)	15-8-55	-19.8	-1.5	-21.3	-21.1[a]	
"	"	-19.8	-1.1	-20.9		
			Station 5-190			
300	16-8-55	-16.5	-3.9	-20.4	-20.1	
"	"	"	-3.3	-19.8		
(400)	16-8-55	-18.5	-1.5	-20.0	-19.8[a]	
"	"	"	-1.1	-19.6		
			Station 5-200			
300	17-8-55	-16.0	-4.0	-20.0	-19.7	-19.6
"	"	"	-3.4	-19.4		
(400)	"	(-18)	-1.6	-19.6	-19.4[a]	
"	"	(")	-1.2	-19.2		

Depth (cm)	Date	Observed temp.	Correction	Mean annual temp.	Average	
			Station 5-210			
300	18-8-55	-15	-4.0	-19.0	-18.75	-18.6
"	"	"	-3.5	-18.5		
(400)	"	(-17)	-1.65	-18.65	-18.5[a]	
"	"	"	-1.3	-18.3		
			Station 5-220			
300	19-8-55	-13.75	-4.1	-17.85	-17.55	-17.5
"	"	"	-3.5	-17.25		
(400)	"	(-16)	-1.7	-17.7	-17.52[a]	
"	"	"	-1.35	-17.35		
			Station 5-230			
300	20-8-55	-11.5	-4.15	-15.65	-15.10	
"	"	"	-3.55	-14.55		
			French Camp VI[e]			
1000	July '50	-12.28			-12.4	
1000	30-8-50	-11.7				
1500	July '50	-12.45				
1500	30-8-50	-12.95				
			Station 0-35[f]			
(300)	31-5-54	(-11.5)	+2.5	-9.0		best value -10
"	"	(-12.0)	+2.5	-9.5		
"	"	(-12.5)	+2.5	-10.0		
"	"	(-13.0)	+2.5	-10.5		
(400)	31-5-54	(-11.5)	+2.5	-9.0		best value -10
"	"	(-12.0)	+2.5	-9.5		
"	"	(-12.5)	+2.5	-10.0		
"	"	(-13.0)	+2.5	-10.5		
(200)	16-5-55	(-14.5)	+2.7	-11.8		best value -12
(300)	"	(-15.0)	+3.25	-11.75		
(400)	"	(-14.5)	+2.7	-11.8		

[a]Temperature values enclosed in parentheses were extrapolated beyond the measured temperature profiles as follows:

Station 1-50, 19-5-55, 300 cm value extrapolated from 260 cm
Station 2-50, 24-5-55, 300 cm value extrapolated from 220 cm

1954 Survey area pit A, 6-8-54, 400 cm extrapolated from 360 cm
1954 Survey area pit B, 9-8-54, 400 cm extrapolated from 380 cm

Station 2-125, 30-5-55, 400 cm value extrapolated from 360 cm
Station 4-325, 11-7-55, 800 cm value extrapolated from 755 cm
Station 4-375, 14-7-55 500 cm value extrapolated between the values at 420 and 740 cm

Station 5-140, 10-8-55, 700 cm value extrapolated from 675 cm
Station 5-160, 13-8-55, 400 cm value extrapolated from 345 cm
Station 5-170, 14-8-55, 400 cm value extrapolated from 358 cm
Station 5-180, 15-8-55, 700 cm value extrapolated from 670 cm
Station 5-190, 16-8-55, 400 cm value extrapolated from 350 cm
Station 5-200, 17-8-55, 400 cm value extrapolated from 370 cm
Station 5-210, 18-8-55, 400 cm value extrapolated from 370 cm
Station 5-220, 19-8-55, 400 cm value extrapolated from 355 cm

[b]This value is about 1.5°C higher than it should be, according to the measurements from Stations 2-0 and 2-20.

[c]Measured by Bader one mile from the 1954 Survey area "pit B"

[d]The climatic warm up as seen in coastal stations (Fig. 39) shows up as a 1°C rise in mean annual temperature at Eismitte between 1930 and 1950. The 1930 data are from Sorge (1935) and the 1950 data are from Heuberger (1954).

[e]Data from French Camp VI are from Heuberger (1954).

[f]The temperature profiles at 0-35 in May of 1954 and 1955 do not quite reach 200 cm depth. But, during the period from 15 May to 30 May the temperature profiles are very nearly vertical, i.e., isothermal, between 200 and 400 cm.

This enables one to extrapolate the profiles below 180 cm. And the resulting range of mean annual temperature is -10 to -12°C.

APPENDIX III

THE DATA SHEETS

This appendix describes the format of the data sheets (in pocket) whose locations are indicated in Figure 55; these sheets contain almost all of the data discussed in this paper. There are 11 sheets, including data sheet 6A (not shown in Fig. 55) which presents the results of the 1953 traverse between 2-100 and 2-200 (see Fig. 2). Four other data sheets summarizing the 1952 and 1953 results have been published (Benson, 1959) and are not reproduced here.

A table showing the location of each test station, its altitude, the date or dates of occupation, and a summary of the work done at the station is available. It is not of sufficient general interest to be reproduced here, but may be obtained from the writer upon request.

Format

Data from each station are plotted around a stratigraphic columnar section which summarizes the appearance of the pit wall. The main emphasis in the column has been placed on features caused by melt and/or wind action.

Grain size is indicated only where it is extremely coarse or fine, or where it undergoes several significant variations over a short depth interval. The symbol depicting grain size

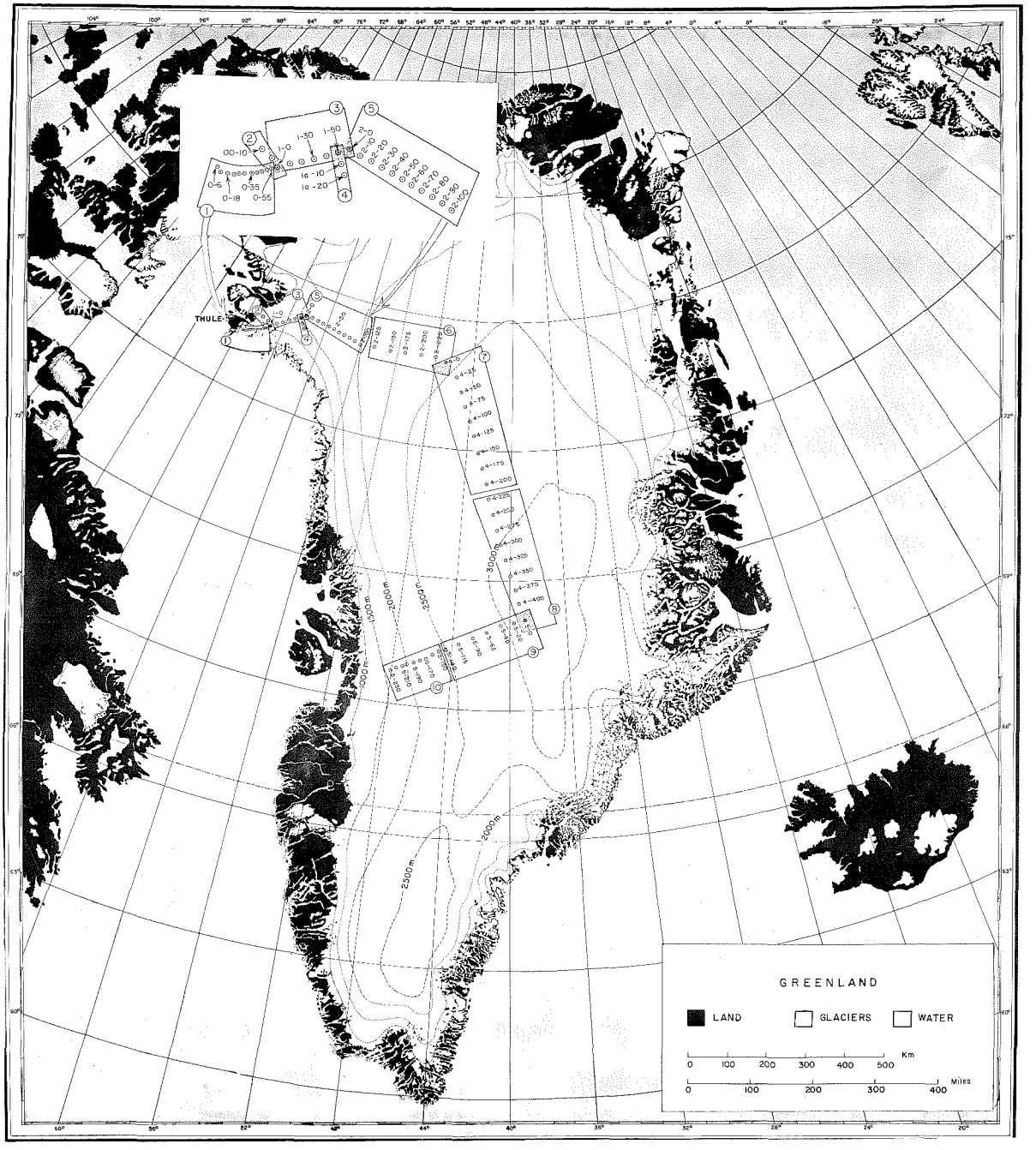

Figure 55.--Location of data sheets. Data sheet 6a (not shown) contains the six stations made in 1953 between Station 2-100 and 2-200, see Figure 2.

of a given layer represents the most abundant size range, typical ranges of grain size in single layers are seen in Figures 17 and 18. In most layers where grain size is not indicated, it lies in the range 1.0 $\pm$ 0.5 mm. Grain size is always indicated where it exceeds 2 mm.

The symbols used in the stratigraphic columns are described on page 205. (See also pages 55-59).

The temperature profile is plotted on the left hand side of the stratigraphic column. The ram hardness profile is also plotted to the left with its scale indicated above the temperature scale. No confusion results from superimposing the temperature and hardness data, because the former consists of observation points connected by lines, whereas the latter is simply a bar graph. The ram hardness profile is cross hatched where it exceeds 50 kg force; snow is very soft below this value.

The density profile is plotted on the right hand side of the stratigraphic column. It begins at 0.25 g/cm^3, and is cross hatched where it exceeds 0.40 g/cm^3. The cross hatching is useful in correlation between stations, and in comparing gross variations in density between facies (see data sheets 1 and 7 for example). The zero point on the density scale coincides with the $-15^{\circ}C$ point on the temperature scale. The depth and density scales were selected in such a way that each square cm under the depth density curve represents 1 cm of water equivalent. This made it an easy

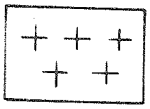

New snow, original crystal forms still recognizable.

1 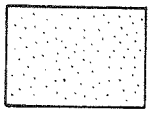 2 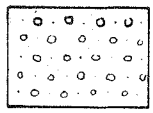 3 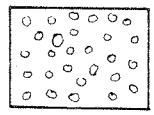 4 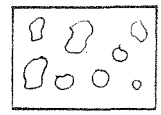

1. Fine- or very fine-grained snow, 1 mm.
2. Medium-grained snow, 1 to 2 mm.
3. Coarse-grained snow, 2 to 4 mm.
4. Very coarse-grained snow, 4 mm.

5 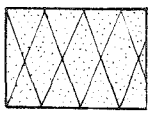 6 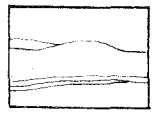 7  8 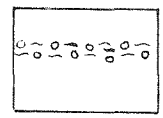

5. Wind slab, consisting of firmly bonded fine or very fine grains; from a little distance it has a dull, lustreless chalky appearance.*
6. Wind crusts, paper thin layers of firmly bonded very fine grains.** A thin line is also used to indicate discontinuities between adjacent layers.
7. Depth hoar, or coarse loosely bonded grains with vugs.
8. Melt crust or iced firn, consisting of coarse grains with small lenses and irregularly shaped chunks of ice scattered throughout.

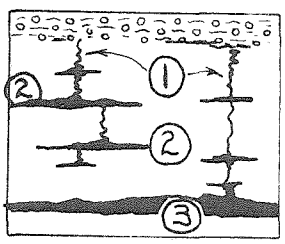

Ice masses in snow, formed by downward percolation from surface melt
1. ice gland
2. ice lens
3. ice layer

---

* Descriptive material on wind slabs is found in Seligman (1936, p. 159-205).

** The term wind crust is used here in a slightly different sense from that of Seligman (1936, p. 167).

matter to integrate the depth-density profiles to obtain depth-load curves. The data sheets reproduced here were reduced to 50% of their original size, thus an area of 1 cm^2 on the paper represents 4 cm water equivalent (each ruled square represents 1 cm water equivalent).

Stratigraphic Correlation

Stratigraphic interpretations have been correlated between stations. The year-labels, and the correlation lines connecting them, are intended to mark the fall layers of each year, i.e., 20 August to 10 September (see pp. 61-71). The location of specifically dated levels are indicated where they are known on data sheets 3 and 5. Correlation lines are dashed where interpretations were not unequivocal.

Several general comments are in order.

(1) The 1954 summer was the warmest one encountered as evidenced by the melt record in the snow and firn and by the meteorological record from Thule (see Fig. 31). Percolation from the mid-July 1954 snow surface penetrated into the snow layers of 1953 and 1952 at elevations of nearly 2000 m in northwest Greenland (see Figs. 24 and 25, and station 2-70 on data sheet 5). However, the extreme nature of the July 1954 melt was restricted to north Greenland. It apparently accompanied the occlusion of a storm over the region of 2-0 (personal communication with G. R. Toney, U. S. Weather Bureau).

(2) The summers of 1941 and 1950 produced the most widespread melt evidence in Greenland, being observed at nearly

all points along the traverse of this study. These years, especially 1941, were the only significant producers of melt evidence in the dry-snow facies (see data sheets 6, 7, and 8; also 5 and 9).

(3) In northwest Greenland the 1941 summer produced melt evidence comparable to that of the 1954 summer. It caused percolation through the 1940 and 1939 snow layers (see data sheet 5).

(4) Greater than average melt also occurred in northwest Greenland during the summers of 1945 and 1949. Localized percolation through the 1948 snow layers, of the percolation facies, apparently occurred during both 1949 and 1950.

(5) The heaviest accumulation recorded between 1937 and 1955 occurred during the year 1945-46. The lightest accumulation during the same 18-year period was during the year 1951-52.

BIBLIOGRAPHY

The Snow Ice and Permafrost Research Establishment is referred to as "SIPRE" in this bibliography. The numbers in parentheses at the end of each reference indicate pages where the reference is cited in the text of this paper.

Ahlmann, Hans W:son, 1935, Contribution to the Physics of Glaciers: Geogr. Jour., Vol. 86, pp. 97-113 (190).

_____, 1936, Scientific Results of the Norwegian-Swedish Spitsbergen Expedition 1934. Part VII. The Firn Structure on Isachsen's Plateau: Geografiska Annaler, Vol. 18, pp. 48-73. (190).

_____, 1940, Scientific Results of the Swedish Icelandic Investigations 1936-37-38: Geografiska Annaler, Vol. 22, pp. 188-205 (190).

_____, 1948, Glaciological Research on the North Atlantic Coasts: Royal Geographical Society Research Series No. 1, 83 p. (1,47,187,188,189).

_____, 1949, The Contribution of Polar Expeditions to the Science of Glaciology: Polar Record, Vol. 5 No. 37 & 38, pp. 324-331 (190).

_____, 1953, Glacier variations and climatic fluctuations, Bowman Memorial Lecture Series 3: American Geographical Society, N. Y. (122).

Anderson, Don L. and Carl S. Benson, 1959, The Densification of Snow (in preparation) (161,166).

Bader, et al, 1939, Der Schnee und Seine Metamorphose: Beitrage zur Geologie der Schweiz, Geotechnische Serie, Hydrologie, Lieferung 3, Bern. Translated into English by Jan C. Van Tienhoven and published as: SIPRE Translation No. 14, 1954 (5,16,34,36,56,62,127,129,189).

Bader, Henri, 1954, Sorges Law of Densification of Snow on High Polar Glaciers: Journ. Glaciology, Vol. 2 No. 15, pp. 319-323--also published as SIPRE Research Paper No. 2, 1953--(155).

_____, 1956, Personal Communication (125).

Bauer, A., 1955, The Balance of the Greenland Ice Sheet: Journ. Glaciology, Vol. 2, No. 17, pp. 456-462 (vi,178, 182,188).

Belknap, R. L., 1934, The Michigan-Pan American Airways Greenland Expedition, Preliminary results: Geogr. Review, Vol. 24, pp. 205-218 (151).

Benson, Carl S., 1955a, Scientific Work of Party Crystal, Preliminary report: SIPRE Report No. 24 (84).

_____, 1955b, Operations and Logistics of Ice-cap Party Crystal, 1954: SIPRE Report No. 25, 21 p. (9).

_____, 1955c, Resupply of Ice-cap Expeditions by Air Drop: SIPRE Special Report 17, 3 p. (9).

_____, 1959, Physical Investigations on the Snow and Firn of Northwest Greenland during 1952, 1953, and 1954: SIPRE Research Report 26, 62 p. (4,7,24,87,129,131,202).

Benson, Carl S. and R. H. Ragle, 1956, Report on special foods provided by the Quartermaster Food and Container Institute: SIPRE Special Report 18--also published in: Activities Report, Quartermaster Food & Container Institute, Vol. 9, No. 1, pp. 8-23, March 1957 (9).

Bey, Paul B., 1951, The Heat Economy of the Snow Pack: Chapter VII of SIPRE Report 4: "Review of the Properties of Snow and Ice," by H. T. Mantis and others (118).

Black, Robert F., 1954, Precipitation at Barrow, Alaska, Greater than Recorded: Trans. A.G.U., Vol. 35, pp. 203-207 (84).

Brooks, C. R., 1938, Need for universal standards for measuring precipitation, snowfall, and snow cover: Bull. 23, Intern. Assocn. of Hydrology, I.U.G.G., Riga (84).

Bull, Colin, 1956, Seismic Investigations on the Northern Part of the Greenland Ice Sheet: Geographical Journal, Vol. 122, pp. 219-225 (125).

_____, 1958, Snow Accumulation in North Greenland Journal of Glaciology, Vol. 3, No. 24, pp. 237-248 (6,85,86).

Butkovich, T. R., 1954, Ultimate Strength of Ice: SIPRE Research Paper No. 11 (133).

Church, James E., 1933, Snow Surveying--its Principles and Possibilities: Geogr. Review, Vol. 23, pp. 529-563 (83).

_____, 1942, Snow and Snow Surveying: Chapter IV of Hydrology, Physics of the Earth, Vol. IX, Dover Publications, Inc., New York (83).

Conrad, Victor, 1944, Methods in Climatology, 228 p., Harvard University Press, Cambridge, Massachusetts (80).

DeQuervain, Alfred and P. L. Mercanton, 1925, Resultats Scientifigues de l'expedition Suisse au Groenland 1912-1913: Meddelelser om Grønland Bind. 59 (text in French) (6,86,118).

DeQuervain, M., 1945, Schnee als kristallines Aggregat: Experimentia, Vol. 1, October, 1945. Translated by C. M. Gottschalk, 1954, and published as SIPRE Translation 21 (36).

Diamond, M., 1958, Air Temperature and Precipitation on the Greenland Ice Cap: SIPRE Research Report 43 (84).

Dorsey, H. G., 1945, Some Meteorological Aspects of the Greenland Ice Cap: Jour. Meteorology, Vol. 2, pp. 135-142 (115).

Epstein, S. and Carl Benson, 1959, Variation of the O^{18}/O^{16} ratios in Greenland Snow (in preparation) (90).

Epstein, S. and T. Mayeda, 1953, Variation of O^{18} Content of Water from Natural Sources: Geochim. et Cosmochim. Acta, Vol. 4, pp. 213-224 (90,94).

Epstein, S. and R. P. Sharp, 1959, Oxygen-Isotope Variations in the Malaspina and Saskatchewan Glaciers: Journal of Geology, Vol. 67, pp. 88-102 (91).

Flint, R. F., 1947, Glacial Geology and the Pleistocene Epoch, 589 p.: John Wiley & Sons, New York (189).

Grout, F. F., 1932, Petrography and Petrology, 522 p.: McGraw-Hill Book Company, N. Y. (189).

Hare, F. K., 1951, Some Climatological Problems of the Arctic and Sub-Arctic, Compendium of Meteorology, pp. 952-964: Published by American Meteorological Society (172).

Henry, A. J., 1919, Increase of Precipitation with Altitude: Monthly Weather Review, Vol. 47, pp. 33-41 (80).

Heuberger, Jean-Charles, 1954, Glaciologie Groenland, Vol. I Forages sur L'inlandsis: Hermann & Cie, Editeurs, Paris (106,151,201).

Holzman, Benjamin, 1937, Sources of Moisture for Precipitation in the United States: U.S. Department of Agriculture, Tech. Bull. No. 589 (174).

Hubley, R. C., 1954, The Problem of Short Period Measurements of Snow Ablation: Jour. Glaciology, Vol. 2, No. 16, pp. 437-440 (73).

Koch, J. P. and A. Wegener, 1930, Wissenschaftliche Ergebnisse der Dänischen Expedition nach Dronning Louises-Land und Quer über das Inlandeis von Nordgrönland 1912-1913 unter Leitung von Hauptmann J. P. Koch: Meddelelser om Grønland, Bind 75, text in German (2,6,61,86,151).

Krumbein, W. C., 1933, Textural and Lithological Variations in Glacial Till: Jour. Geol., Vol. 41, pp. 382-408 (53).

_____, 1943, Size Frequency Distributions of Sediments: Jour. Sed. Petrology, Vol. 4, pp. 65-77 (50,51).

_____, 1936, The Use of Quartile Measures in Describing and Comparing Sediments: Am. Jour. Sci., Vol. 32, pp. 98-111 (53).

Krumbein, W. C. and L. L. Sloss, 1951, Stratigraphy and Sedimentation, 497 p.: W. H. Freeman & Company, San Francisco, California (53,184).

Landauer, J. K., 1959, From Discussion at Symposium de Chamonix: Bull de l'assoc. Int. Hydrol. Sci., No. 13, p. 43, March, 1959 (154).

Lee, Charles H., 1941, Total Evaporation for Sierra Nevada Watersheds by the Method of Precipitation and Runoff Differences: Trans. A.G.U., Part I, pp. 50-71 (80,81,83).

Loewe, F., 1936, Höhenverhältnisse und Massenhaushalt des Grönländischen Inlandeises: Gerlands Beiträge zur Geophysik, Band 46, Ht. 3, pp. 317-330 (vi, 178,181,182).

Matthes, F. E., 1942, Glaciers, Chapter V in Hydrology Physics of the Earth IX: McGraw-Hill Book Company, N. Y. (150,187).

_____, 1946, The Glacial Anticyclone Theory Examined in the Light of Recent Meteorological Data from Greenland, Part I: Trans. Amer. Geophys. Union, Vol. 27, pp. 324-341 (115,172,173).

Matthes, F. E. and A. D. Belmont, 1950, The Glacial Anticyclone Theory Examined in the Light of Recent Meteorological Data from Greenland, Part II: Trans. Amer. Geophys. Union, Vol. 31, pp. 174-182 (115,172).

Meyer, C. B., 1941, Discussion of Paper by Lee: Trans. A.G.U., Part I, pp. 67-71 (81).

Moore, R. C., 1949, Meaning of Facies: G.S.A. Memoir 39, pp. 1-34 (185).

Muskat, M., 1937, The Flow of Homogeneous Fluids Through Porous Media, 763 p.: McGraw-Hill Book Company, N. Y. (159).

Nakaya, V. and A. Matsumoto, 1953, Evidence of the Existence of a Liquidlike Film on Ice Surfaces: SIPRE Research Paper No. 4 (36).

Nyberg, Alf, 1938, Temperature Measurements in an Air Layer Very Close to a Snow Surface: Geografiska Annaler, Vol. 20, pp. 234-275 (96).

Perutz, M. F. and G. Seligman, 1939, A Crystallographic Investigation of Glacier Structure and the Mechanism of Glacier Flow: Proc. Roy. Soc. London, Series A, No. 950, Vol. 172, pp. 335-360 (190).

Schaefer, V. J, G. J. Klein, and M. DeQuervain, 1951, Entwurf einer internationalen Schneeklassifikation (Draft of an international snow classification): Union geodesique et geophysique internationale, Assembe Generale de Bruxelles (50,51).

Schuster, Robert L., 1954, Project Mint Julep, Part III--Snow Studies: SIPRE Report 19, 7 p. (6,17,151,179).

Schytt, Valter, 1954, Report on Glaciological Investigations During the Norwegian-British-Swedish Antarctic Expedition, 1949-1952: Publication No. 39 de l'Association Internationale d'Hydrologie (Assembee generale de Rome, Tome IV), Extrait (148,156,158,190).

_____, 1955, Glaciological Investigations in the Thule Ramp Area: SIPRE Report 28, 88 p. (42,83,179).

Seligman, Gerald, 1936, Snow Structure and Ski Fields, 555 p.: MacMillan & Company, London (63,64,189,205).

Sharp, Robert P., 1951, Features of the Firn on Upper Seward Glacier, St. Elias Mountains, Canada: Journal of Geology, Vol. 59, pp. 599-621 (43,138,139,146,157,163).

Sorge, Ernst, 1933, The Scientific Results of the Wegener Expeditions to Greenland: Geographical Jour., Vol. 81, pp. 333-344 (1,160).

_____, 1935, Glaziologische Untersuchungen in Eismitte, in Wissenschaftliche Ergebnisse der Deutschen Grönland Expedition Alfred Wegener 1929 und 1930/1931; Band III Glaziologie, pp. 62-263: F. A. Brockhaus, Leipzig, 1935 (1,96,101,107,108,119,138,201).

Thiel, G. A., 1935, Sedimentary and Petrographic Analysis of the St. Peter Sandstone: Bull. G.S.A., Vol. 46, pp. 559-614 (53).

Varney, Burton M., 1925, Seasonal Precipitation in California and its Variability: Monthly Weather Review, Vol. 53, pp. 148-163 and 208-218 (80).

Wade, F. Alton, 1945, Physical Aspects of the Ross Shelf Ice: Proc. Am. Phil. Soc., Vol. 89, pp. 160-173 (148).

Warnick, C. C., 1953, Experiments with Windshields for Precipitation Gages: Trans. A.G.U., Vol. 34, No. 3, pp. 379-388 (84).

Wexler, H., 1936, Cooling in the Lower Atmosphere and the Structure of Polar Continental Air: Monthly Weather Review, Vol. 64, pp. 122-136 (114,186,187).

Weyl, W. A., 1951, Surface Structure of Water and Some of its Physical and Chemical Manifestations: Journ. Colloid. Sci., Vol. 6, No. 5, pp. 389-405 (36).

Wilson, Walter T., 1954, Discussion of paper by Black: Trans. A.G.U., Vol. 35, pp. 206-207 (84).